UNIVERSITY OF CALIFORNIA, MERCED

# An Examination of Dynamic Molecular Interactions in Triple Negative Breast Cancer Tumors Towards Improved Preclinical Approaches

A dissertation submitted in partial satisfaction of the requirements for the degree Doctor of Philosophy

in

Quantitative and Systems Biology

by

Nicholas Hum

Committee in charge:
Dr. Michael D. Cleary, Chair
Dr. Jennifer O. Manilay
Dr. Kara E. McCloskey
Graduate Advisor:
Dr. Gabriela G. Loots

2021

## Signature Page

The Dissertation of Nicholas Hum is approved, and it is acceptable in quality and form for publication on microfilm and electronically:

Michael D. Cleary

Jennifer O. Manilay

Kara E. McCloskey

Gabriela G. Loots

Date

University of California, Merced

2021

## Dedication

To Olivia and Lucas, you were the motivation to strive to be a better everything.

Table of Contents

## List of Abbreviations

2D - 2-dimensional
2D - monolayer
3D - 3-dimensional
3DG - 3D spheroids in hydroGel
3DM - 3D spheroids in Media
AKT - protein kinase B
B2M - Beta-2-microglobulin
BC - breast cancer
BFP - blue fluorescent protein
BRCA1 - Breast cancer type 1 susceptibility
CDE - cancer derived exosomes
DCIS - ductal carcinoma in situ
DEGs - differentially expressed genes
DOX - doxorubicin
ECM - extracellular matrix
EMT - epithelial to mesechymal transition
EV - extracellular vesicle
EV2D - ex vivo monolayer
EV3D - ex vivo spheroid
FACS - fluorescently activate cell sorting
FDR - false discovery rate
GEMM - genetic engineered mouse model
GO - gene ontology
HR- hormone respetor
IDC - invasive ductal carcinoma
lincRNA - long non-coding RNA
MAPK - mitogen-activated protein kinase
MDSC - myeloid derived supressor cells
MFP - mammary fat pad
miRNA - micro RNA
NK - natural killer
NKT - natural Killer T
NOG - NOD.Cg-PrkdcscidIl2rgtm1Sug/ShiJic
NSG - NOD.Cg-PrkdcscidIl2rgtm1Wjl/SzJl
PD-1 - programmed cell death-1
PD-L1 - programmed death ligand-1
PDX -patient derived xenograft
PI3K - phosphoinositide 3-kinase
p-Stat1 - phosphorylated Stat1
SBM - sorted Balb/c derived MFP
SBM - Sorted BALB/c Mammary fat pad;
SBS - Sorted BALB/c Subcutaneous;
scRNA-seq - single cell RNA sequencing
SNM - Sorted NSG Mammary fat pad;

snoRNA - small nucleolar RNA

SNS - Sorted NSG Subcutaneous

SQ - subcutaneously

TBM - whole Tumor from BALB/c Mammary fat pad

TBS - whole Tumor from BALB/c Subcutaneous back flank 2D monolayer

TME - tumor microenvironment

TNBC - triple negative breast cancer

VEGFR1 - vascular endothelial growth factor receptor 1

## List of Figures

## List of Tables

## Acknowledgements

The research was supported by LLNL LDRD-19-SI-003, LDRD-17-ER-121, DOD BC151687, and the LLNL Education Assistance Program. This work was conducted under the auspices of the USDOE by LLNL (DE-AC52-07NA27344).

I would like to acknowledge my thesis committee, Dr. Michael Cleary, Dr. Jennifer Manilay, and Dr. Kara McCloskey, for the time and effort invested into my doctoral studies at UC Merced. The guidance and critiques that you have provided me throughout my doctoral education will have lasting effects on my scientific career. I am grateful of your responsiveness and dedication to education that has assuredly improved my scientific skills and prepared me for my post-graduate endeavors.

I am blessed to have too many loved individuals to name but this document and breadth of work would not be possible without the support, encouragement, and motivation derived from my family and friends. Extra gratitude to Breezy, Olivia and Lucas for the constant love and support that has meant the world to me.

To all my LLNL co-workers who have contributed advice and perked up my spirits on the long single-cell sequencing days and listened to my data analysis strife, thank you for getting me through the anguish of biological research to get to see the impact of novel science. In particular, Kelly Martin your constant encouragement, endless proofreading, and most importantly the abundance of coffee and snacks that have fueled my entire graduate experience.

Finally, a very special acknowledgement is devoted to Dr. Gabriela Loots. It has been a privilege to work under your mentorship for over a decade

now from my Master's research culminating in this document and doctorate. We have evolved through numerous personnel and project changes, but our working relationship never faltered and my confidence in your direction only increased over time. I owe so much of my scientific career to your mentorship, direction, and friendship. This accomplishment belongs to us both and deserves its celebration however I am motivated more than ever to get back to work by your side. Thank you Gaby!

## Curriculum Vitae

Nicholas Hum
Biomedical Scientist
Human Health Sciences Group
Biosciences & Biotechnology Division; Physical and Life Sciences Directorate
Lawrence Livermore National Laboratory
925-216-9837
Hum3@llnl.gov

### Professional Preparation

| | | |
|---|---|---|
| University of California, Davis | Microbiology | BS, 2007 |
| California State University, East Bay | Biology | MS, 2011 |
| University of California, Merced | Quantitative & Systems Biology | PhD, 2021 |

### Professional Experience

2008-2009 Research Associate; Biolog Inc, Hayward, CA
2010-2011 Graduate Researcher; BBTD/PLS, LLNL, Livermore CA
2011-pres Biomedical Scientist; BBTD/PLS, LLNL, Livermore CA

### Research Experience

**UC Merced Quantitative & Systems Biology, Merced, CA**
**Doctoral Graduate Student, January 2018 – Present**

- Conception, execution, analysis, and presentation of the following cancer projects in support of Elizabeth Wheeler's "Engineered and Instrumented Three-Dimensional Tumor-Immune Model System" strategic initiative LDRD funded project (19-SI-003).
- Assessment of molecular shifts in cancer cell behavior as a result of altered culturing conditions.
- Characterize tumor stromal cell subtypes in response to cytotoxic chemotherapeutics.
- Optimization of *ex vivo* tumor culturing platform utilizing multiomic based analytics for recapitulation of *in vivo* tumor behavior

**Lawrence Livermore National Laboratory, BBTD/PLS, LLNL, Livermore CA**
**Biomedical Scientist, June 2011 – Present**

- Primary technical lead on multiple projects focused on cancer including:
- Identification and impact of tumor heterogeneity
- Examination of extracellular vesicle cargo and trafficking characterization
- Analysis of transcriptional and translational regulation underlying prostate cancer metastasis in bone
- Development of novel *in vivo* metastasis assays
- Senior technical expert single-cell sequencing, nucleic acid sequencing, flow cytometry, cell based assays, small rodent imaging, and cancer research
- Analysis of genomic response *in vivo* and *in vitro* in bone and joint related disease
- Mentor to numerous interns, graduate students, and post-doctoral researchers
- Generation of internal and external grant applications in collaboration with LLNL and external co-investigators as well as a Principal Investigator

**Master's Research, January 2010 – June 2011**

- Performed all work on thesis project entitled "Functional analysis of conserved cis-acting enhancer elements for tissue specific regulation and significance in vertebrate evolution"
- Optimization and execution of frog (Xenopus) transgenic enhancer assay
- Testing predicted enhancer regions for tissue specific enhancer abilities
- Performing various molecular biology techniques with chicken, mouse, and frog specimens including whole mount in situ hybridizations, plasmid creation, cloning, and PCR
- Frog *in vitro* fertilization and microinjection of fertilized embryos
  See less

**Biolog Inc, Hayward, CA**
**Research Assistant, January 2008 – November 2009**

- Setup, execute, troubleshoot, analyze, and report phenotype microarray (PM) experiments
  - Including work on numerous species of microbes under differing conditions (temperature, incubation time, culture technique, anaerobic preparation)
- Develop new antibiotic sensitivity plates for fungal PM
- Maintain database of microbial customers, strains, and assays
- Aid in protocol, assay, product, and software development for PM

**IDEXX Laboratories, West Sacramento, CA**
**Microbiology Clinical Laboratory Technician, April 2007 – August 2007**

- Operate bioMerieux Vitek machine
- Setup Kirby Bauer antibiotic plates, BBL Crystal and API Identification systems
- Perform weekly and monthly laboratory quality control tests

**Teaching Experience**

Spring 2018 Teaching assistant, Nutrition

**Select Poster Presentations**

1. **Hum NR,** Sebastian A, Gilmore SF, Gravano DM, Rios-Arce ND, Martin KA, Wheeler EK, Coleman MA, Loots GG. Single cell transcriptomics of triple negative breast cancer allografts following chemotherapy treatment reveals increased T cell abundance in doxorubicin-sensitive tumorsAACR Virtual Special Conference: Tumor Immunology and Immunotherapy; October 19-20, 2020. Poster PO065
2. **Hum NR**, Martin KA, Sebastian A, Wheeler EK, Coleman MA, Loots GG. Epithelial-mesenchymal hybrid population changes from monolayer, spheroid, and tumoroid *ex vivo* culture of syngeneic murine mammary tumors. American Association for Cancer Research 2020. Poster 2810
3. **Hum NR,** Sebastian A, Gilmore SF, Wheeler EK, Coleman MA, Loots GG. Characterization of the tumor microenvironment using single cell transcriptomics of triple negative breast cancer allografts treated with doxorubicin. American Association for Cancer Research 2019. Abstract 130
4. **Hum NR,** Sebastian A, He W, Moya ML, Hynes WF, Adorno JJ, Hinckley A, Wheeler EK, Coleman MA, Loots GG. RNA-seq comparisons of *in vitro* and *in vivo* cancer model platforms: Monolayer, spheroids, immunodeficient, and syngeneic mouse model. American Association for Cancer Research 2019. Abstract 37
5. **Hum NR**, He W, Sebastian A, Wheeler EK, Coleman MA, Loots GG. Determining gene expression variability between *in vitro* and *in vivo* cancer models: Monolayer, spheroids, and mouse allografts. American Association for Cancer Research 2018. Abstract 2528
6. **Hum NR**, Martin KA, Sebastian A, Loots GG. Transcriptome Analysis Of Osteoblasts Fused With Cancer-Derived Exosomes. American Association for Cancer Research 2018. Abstract 7985

7. **Hum NR**, Martin KA, Malfatti M, Haack K, Buchholz BA, Loots GG. Tracking cancer colonization in xenografts using ultrasensitive accelerator mass spectrometry methods. American Association for Cancer Research 2017. Abstract 5791

## Selected Publications

Full list of publications can be found at the following link: https://www.ncbi.nlm.nih.gov/sites/myncbi/1F7Xg4Pmf6gQf/bibliography/45815671/public/?sort=date&direction=ascending

1. **Hum NR,** Sebastian A, Gilmore SF, He W, Martin KA, Hinckley A, Dubbin KR, Moya ML, Wheeler EK, Coleman MA, Loots GG. Comparative Molecular Analysis of Cancer Behavior Cultured *In Vitro*, *In Vivo*, and *Ex Vivo*. Cancers (Basel). 2020 Mar 14;12(3). doi: 10.3390/cancers12030690. PubMed PMID: 32183351.
2. Zhu K, **Hum NR**, Reid B, Sun Q, Loots GG, Zhao M. Electric Fields at Breast Cancer and Cancer Cell Collective Galvanotaxis. Sci Rep. 2020 May 26;10(1):8712. doi: 10.1038/s41598-020-65566-0. PubMed PMID: 32457381; PubMed Central PMCID: PMC7250931.
3. Martin KA, **Hum NR**, Sebastian A, He W, Siddiqui S, Ghosh PM, Pan CX, de Vere White R, Loots GG. Methionine Adenosyltransferase 1a (MAT1A) Enhances Cell Survival During Chemotherapy Treatment and is Associated with Drug Resistance in Bladder Cancer PDX Mice. Int J Mol Sci. 2019 Oct 9;20(20). doi: 10.3390/ijms20204983. PubMed PMID: 31600961; PubMed Central PMCID: PMC6829260.
4. **Hum NR,** Sebastian A, Gilmore SF, He W, Martin KA, Hinckley A, Dubbin KR, Moya ML, Wheeler EK, Coleman MA, Loots GG. Comparative Molecular Analysis of Cancer Behavior Cultured *In Vitro*, *In Vivo*, and *Ex Vivo*. Cancers (Basel). 2020 Mar 14;12(3). doi: 10.3390/cancers12030690. PubMed PMID: 32183351.
5. Martin KA, **Hum NR**, Sebastian A, He W, Siddiqui S, Ghosh PM, Pan CX, de Vere White R, Loots GG. Methionine Adenosyltransferase 1a (MAT1A) Enhances Cell Survival During Chemotherapy Treatment and is Associated with Drug Resistance in Bladder Cancer PDX Mice. Int J Mol Sci. 2019 Oct 9;20(20). doi: 10.3390/ijms20204983. PubMed PMID: 31600961; PubMed Central PMCID: PMC6829260.
6. **Hum NR**, Martin KA, Malfatti M, Haack K, Buchholz BA, Loots GG. Tracking Tumor Colonization in Xenograft Mouse Models Using Accelerator Mass Spectrometry. Scientific Reports. 2018; 8:15013.
7. Sebastian A, **Hum NR**, Morfin C, Murugesh DK, Loots GG. Global gene expression analysis identifies Mef2c as a potential player in Wnt16-mediated transcriptional regulation. Gene. 2018;675:312–21.

8. Sebastian A, **Hum NR**, Murugesh DK, Hatsell S, Economides AN, Loots GG. Wnt co-receptors Lrp5 and Lrp6 differentially mediate Wnt3a signaling in osteoblasts. Kim J-E, editor. PLoS ONE. Public Library of Science; 2017;12:e0188264.
9. Sebastian A, **Hum NR**, Hudson BD, Loots GG. Cancer-Osteoblast Interaction Reduces Sost Expression in Osteoblasts and Up-Regulates lncRNA MALAT1 in Prostate Cancer. Microarrays (Basel). Multidisciplinary Digital Publishing Institute; 2015;4:503–19.
10. Hudson BD, **Hum NR**, Thomas CB, Kohlgruber A, Sebastian A, Collette NM, et al. SOST Inhibits Prostate Cancer Invasion. Languino LR, editor. PLoS ONE. Public Library of Science; 2015;10:e0142058.

## Abstract

Breast cancer is the most common cancer in women and 1 in 8 women nationally will develop this disease in their lifetime. Preclinical cancer models have driven novel therapeutic regimens over the last half century yielding progressively improved survival yet 95% of new anticancer drugs will fail in clinical trials and greater than 42,000 people will still succumb to this disease per year. This research focuses on characterization of triple negative breast cancer (TNBC), a clinically difficult form of breast cancer characterized by lack of targetable receptors, advanced diagnosis, and increased aggressiveness, towards identification of current limitations and future direction for optimized preclinical models.

Transcriptional profiling of 4T1, a murine TNBC cell line, at the bulk and single cell level were utilized to culture induced alterations of tumor cells cultured in vitro, in vivo, and ex vivo. Flow cytometric analysis was also used to validate and further the molecular alterations imparted on cancer cells. Furthermore, proteomic and transcriptomic analysis of cancer derived exosomes was performed to identify biomarkers of cancer behavior.

I was able to identify in vitro culturing induced behavioral bias towards proliferative behavior while in vivo conditions favored cell signaling and cancer progressive biological processes such as a transition from epithelial to mesenchymal cell states. Non-cancer stromal cells were also proven to be an essential component for clinical cancer behavior recapitulation in vitro. This key finding was then followed by examination of heterogenous ex vivo tumor cell cultures utilizing numerous culturing techniques finding that retention of not only tumor cell populations, but spatial organization and extracellular matrix composition retention is optimal for native cancer behavior recapitulations. Additionally, TNBC stromal cell effects on chemotherapeutic sensitivity were found to play a significant role towards inhibiting tumor

growth. IL17A secreted from γδ T cells are capable of increasing cancer cell sensitivity to Doxorubicin and increased efficacy of antitumor cytotoxic T cell populations. Furthermore, human cancer exosomes derived from cultured cells discovered putative biomarkers of cancer subtypes that were validated with clinical data sets to identify 2 exosomal miRNA (hsa-mir-375, hsa-mir-138-1) and 2 protein biomarkers (FBP1, HLA-A) were found to correlate to breast cancer subtype and aggressiveness.

In summation, the tumor microenvironment is a complex and dynamic tissue to recapitulate under in vitro conditions, multiple effects and approaches have been identified in this work to serve as a basis for future pre-clinical approaches.

# Chapter 1. Introduction

According to the World Health Organization, cancer remains a leading cause of death before the age of 70 and predicts that the incidence, mortality, and financial burden of cancer will continue to increase globally over the next decade (1). It is estimated that over 1.8 million new cases of cancer will be diagnosed in the United States and the rate of cancer remains high with an estimate that ~39.5% of the US population will be diagnosed with some form of cancer in their lifetime based on 2015-2017 data. While advances in basic cancer research, diagnostics, and therapeutics have decreased the death rates on average 1.7% each year over 2009-2018, some cancer types are still on the rise, and more than 600,000 people will still succumb to the disease where the 5-year relative survival rate is still only 67.4% (based on 2010-2016 data) (2). Biomedical advances facilitated by cancer research to have significantly contributed to reducing mortality of this huge public health burden, yet many challenges remain and more thorough characterizations of the dynamic nature of cancer biology will undoubtedly aide in the continuing improvement in survivability of this disease.

## 1.1 Breast cancer

### 1.1a Incidence and burden

Nationally and globally, breast cancer (BC) is the most common cancer among women and the second most common amongst all cancers. Since 2008, the incidence of BC has increased by 20% and the mortality has increased by 14%, worldwide (3). In 2018 alone, ~2 million new cases of BC were diagnosed worldwide, of which 276,480 were in the United States (2). The incidence of BC varies regionally, with higher rates in high-income countries (92 per 100,000 in North America) than in low-income ones (27 per 100,000 in middle Africa and eastern Asia) (4). These patterns reflect heterogeneity in risk factors and access to healthcare and preventative measures like routine mammograms

(and, therefore, detected breast cancers); but since the highest breast cancer incidences occur in North America, Australia, New Zealand and northern and western Europe, it could also be attributed to overdiagnosis and socioeconomics, where developed countries have new environmental factors contributing to BC that may not exist in countries that less industrialized. New BC cases are expected in 2020 with an associated cost burden of ~$158 billion based on 2018 breast cancer cost estimated at $19.3 billion (5). While numerous studies have implicated both genetic and environmental factors driving the high incidence and lethality, this global challenge has proven to be a heterogenous disease manifesting in different regions of the breast and driven by a complex combination of molecular drivers.

### 1.1b Origins of breast cancer

Breast tissue is an apocrine gland that can produce milk in response to hormones. It is primarily composed of subcutaneous fat and connective tissue surrounding a network of ducts that converge at the nipple. Throughout development the breast responds to complex interactions with hormones including estrogens, progesterone, and growth hormones mediating major developmental events (6,7). Cells residing in breast tissue possess specific receptors for these hormones that respond to influxes during puberty while lactation is induced during pregnancy. During menopause decreased hormonal levels induce glandular tissue atrophy (8).

While it remains unclear the exact mechanism of BC initiation, current evidence suggests that BC develops and evolves in two divergent pathways. The first pathway is characterized by mutations on chromosomes 1q, 16q, and sometimes the chromosomal region 17q12 (containing ERBB2, encoding HER2) and a gene expression signature with most genes associated with the hormone receptor phenotype. The second pathway identified is characterized by mutations on chromosome 11, region 11q13, and amplification of 17c12

region with an expression signature comprised of genes involving cell cycle and proliferation (9).

Once initiated in the normal epithelium of the breast, BC matures into progressive stages of disease. First a flat epithelial atypia develops in the mammary epithelium followed by atypical ductal hyperplasia characterized as a proliferative lesion that have some, but not all, of the architectural and cytologic features of low-grade ductal carcinoma in situ (DCIS) (10). This can progress into a DCIS as the abnormal accumulation of epithelial cells in the duct increases in abundance which can in turn culminate in an invasive ductal carcinoma (IDC)(11). DCIS is an early-stage, non-invasive form of BC characterized by the retention of cancerous cells in the milk duct and no evidence of spread into the surrounding breast tissue. In 2019, 48,100 US women were diagnosed with DCIS and surgical resection is considered the most effective treatment prescribed therapy at this early stage of the disease. If untreated or resected, DCIS tumors can progress into IDC, a more life threatening, malignant form of the cancer, where the cancerous cells have escaped the wall of the ducts and invaded the surrounding breast tissue. In 2019, 85% (268,600 patients) of BC cases in the US were diagnosed at this stage (2).

### 1.2 Breast cancer diagnosis and subtype classification

#### 1.2a Clinical Diagnosis

The diagnosis of BC encompasses a combination of physical and pathological assessments. A clinical examination is first conducted utilizing a bimanual palpation of the breasts and lymph nodes. If unusual masses are detected in either tissue, a core needle biopsy is extracted and assessed via pathology to identify disease grade and classification based on histological and molecular assessment of cellular morphology, immune infiltration and identification of specific molecules such as hormone receptors. Mammography

using low dose radiation is also utilized to analyze the prevalence of tumors throughout the breast tissue. Additionally, potential sites of metastasis are also examined to assess the extent of the disease spread beyond the breast tissue. This diagnosis includes needle-biopsy of draining lymph nodes, chest X-ray to search for lung metastasis, in addition to CT scans to examine bone density disruption induced by bone metastasis. Based on this initial diagnosis BC is then binned into subtypes that will dictate therapeutic options and prognosis.

### 1.2b HR and HER2 positive breast cancers

The dysfunction of hormone receptors in breast epithelial cells are significant driving factors in most BC patients and clinical classification of BC is associated with characterization of the presence or absence of three key hormone receptors: estrogen receptor, progesterone receptor, and HER-2. Hormone receptors (HRs) encompass estrogen and progesterone receptors. The imbalance of these hormones during menstrual cycles triggers enhanced cell proliferation in regions of the breast (12). In turn, the proliferative cycling of breast cells may cause the accumulation of oncogenic mutations over time. At this stage in HR positive BCs, estrogen can stimulate pre-malignant cells through its binding to the estrogen receptor (a ligand-activated transcription factor) in the nucleus where it can modulate the transcription of genes through interaction with estrogen response elements found in the promoter regions of target genes (13).

ERBB2 is amplified in 13–15% of breast cancers, causing an activation of the HER2 pathway(14). HER2 is a member of the human epidermal growth factor family capable of activating different pathways such as the RAS pathway and the phosphoinositide 3-kinase (PI3K)–protein kinase B (AKT)–mitogen-activated protein kinase (MAPK) pathway. This activation can result in increased proliferation, cell survival, metastasis and adhesion in BC (15).

Most breast cancer cases are positive for HR. Nationally, the predominant subtype of BC is HR positive and negative for HER-2 receptor (also referred to as a Luminal tumor) accounting for 68% of BC and 4% are HR positive and HER-2 positive. Tumors negative for HR and positive HER-2 account for 10% of diagnosed BC (or non-luminal). Furthermore, BC tumors lacking both HR and HER-2 (TNBC or Basal) account for 10-15% of BC cases (16).

Progression of disease is also a critical measurement in clinical evaluation and is based on localization of cancer cells and morphology of the tumor. Invasive BC is further subcategorized according to disease progression. The American Joint Committee on Cancer has standardized a staging system (TNM system) to characterize cancer progression based on size and/or extent of the primary tumor [T1 (smallest)-T4 (largest)] in addition to metastatic progression first in the draining lymph nodes (N1 (minimal cancer presence) - (N3 (high incidence of cancer cells)) then in other distant tissues (M1). Most cases of invasive BC will have some type of surgical removal of the tumor. Depending on the type of BC and how advanced it is other pre and postoperative treatment options can also be utilized for invasive BC cases, which will be discussed later.

Genetic profiling tests, such as MammaPrint (17) and Oncotype DX (18), that analyze transcriptional levels of genes linked to treatment efficacy and prognosis are also available for further molecular characterization of cancer genotypes. These genomic characterizations improve personalized treatment selection and disease prognosis however this is not a prevalent diagnostic tool in a clinical setting. Somatic mutation burden has been analyzed in a research setting on BC subtypes as it relates to oncogenic driver mutations. In a study, whole genome DNA sequencing performed on 530 tumors revealed that the most frequently mutated and/or amplified genes in BC cells are *TP53* (41% of

tumors), *PIK3CA* (30%), *MYC* (20%), *PTEN* (16%), *CCND1* (16%), *ERBB2* (13%), *FGFR1* (11%) and *GATA3* (10%) (19). With HR positive tumors showing increased frequency of mutations in *PIK3CA*, *CCND1*, and *GATA3* relative to HR negative tumors. HR negative tumors show increased abundance of oncogenic mutations in *TP53*, *MYC*, *PTEN*, and *RB1* driver genes (6). The differential preference for oncogenic driver genes provides evidence that the genetic drivers of the cancer cells may play a critical role in BC tumor phenotype, classification, and prognosis.

### 1.2c Triple negative breast cancer (TNBC)

Globally, TNBC accounts for up to 15% of all breast cancers and~20% of invasive breast cancer (20). Additionally, this subtype of BC has been associated with younger diagnosis age, familial history of BC, carrying mutations in breast cancer type I susceptibility gene (*BRCA1*) and is more common among specific ethnic groups, such as Latin and African women (21–24). Moreover, this subtype has been characterized with increased growth rates and metastasis, and shorter overall relapse-free survival when compared to other breast cancer subtypes (6). Patients with TNBC also present more advanced stage disease progression at the time of diagnosis with detectable cancer in the lymph nodes and larger primary tumor size. TNBC is also characterized by aggressive behavior due to increased correlation to metastatic spread to the lung, liver, and central nervous system in addition to early relapse. Within 5 years of diagnosis, TNBC patients have the highest morality when compared to other BC subtypes (hazard ratio, 3.2; 95% confidence interval, 2.3-4.5; $P < 0.001$) however the long-term prognosis does not show significant differences (25).

The absence of targetable oncogenic driving receptors makes this BC subtype especially difficult to treat with targeted therapy and most patients are treated with nonspecific chemotherapy. Patients exhibit diverse response

rates either to traditional treatments or to new targeted therapies, often leading to discrepant times of survival. The diverse response rates observed in response to traditional therapies or to new targeted treatments leading to varied times of survival in TNBC clinical trials has been widely attributed to the heterogeneity of this subtype of BC (26). TNBC is not a unique disease possessing wide heterogeneity in histopathological, transcriptomic, and genomic levels of characterizations.

### 1.3 Tumor microenvironment

BC is a remarkably heterogeneous disease not only in terms of subtypes and oncogenic drivers but in the stromal composition of the tumor microenvironment. The majority of BC stromal cells, benign tumor residing cells, are comprised of a myriad of immune cells (including lymphocytes, macrophages, and myeloid derived suppressor cells), cancer associated fibroblasts, and endothelial cells. These cells have multiple functions that can both inhibit and encourage cancer progression through dynamic interactions with BC cells.

#### 1.3a Immune component

Immunogenicity of BC varies by subtype with TNBC and HER2-positive having the highest relative abundance and HR positive subtypes having the lowest relative abundance of immune infiltrate (27,28). BC tumors can contain both innate and adaptive immune components that impart pro- and anti-tumor abilities depending on cellular composition and condition of the microenvironment (29). The current understanding of immune cells residing in BC tumors results in increased $CD8^+$ T cells, $CD4^+$ Th1 cells, natural killer (NK) cells, B cells, M1 macrophages, and dendritic cells result in an anti-tumor effects. Conversely, $CD4^+$ Th2 cells, regulatory B cells, $CD4^+$ regulatory T cells, myeloid-derived suppressor cells, and M2 macrophages contribute to pro-tumorigenic behavior (30–33).

In early stages of cancer development, malignant cells are detected and killed by the innate immune system (Natural Killer T (NKT), NKT, NK, γδ T cells, macrophages, and dendritic cells)(34). These early phases of carcinogenesis possess largely anti-tumor activity with an abundance of cytokines secreted into the tumor microenvironment from activated $CD8^+$ and $CD4^+$ T cells (35). However, this immune pressure is also believed to select for specific mutations with immune-evasive phenotypes, contributing to the development of more aggressive cancer phenotypes (36).

The failure of immune-mediated cancer control at early stages of the disease results in the progression of the tumor. As BC becomes more invasive, the cytokine and cellular composition shifts towards a more pro-tumor behavior. Malignant cells can induce suppression of the immune response by expressing immune checkpoint regulators (CTLA-4 and PD-1) which are upregulated by T cells because of chronic exposure to tumor antigens (37). Additionally, pro-tumor immunosuppressive cells like T regulatory cells and myeloid-derived stromal cells are also recruited into the tumor microenvironment and aid in reducing the activity of $CD4^+$ and $CD8^+$ T cells (38). Furthermore, reduction in MHC I levels and increased production costimulatory molecules that suppress the immune system (IL10, TGF-B, CCL2), which enables them to further avoid recognition by the immune system (39).

### 1.3b Non-immune component

Non-immune stromal cells are also recruited into the tumor. These cells perform multiple functions critical to tumor progression including generation of extracellular matrix (ECM), vascularization, and recruitment of immune and non-immune stromal cells into the tumor microenvironment (40). Cancer associated fibroblasts (CAF) and endothelial cells represent most non-immune stromal populations found in the tumor yet other cell types like adipocytes,

pericytes, and mesenchymal stem cells also occupy the tumor microenvironment and play roles in tumor progression (40–43).

CAF populations maintain the homeostasis of the ECM through secretion and assembly of fibrotic ECM proteins (collagens, fibronectin, lysyl oxidase, hyaluronan laminins) for structural integrity of the tumor and allowing for adhesion of cancer cells as well as ECM degradation proteins (MMPs and transglutaminase) promoting cancer motility (44). Interestingly, CAFs adopt an activated state in tumors with upregulation of alpha-smooth muscle actin, fibroblast activating protein, and matrix metalloproteinases as opposed to fibroblasts found in normal tissues (45).

Like CAFs, endothelial cells are activated in the tumor microenvironment to support tumor growth and invasion. Activated endothelial cells have been shown to transition into a more mesenchymal state in the presence of cancer derived TGF-beta and adopt a more fibroblast-like behavior as exhibited by downregulation of CD31 and upregulation of Fsp1 (46). Furthermore, endothelial cells aide in metastasis by chaperoning and protecting extravasated tumor cells from anoikis in circulation (47). As shown, stromal cells in the tumor microenvironment play a major role in progression or eradication of tumors. This emphasizes the importance of BC research inclusive of the native cellular heterogeneity and may contribute to the identification of novel therapeutic targets.

### 1.4 Breast cancer therapies

#### 1.4a HR and HER2 positive breast cancer therapies

Standard of care treatments for BC is dependent on stage of the disease and subtype classification. Early-stage BC is most likely to be treated surgically by removal of the tumor regardless of subtype, followed by post-operative therapy in the form of radiation and/or systemic chemotherapy depending. The post-operative treatment usually depends on the tumor

subtype and level of progression at the time of diagnosis. Advanced invasive BC poses more complications due to the inoperable state of cancer burden on not only the breast but metastasized tissues. BC patients at advanced stages of disease are much more difficult to treat but will still be administered systemic treatments of radiation and chemotherapeutics. Increased monitoring of response to therapy with imaging is also recommended to guide personalized treatments for each BC patient. Patients with late-stage invasive BC receive therapies aimed at prolonging quality of life as this form of BC is treatable but virtually incurable with a median overall survival of 2–3 years caused by metastases in nearly all patients (48).

Standard therapies for HR positive, the predominate subtype of BC, regardless of stage, include at least a 5-year treatment with endocrine based chemotherapy with tamoxifen, a selective estrogen receptor modulator, acting as an agonist to the estrogen receptor activation in cancer cells. HER2 positive BC standard of care is an anti-HER2 therapy (trastuzumab and/or pertuzumab) with systemic chemotherapy with an anthracycline-taxane sequence for 1-year (49,50). Following standard therapeutic regimens, BC will be reassessed and addressed on a per case basis to evaluate response to therapy and its effects on disease progression.

More personalized therapeutic options have emerged in the last decade. Oncogenic driving pathways, including PIK3CA, mTOR, and AKT, have been identified in BC subtypes and offer targetable biological processes (51). Current FDA approvals for these treatments are limited to defined subtypes in advanced stages however clinical trials are ongoing to evaluate therapeutic value for additional BC subtypes (52). Treatment options are rapidly evolving with the hope that in the not-too-distant future, more effective targeted treatments will come on the market.

### 1.4b Therapeutic options for TNBC

Due to the lack of targetable receptors driving the disease, TNBC is especially challenging to treat with very few effective therapies available. TNBC is insensitive to hormone therapy and typical treatments are limited to a combination of surgery, radiation, and systemic chemotherapy depending on genetic drivers and disease progression status. Late stage TNBC patients are faced with very poor prognosis with just a 15% to 20% response rate and a median progression-free survival of 4.2 months (53,54). Regardless of BC status, systemic non-specific cytotoxic chemotherapy remains the recommended therapeutic option with no clinically significant difference in efficacy when utilized in a neoadjuvant (prior to surgical intervention) or an adjuvant (post-surgery) administration (55). Neoadjuvant administration of chemotherapy is preferred as it allows for assessment of treatment efficacy and optimization of therapy on the primary tumor in an effort to predict post-operative treatment response in case of residual disease.

In TNBC, standard chemotherapeutic therapy is comprised of an anthracycline (doxorubicin, daunorubicin, epirubicin) and a taxane (paclitaxel, docetaxel) in sequence to avoid excessive toxicity(56). Anthracyclines have numerous mechanisms of actions to eradicate BC including inhibition of topoisomerase II, DNA intercalation, and generation of reactive oxygen species. Taxane based chemotherapies function through stabilization of microtubule assemblies thus blocking mitotic progression and chronic activation of the spindle assembly checkpoint followed by induction of apoptosis (57). This combinatorial therapy does have limitations to specific TNBC subtypes. For example, BC containing p53 mutations have shown increased resistance to anthracyclines (58) as well as multidrug chemotherapy resistance imparted by upregulation of ATP-binding cassette transporters in TNBC (59).

Despite these standard chemotherapeutic options, TNBC remains a difficult to treat BC subtype associated with poor prognosis and as a result alternative therapeutic regimens are continuously being explored and utilized in TNBC subtypes. For example, the use of docetaxel and cyclophosphamide has proven to be an effective therapy for cases where anthracyclines need to be avoided. Adding a platinum-based agent (cisplatin, oxaliplatin) to standard chemotherapeutics has also shown increased efficacy on TNBC, specifically in TNBC patients harboring *BRCA1/2* mutations, due to the high prevalence of DNA repair pathway defects (60,61). The dependence of TNBC containing BRCA mutations on DNA repair function are additionally being exploited using poly (ADP-ribose) polymerase (PARP) inhibitors (Olaparib) as a promising neoadjuvant (62). Augmentation of dosing scheduling and concentration is also an attractive option to increase efficacy of treatment for TNBC due its more aggressive and highly proliferative nature however dose dense strategies have yet to show consistent advantages for progression free survival or long-term outcomes (63). No single therapy has proven universally effective for TNBC which may be linked to the disease heterogeneity with therapeutic innovation focused on more personalized approaches to identify TNBC subtype dependencies and treatment escalation regimens (6).

### 1.4c Stromal cell mediated therapy

In recent years, immunotherapy is transforming the cancer therapeutic landscape through exploitation of the recognition and cell-mediated toxicity the immune system has for malignant cells. Clinical data has revealed that some BC subtypes in advanced metastatic stages with increased inflammatory signaling are responsive to programmed cell death-1/programmed death ligand-1 (PD-1/PD-L1) antagonists (64). Specifically, prolonged response has been observed in TNBC patients treated with atezolizumab (anti-PD-L1) and pembrolizumab (anti-PD-1)(65). PD-1/PD-L1 inhibition are leading candidates for alterations in stromal populations induction of cancer clearance yet several

other therapeutics targeting non-malignant cells are undergoing clinical evaluations (66–68)

### 1.5 Breast cancer culturing methodologies

Despite thorough development and analysis of BC and its associated therapeutic options, modern understanding of BC is still unable to deconvolute the disease heterogeneity resulting retention of high mortality incidence and the necessity of chronic observation for disease relapse. Preclinical BC research remains an essential tool in combating this global health burden, and the ability to culture BC *in vitro* and *in vivo* has proven a critical barrier in advancing our understanding of this disease. Only ~5% of new cancer drugs reach FDA approval due mostly to lack of efficacy in the clinic despite promising preclinical results. This failure imparts a large burden financially and on the quality of human life of BC patients. Improved BC culturing approaches will prove to be an invaluable tool in advancing therapeutics and predicting successful clinical outcomes. Here I will review current culturing methodologies for BC propagation.

#### 1.5a *In vitro* breast cancer approaches

The challenges and time-consuming nature of *in vivo* work has classically been circumvented and supplemented with *in vitro* models performed using 2-dimensional (2D) culturing in which cancer cells adhere as a monolayer to an inert substrate. Conventional *in vitro* 2D culture of human cancer cell lines has been fundamental in the study of cancer biology as well as for screening and evaluating therapeutic efficacies of anticancer agents. This approach promotes fast growth, ample area to adhere to substrates, and uniform access to nutrients and growth factors. Overall, 2D cancer models generate highly reproducible results, but lack the complexity of the cellular and extracellular matrix associated with solid tumors (3).

Techniques and tools have improved by moving from 2D cell culture to 3-dimensional (3D) culture platforms capable of generating spheroids, organoids, or cultures suspended in ECM. The increased complexity in cell-to-cell contact, necessity for ECM generation, and spatial organization of cells are thought to mimic the native tumor environment more accurately. These methods encourage cancer cells to more tightly attach to other cancer cells, other cell types, and the ECM to form tissue-like structures (69,70). Research has also shown that 3D grown cancer cells also display a hypoxic core thus facilitating the necessity for angiogenesis for larger 3D cultures (71). The resulting decreased external surface area of spheroids and organoids results in diffusion gradients of nutrients and drugs through the culture (72). This phenomenon is evident in decreased drug efficacy and enhanced cellular heterogeneity (73), characteristics usually noted for the resected tumor from which these cells originate. Yet these culture methods currently fail to incorporate the complex heterogeneous cell composition and transient fluxes in nutrients or drugs that occur *in vivo*.

The incorporation of the heterogenous cellular composition of tumors is a rapidly advancing field in cancer research. Several methodologies have been developed to include increased complexity of cancer cultures. The simplest of these methods is indirect contact with stromal components by replacing of culture media with stromal-preconditioned media containing secreted biomolecules. Exposing cancer cells to live stromal cells builds upon this premise and allows for the bi-directional dynamic cell-cell communication to occur (74). This co-culture technique has been demonstrated with cancer cells physically separated using a porous barrier like a transwell insert or in direct physical contact in the same culture medium (75). This co-culture approach is the basis for numerous culturing technologies with a multitude of combinations of cellular compositions and culturing substrates developed

specifically for cancer applications (76–78). Even the most complex of cellular formulations has limitations on the spatial organization of a tumor. *Ex vivo* organ/organoid cultures have also been implemented to retain the architecture of tumor residing cells however increasing complexity also includes the necessity for complex fluxes in nutrient accessibility found *in vivo* (79,80). While inclusion of complexity (dimensionality, cellular composition, culturing substrate, and media composition) into *in vitro* models has proven to be an improvement upon classic approaches, the need for continued development to continue to improve these pre-clinical *in vitro* platforms remains, and we have yet to fully mimic the comprehensive behavior of human tumors, *ex vivo* .

### 1.5b *In vivo* breast cancer culturing approaches

While *in vitro* pre-clinical models are improving as increased complexity is being incorporated into culturing conditions, the most faithful surrogates of human disease are still cancer cells derived from live tumor. Laboratory mice have classically been utilized for this research with three main models (patient derived xenografts, allografts of mouse derived cancer cells, and genetically engineered mouse models) routinely utilized in for pre-clinical tumor modeling. *In vivo* cultured cancer cells best recapitulate the dynamic nature of tumors and complex interactions with non-malignant cells.

Patient derived xenografts (PDX) have been increasingly used to expand our understanding of factors affecting tumor growth, drug response and metastasis (9); however, the absence of a complete immune system allows human tumors to evolve in a murine-specific manner (81). PDX are generated by this direct transfer of human tumors into genetically induced immunodeficient mice. The absence of a competent immune system eliminates the rejection of foreign cells induced by immunogenicity of the foreign tissue (82). Three commonly used mouse lines for PDX include non-obese diabetic (NOD)-scid, NOD.Cg-Prkdc$^{scid}$Il2rg$^{tm1Wjl}$/SzJl (NSG), or NOD.Cg-

Prkdc$^{scid}$Il2rg$^{tm1Sug}$/ShiJic (NOG) mice and function through the inhibition of T, B, and NK cell maturation and prevention of cytokine signaling required for differentiation and function in many hematopoietic cells (83)-(84). PDXs are continuously maintained by passaging from mouse to mouse. PDX models have been shown to maintain the patient tumors features such as oncogenic driving mutations and drug (85). However, PDX models cannot completely predict drug efficacy because they lack stromal contributions and spatial organization found in the original tumor microenvironment. In recent years, next generation PDX models with transplanted human hematopoietic stem cells have been utilized to incorporate a human immune component into growing tumors with promising results in recapitulating immunotherapy based anti-cancer therapies yet this technique is a time, cost, and labor-intensive approach (80–82).

Allograft rodent models follow a similar inoculation of cancer cells into host animals yet utilize mouse derived cancer cell lines transplanted into immune-competent host animals. This methodology allows for the study of tumor interactions with the immune system without the immunogenicity induced by foreign human cells (86). Due to a complete complement of stromal cells in the TME, allograft models are critical for immune-oncology research and considered to be the most native environment for cancer cell culturing. However, the allograft approach still poses some limitations including the strong selection process for first expanding cell lines *in vitro*. While it is known that these cells maintain their cell type of origin signature and malignant phenotypes (87)-(88) the clonal nature of the resulting mouse cancer cell lines often lack the heterogenic behavior and therapeutic response observed clinically. Furthermore, species specific variability including immune responses absent in humans and altered drug metabolism still hinders complete clinical recapitulation (89).

Genetic engineered mouse models (GEMM) (e.g., MMTV-PyMT(90))are an additional well utilized *in vivo* preclinical model in which transgenic constructs are introduced into the mouse genome to promote well-defined tumorigenesis. Multiple BC GEMMs have been engineered with spatial/cell type specific control of the oncogenic alleles utilizing tissue specific promoter regions driving the transgenes which then allows for orthotopic generation of tumors without the need for invasive introduction of cancer cells (91,92). Temporal control is also often designed to be inducible and/or constitutively active mutant alleles (93) with introduction of inducible expression systems like tetracycline controlled or estrogen receptor-controlled activation. An additional advantage of GEMMs is the ability to introduce targeted oncogenic mutations of increased clinical relevance. As a result, many GEMMs of breast cancer have been developed that reflect some of the diversity of genetic lesions seen in human BC (94,95). While these models can initiate tumors in the correct microenvironment with minimal manipulation, this model is not without limitations as well, such as the lack of well-defined transgene expression domains which could result in non-specific activation of oncogenic drivers in turn producing deleterious results and the similarity to human-like tumor behavior in a mouse, even when driven by clinically relevant oncogenes, needs to be analyzed for each GEMM.

## 1.6 Cell-cell communication via extracellular vesicles

### 1.6a Extracellular vesicle biogenesis

Cancer cells depend on dynamic signaling to each other and stromal cells within the tumor microenvironment as well as throughout the body to expand and allow for disease progression. Extracellular vesicle (EV) secretion is a method of cellular communication of biomaterials encased in a lipid membrane allowing for shuttling of biological compounds typically unstable in the extracellular space. EVs are highly heterogenous in content, size, and method of generation and segregate into several subtypes.

One extracellular vesicle of interest is the exosome. First characterized in 1983 as a waste excretion mechanism of cells (96) further studies have identified the multitude of roles exosomes have in cellular communication. This field has vastly expanded in the last decade due to the technological advances like next generation sequencing and enhanced resolution of microscopy and biomolecule identification. Exosomes are relatively small EVs (30-200nm in diameter, averaging 100nm). A key differentiating factor of exosomes from other EVs is that exosomes are not generated directly from the cell membrane but from the endocytic pathway. This process initiates from the encapsulation of the cell membrane through endocytosis followed by generation of multiple vesicles (intraluminal membrane vesicles [ILV]) inside the endosome. Multiple proteins have been identified to play a role in trafficking of specific biomolecules into these ILVs such as ESCRT proteins and CD63 (97). The biological content or cargo capable of encapsulation into exosomes can include proteins, DNA, mRNA, small non-coding RNAs, and lipids incorporated into the membrane. Additionally, several proteins are also required for exosome secretion such as n-SMase2 and RAB proteins. These multivesicular bodies are then fused back to the cell membrane thus releasing the exosomes into the extracellular space. This unique generation of EVs also imparts specific exterior markers that allow for simpler identification in relation to EVs blebbed off the cell membrane. Exosomal membranes contain increased levels of cholesterol, sphingolipids and phosphatidylserines classically found on the inner side of cell membranes (98). Furthermore, exosomal protein markers (tetraspanins, and MHC molecules) have also been well characterized.

### 1.7b Cancer derived exosomes

The specific intracellular packaging of biomolecules into exosomes and identifiable external markers have promoted exosomal research in numerous diseases including cancer. In breast cancer, numerous studies have

demonstrated that cancer derived exosomes (CDE) affect disease progression tumor and cancer cell homeostasis in the local tumor microenvironment through a wide range of cell types. The dynamic nature of CDE in breast cancer cell has been shown to interact in an autocrine function in signaling to local cancer cells; paracrine effecting stromal cells in the tumor microenvironment; and endocrine aiding in metastasis to distant tissues (28).

CDE can aide in tumor progression in the local tumor microenvironment through delivery of packaged protein and miRNA. The aggressive MDA-MB-231 human cell line has been shown to promote malignancy and increase aggressive cancer phenotypes (invasion, migration, conversion to EMT phenotype) of less aggressive BC or breast epithelial cells in co-cultures and these effects were mediated by exosomes (99–101) Additionally, exosome production can be induced from cellular stress and in turn emerging evidence indicates that therapeutic efficacy is altered via CDE(102). Radiation induced CDE has been previously shown to increase tumor burden, decrease survival and promote radioresistance (103). Furthermore, systemic chemotherapeutics can also induce CDE specific responses by conferring resistance to these drugs through several mechanisms including drug export, transport of drug efflux pumps and miRNAs exchange among cells (104).

The local effects of CDEs have also been shown through modulation of stromal cells. Endothelial cell recruitment and activation in the tumor are prime examples of the stromal effects of CDE. Angiogenesis, the development of intratumoral vasculature, is impacted by cell signaling mediated through Annexin II and miRNAs packaged in exosomes(105). Previous studies have demonstrated that CDE BC patient serum samples are able to increase angiogenesis in *in vitro* and *in vivo* mouse tumors(106),(107). Additionally, CDE can mediate vascular leakiness in endothelial cells to aide cancer cells to enter the circulation and enable their metastasis(108). Furthermore,

modulation of the tumor microenvironment can be mediated through cancer associated fibroblasts which can be stimulated to degrade the extracellular matrix through MMP activity induced by CDE therefore promoting BC invasive and migratory behaviors involved in disease progression(109). The immune component of BC tumors has also been demonstrated to be influenced by CDE. Decreased cell cytotoxicity, increased apoptosis, and decreased proliferation of natural killer, $CD8^+$ and $CD4^+$ T cells has been directly linked to BC exosomal effects (110). Myeloid derived cells are also recipients of CDE. Upon delivery into macrophages, pro-inflammatory tumoral responses are elicited (stimulation of NF-kB; increased M1 to M2 polarization; secretion of IL-6, TNFα GCSF, and CCL2) only through uptake of BC cell lines and not from benign cell lines (111)(112).

The stability and specificity of delivery of CDE is further utilized at distant sites outside the primary tumor to distant sites of metastasis where they can facilitate fertilization of a pre-metastatic niche for subsequent extravasated cancer cells to seed metastatic tumors(113). Studies of CDE and metastasis have identified the principles of exosome-mediated pre metastatic niche formation which includes recruitment of immune cells, education of resident cells, and stromal alterations. An initial description of PMN formation demonstrated that BMDCs expressing vascular endothelial growth factor receptor 1 (VEGFR1) homed to the lungs before the arrival of cancer cells and generated receptive sites for future metastatic cells (114). CDE also mediated bone phenotypes (osteolysis or osteoclastic) through activation of EGFR and alteration in bone cell development to promote bone tumor growth and metastasis (115–117).

### 1.7 Significance & statement of work

The global burden, prevalence, and mortality of BC underlies the necessity for improved *in vitro* pre-clinical models to hasten the development

of effective therapeutics. Basic research and technological advances have increased our understanding of TNBC biology and yielded vast possibilities for novel therapeutic strategies such as immune activation, targeted therapies, and combinatorial administration of therapeutics. However, our increased understanding also highlighted the complexity of biological processes driving cancer progression and other properties of the disease. Tumor heterogeneity is a large contributor to this complexity and represents the principal challenge to overcome in a preclinical setting. The diversity of stromal cell types with genetically diverse cancer cells across tumors with differing molecular composition create an immensely dynamic disease that is difficult to generalize or treat. This heterogeneity has been shown to contribute to a wide array of cancer phenotypes from drug efficacy, growth rates, and metastatic potential (118,119) and have been observed clinically through modern imaging (120).

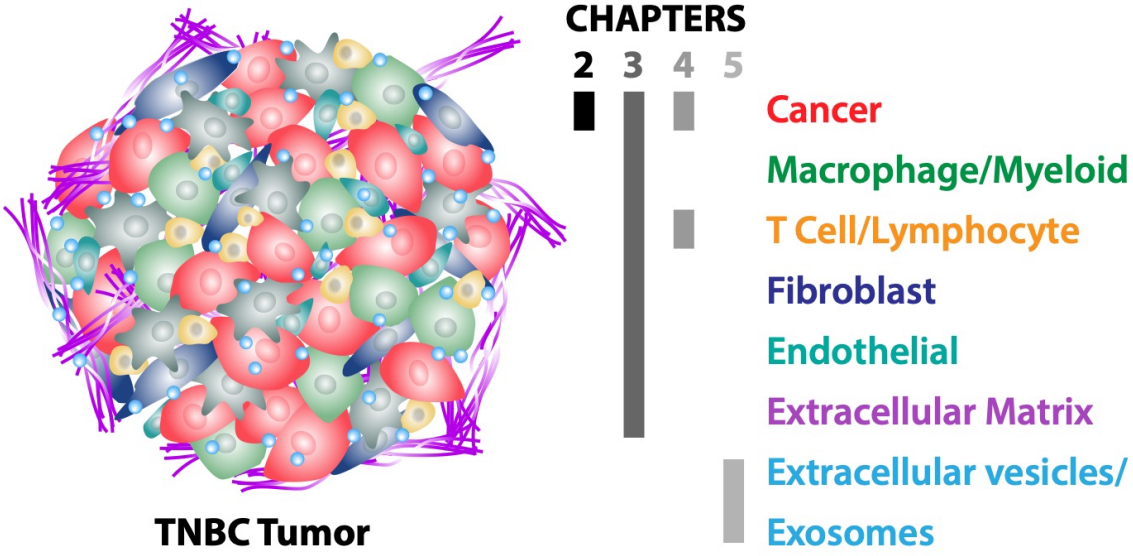


**Figure 1. Project Overview.** Research presented in this thesis dissect the complexity of TNBC tumors highlighting four aspects of tumor biology.

Despite the promise of existing pre-clinical models, about 95% of new drugs fail to receive approval due to lack of efficacy (85). Additionally, resistance to chemotherapeutics in local and metastatic breast cancer remain

a major challenge (121) yet conventional homogenous culturing techniques fail to incorporate tumor stromal components that have been shown to play a role in chemoresistance (119,122). Inadequacy of preclinical models fail to recapitulate clinical efficacy and outlines the necessity of understanding current cancer model limitations as well as the creation of a high throughput adaptable *in vitro* tumor model for preclinical research. This research examines multiple facets of tumor biology from cancer cell behavior to stromal cell contributions to the cell-cell communication used by cancer cells to alter the behavior of all tumor cells (Fig 1).

Chapter 2 utilizes gene expression analysis of cancer cells in existing methodologies to address key deficiencies in existing preclinical tumor models. By analyzing across several culturing platforms and utilizing endogenously labeled cancer cells coupled with fluorescently activate cell sorting (FACS) technology to exclude tumor stromal cells from the bulk RNA analysis, this study will be able to produce an unbiased approach to analyze the *in vitro* and *in vivo* transcriptional profiles of cancer cells cultured in different conditions. RNA-seq data across methods with 4T1, a murine TNBC cell line, cells illustrate the significant alterations in global gene expression patterns from altered culturing (monolayer vs *in vivo*) or collection methods (sorted cancer cell fraction vs whole tumor). In Chapter 3, the altered cancer cell behaviors previously identified are further examined in longitudinal studies in co-culture with stromal cell heterogeneity. This research highlights the dynamic nature of cancer cells in *ex vivo* conditions.

The impact of non-malignant, host recruited, stromal cells present in the tumor is examined in Chapter 4. This research focuses on the impact that a T cell secreted cytokine, IL17a, can have on the tumor response to systemic neoadjuvant chemotherapy. This work emphasizes the importance of secreted molecules in the tumor microenvironment which is further examined in

Chapter 5 where I characterize the generation and cargo of exosomes secreted by different BC cell lines. The study of CDE deepens our understanding of cancer signaling and provides novel opportunities for biomarkers of aggressive BC. The research presented here increases our understanding of BC culturing dynamics, stromal cell impacts on tumor biology, and the communication of the community of cells residing in the tumor microenvironment. This new knowledge will help inform and improve future BC culturing conditions and aid the development of new, more personalized and more effective therapeutics for the treatment of difficult to treat breast cancers.

## Chapter 2. Comparative molecular analysis of cancer behavior cultured *in vitro*, *in vivo*, and *ex vivo*


### Abstract

Current preclinical tumor models fail to recapitulate the native cancer cell behavior primarily due to the lack of a deeper understanding of effects the microenvironment has on cancer cell phenotype. To examine our ability to recapitulate the native tumor microenvironment, we performed transcriptomic profiling of 4T1 murine mammary carcinoma cells from 2D and 3D cultures, subcutaneous or orthotopic allografts as well as *ex vivo* tumoroids and validated at the protein level using flow cytometric analysis and western blots. Subsequent analysis of cancer cells undergoing an epithelial-to-mesenchymal transition (EMT) were assayed using a flow cytometric panel elucidating culture induced EMT hybrid heterogeneity. Altered expression of biological processes involved in cell cycle progression, cell signaling, and extracellular matrix remodeling were discovered to be affected by culturing technique. 3D culture platforms had more in vivo-like transcriptional profiles than 2D cultures in relation to biological processes of interest as well as showing upregulation of genes enriched in differentiation processes. *In vivo* tumors had more cells undergoing EMT while in vitro cultures had cells residing primarily in an epithelial or mesenchymal state. *Ex vivo* tumoroids incorporated aspects of *in vivo* and *in vitro* culturing, retaining higher abundance of cells undergoing EMT while shifting cancer cell fate towards a more mesenchymal state. Cellular heterogeneity surveyed by scRNA-seq revealed that *ex vivo* tumoroids, while rapidly expanding cancer and fibroblast populations, lose a significant proportion of endothelial and immune components. This study emphasizes the need to improve *in vitro* culture systems and preserve syngeneic-like tumor composition by maintaining similar EMT heterogeneity as well as inclusion of stromal subpopulations.

## Introduction

Cancer has a major impact on society and poses a significant financial burden globally (123). The American Cancer Society predicts that ~1.7 million new cases of cancer will be diagnosed this year and ~20% of all deaths will be cancer associated. While the overall cancer death rate has dropped steadily since 1991, this decline is mostly due to changes in lifestyle (smoking cessation) and early detection (breast and colorectal). Cancer remains a challenging health burden as the second leading cause of death, in both men and women, with death rates continuing to rise for liver, pancreatic, endometrial, and brain cancers (124). The past two decades have expanded our understanding of the mutational landscape and signal transduction pathways that drive tumorigenesis, guiding the development of more effective therapies and improving survival outcomes for numerous cancer types (125); however, advances have remained slow for patients at later stages of the disease or those with highly aggressive cancer subtypes (126). Most significantly, >95% of new therapies that exhibit superior performance in animal models fail in the clinic due to therapeutic inefficacy or unwarranted toxicity (85).

In order to improve future preclinical cancer models, a thorough understanding of molecular changes underlying cancer cell behavior *in vivo* or *ex vivo* is essential (125) however the vast accumulation of gene expression data generated from clinical tumor samples are primarily collected *via* bulk tumor RNA sequencing or microarray analysis. These datasets represent the transcriptional output of all stromal and malignant cells combined, making it difficult to deconvolute deviations accounted solely by cancer cell response (127). As a result of this technical challenge, heterogeneity found in a pre-clinical screening has classically been underrepresented and initial screens are typically performed on *in vitro* cultures of solely cancer cells.

Conventional *in vitro* 2-dimensional (2D) culture of human cancer cell lines have been fundamental in the study of cancer biology as well as for screening

and evaluating therapeutic efficacies of anticancer agents. This approach promotes fast growth, ample area for adherence to substrates, and uniform access to nutrients and growth factors. Overall, 2D cancer models generate highly reproducible results, but lack the cellular complexity and extracellular matrix (ECM) associated with solid tumors (125). Three-dimensional (3D) cancer cell culture methods that generate spheroids, organoids, or cells embedded in various ECM compositions have been shown to display enhanced cell-cell interactions (128,129) yet are only superficially accessible to nutrients and diffusible drugs. In general, 3D cultures exhibit enhanced cellular heterogeneity and preserve characteristics apparent in the original tumor (128). However, these culture methods currently fail to incorporate the complex heterogenous cell composition and diffusion of nutrients or drugs that occur *in vivo*.

Animal models such as patient derived xenografts (PDX) allow for aspects of *in vivo* tumor progression and incorporate components of the physiologically relevant microenvironment. In recent years, PDXs have been increasingly used to expand our understanding of factors affecting tumor growth, drug response and metastasis (129); however, the absence of a complete immune system allows human tumors to evolve in a murine-specific manner and these models are not useful for testing many immune-based therapies (81). Allograft rodent models utilizing mouse derived cancer cell lines or genetic mouse models capable of spontaneous generation of tumors represent the most clinically relevant cancer models due to the presence of *in vivo* conditions as well as a full repertoire of stromal cell types, including immune cells. Yet less than 8% of animal model findings are successfully translated to clinical cancer trials (85,130). Additionally, *in vivo* culturing is hindered by labor and financial burdens posed by the lengthy process associated with establishing tumor engraftment and generating cohorts for experimentation.

Heterogenous *ex vivo* organoid cultures from primary clinical tumors (tumoroids) have gained considerable traction in recent years due to ease of culturing and the ability of tumoroids to maintain stromal cellular complexity. Tumoroids permit a faster culturing method, amenable to multiplexing a wider range of analysis tools in a preclinical setting. Several studies have shown promising results of tumoroid cultures mimicking histological morphology and drug responses across multiple cancer types (131–135). However, a thorough analysis of the shifting stromal cell populations and the resulting effects on cancer cell behavior as a product of culturing method have yet to be thoroughly investigated.

In order to understand the relationship and limitations of various culturing approaches, we examined the transcriptome of a triple negative mammary carcinoma murine cell line, 4T1, in various culturing environments (*in vitro*, *in vivo*, or *ex vivo*). 4T1 cells are well suited as they closely mimic human breast cancer and can form syngeneic tumors in fully immune competent mice. Transcriptional analysis identified distinct molecular profiles corresponding to *in vitro* and *in vivo* culturing conditions while *ex vivo* tumoroids exhibited molecular characteristics associated with both approaches. Several key biological processes [cell cycle progression, ECM remodeling, cell signaling, and epithelial-mesenchymal transition (EMT) progression] critical to tumor progression also varied across culturing conditions. Tumoroids were found to represent the most similar *in vitro* method to tumors established in syngeneic mice. However, despite the high similarity in cancer cell behavior, tumoroid composition, as assessed by single cell RNA sequencing (scRNA-seq), displayed significant shifts in stromal subpopulations after 5 days of *ex vivo* culture; changes that may play important roles in modulating cancer cell behavior. Faithful recapitulation of the transcriptional behavior, EMT heterogeneity, and stromal heterogeneity will be critical to understanding key deficiencies in existing culturing systems as well as educating future engineered tumor

platforms in fully recreating endogenous tumor architecture and response to therapy.

## Materials and Methods

### *2D and 3D cell culture.*

The 4T1 cells were acquired from the American Type Culture Collection (Manassas, MA, USA), are syngeneic and form tumors in immune-competent BALB/c mice. Monocultures, spheroids and 3D gel culture of 4T1 cells were maintained in RPMI Medium 1640 containing 10% FBS with 100,000 U/L of penicillin and 100 mg/L of streptomycin at 37°C with 5% $CO_2$. For monolayer 4T1 RNA collection, 400 cells were seeded into 96 well flat bottom plates. Aggregates of 4T1 cells were created by incubating 400 4T1 cells into nonadherent U-bottom 96-well plates (Griener, Germany) in 150 μL of complete RPMI containing 0.25% (wt/vol) of caboxymethylcellulose (Sigma Aldrich) for 4 days. On Day 4 spheroids were cast into hydrogels composed of 7.5 % (wt/vol) Type A gelatin from porcine skin (Sigma) and 1% (wt/vol) fibrinogen (Sigma) with thrombin and transglutaminase as crosslinking agents for a final concentration of 100 spheroids/mL of gel solution. Unencapsulated spheroids were cultured in 96 nonadherent U-bottom well plates. Both spheroids encapsulated in gel and unencapsulated spheroids were cultured for an additional 7 days submerged in complete media (Fig.1A). Replicates were isolated from cultures from at least two independent experiments. For imaging, unencapsulated spheroids and spheroids in gels were fixed using 4% paraformaldehyde for 30 minutes, followed by 3 washes in PBS for 5 minutes each. Spheroids were stained using phalloidin and DAPI and imaged using a Zeiss LSM 700 confocal microscope.

### *4T1-BFP generation.*

4T1 cells were transfected using Lipofectamine 3000 (Invitrogen) with the ptagBFP-C plasmid (Evrogen) following manufacturer's protocol for 48 hours. Stable transfected cells were selected with 0.5mg/ml of G418 for 7 days, followed by FACS sorting for high BFP expression then an additional sort was performed following 7 days of cell expansion in selection media. 4T1-BFP cells were then inoculated into BALB/c mice until tumors formed, then tumors were resected, dissociated, and then expanded in selection media followed by a final sort for BFP expression. Sublines were established and used in subsequent *in vivo* allograft experiments.

*Allograft Generation and Tumor Digests.*

All animal experimental procedures were completed under an approved IACUC protocol at LLNL and conforming to the NIH *Guide* for the care and use of laboratory animals. Female mice (6-8 weeks old) NOD.*Cg-Prkdc*$^{scid}$*Il2rg*$^{tm1Wjl}$/SzJ (NSG) or BALB/c mice (Jackson Laboratories) were injected with 25,000 cells into either mammary fat pad (MFP) or subcutaneously (SQ) into the back flank to establish tumors (N=5-10 mice per group) in 100µL of 50% PBS and 50% Matrigel (Corning). All experimental replicates were generated from at least two independent cohorts. Mice were euthanized 19-26 days post injection then tumors were dissected. Terminal tumor volume ranged from 70-140mm$^3$. Single cell suspensions of tumor cells were prepared by passing the tumor through a syringe without a needle followed by a 1h digest with shaking at 37°C in 100 ug/mL DNase I (Roche, catalog no. 11284932001), 300 U/mL collagenase/ 100U/mL hyaluronidase (STEMCELL Technologies, catalog no. 07912), 0.6 U/mL Dispase II (Roche, catalog no. 4942078001) in DMEM/D12 with 10% FBS (Gibco). Digests were filtered through a 100 µm cell strainer prior to debris removal (Miltenyi Biotec, catalog no. 130-109-398) and resuspended in BD FACS Pre-Sort Buffer (BD, catalog no. 563503).

*Histological Sectioning/Staining.*

Tumors were excised and flash frozen immediately in liquid nitrogen. Frozen tumors were embedded in O.C.T. compound (Fisher Healthcare), and sectioned into 40 μm slices, which were placed onto Superfrost Plus microscope slides (Fisher Scientific) and stored at -80°C until further use. To stain sections, slides were warmed to room temperature then immersed in PBS with 4% formaldehyde for 15 minutes. Sections were then immersed in PBS with 0.5% Triton-X for one hour. The samples were then stained with phalloidin for 45 minutes and washed three times with PBS. Sections were mounted using Fluoroshield mounting medium containing DAPI (Abcam) then sealed with a coverslip.

*Flow Cytometry and Fluorescent Activated Cell Sorting (FACS).*

Dissociation of monolayer and spheroid cultures were accomplished using Accutase (Stemcell Technologies) until single cell suspensions were achieved. Prior to Accutase treatment, spheroids were released from hydrogels by first mincing gels into ~1mm fragments followed by incubation in Collagenase 1 (Gibco 17100-017, 2mg/ml) in complete media shaking at 37°C for 1-1.5 hours or until gel is completely dissolved. Cell Sorting was performed using either a FACSMelody (BD Biosciences) or FACSAria Fusion (BD Biosciences) instrument. Protein expression was quantified using Biolegend antibodies FITC anti-mouse/human CD11b (ITGAM) (101206), APC anti-mouse CD49d Antibody (ITGA4) (103621), PE/Cy7 anti-mouse β2-microglobulin (154507), FITC anti-mouse CD326 (Ep-CAM) (118207), PE anti-mouse CD51 (104105), Fluor® 647 anti-mouse/rat CD61 (104313), PerCP/Cy5.5 anti-mouse CD106 (105715) were used at a 1:100 dilution prior to analysis on a BD FACSMelody cell sorter. Protein expression for *in vivo* samples was analyzed for 4T1 BFP+ populations only.

*RNA Sequencing and Analysis.*

RLT buffer with β-mercaptoethanol served as the lysis buffer for monolayer, unencapsulated spheroids, and *in vivo* sorted samples. Spheroids encapsulated in hydrogel and whole tumor samples were lysed using a bead-based homogenization (Lysing Matrix A, MP Bio) in Qiazol (Qiagen). Total RNA was isolated using RNeasy mini spin columns (Qiagen). Sequencing library preparation was performed using Illumina TruSeq RNA Library Preparation Kit v2 (Illumina, Catalog no. RS-122-2002) and single end 75 base pair sequencing was performed using an Illumina NextSeq 500. Sequencing data quality was checked using FastQC software [http://www.bioinformatics.bbsrc.ac.uk/projects/fastqc]. Reads were mapped to the mouse genome (mm10) using STAR (version 2.6) (136) and read counts per gene were determined using "featureCounts" from Rsubread package (version 1.30.5). Only genes with ≥10 reads in at least 3 samples were selected for analysis. Subsequently, a between-sample normalization was performed using EDASeq (version 2.16.0) (137). RUVseq (version 1.16.0) was used to estimate the factors of unwanted variation (138). Differentially expressed genes were identified using edgeR (version 3.22.3), controlling for factors of unwanted variation (139). A gene was significantly differentially expressed when its false discovery rate adjusted p-value was < 0.05 and fold change was >2. Gene ontology (GO) and pathway enrichment analysis was performed using ToppGene (140). Heatmaps were generated using heatmap.2 function in 'gplots' R package. Violin plots were generated using 'ggplot2' R package. Cytoscape was used for network visualization (141,142).

*Western Blot.*

Cell preparations were prepared as previously described. Duplicate samples were pooled then lysed in RIPA buffer followed by centrifuging at 14,000 rcf for 5 mins. The supernatants were collected and analyzed using the

Jess automated Western blotting system (ProteinSimple, San Jose, CA). Jess reagents (biotinylated molecular weight marker, streptavidin-HRP fluorescent standards, sample buffer, DTT, stacking matrix, separation matrix, running buffer, wash buffer, matrix removal buffer, fluorescent labeled secondary antibodies, antibody diluent, and capillaries) were purchased from the manufacturer and used according to the manufacturer's standard protocol. Antibodies were diluted with ProteinSimple antibody diluent at the following dilutions: anti Phospho-Cdk1 (Tyr15) (1:12.5, Cell Signaling, Catalog no. 4539), anti-Phospho-MCM2 (Ser139) (1:50, Cell Signaling, Catalog no. 12958), PE/Cy7 anti-STAT1 Phospho (Ser727) (1:12.5, Biolegend, Catalog no. 686407), and β-Tubulin (1:100, Licor,Catalog no. 926-42211). Target protein concentration is quantitated using Compass for SW 4.0 software. The expression of each target protein is normalized to the expression of β-tubulin.

*Ex vivo tumoroid culture.*

4T1-Thy1.1 cell line was graciously provided as a gift from Dr. Julian Lum (143) for *ex vivo* experiments. $2.5x10^4$ 4t1-Thy1.1 cells were injected into the MFP of BALB/c mice then cultured to 70-140 $mm^3$, isolated and digested as previously described in Allograft Generation and Tumor Digests. Following debris removal of tumor digests 10,000 cells were then plated into a well of a 96-well flat bottom cell culture plate or a nonadherent U-bottom 96-well plates (Griener, Germany) in 150 μL of complete RPMI. Following 5 days of culture, cells were dissociated with Accutase then either sorted prior to cancer cell RNA isolation, analyzed via flow cytometry, or processed for single cell RNA sequencing. Cancer cell identification was performed using anti-CD90.1-VioBlue antibody (Miltenyi Biotec, catalog no. 130-102-637).

*Single cell sequencing and data analysis.*

Tumor growth, digestion, and isolation of cell suspensions were prepared as previously described for tumor digests and tumoroids were dissociated as previously described. 2 subsequent washes in sterile PBS + 0.04% non-acetylated BSA were performed to further remove debris from final suspension. Cell pellets were resuspended in PBS with 0.04% non-acetylated BSA prior to single cell sequencing preparation using Chromium Single Cell 3′ GEM, Library & Gel Bead Kit v3 (10X Genomics, Catalog no. 1000075) on a 10X Genomics Chromium Controller following manufacturers protocol.

Sequencing data was demultiplexed, quality controlled, and analyzed using Cell Ranger (10X Genomics) and Seurat (144). The Cell Ranger Single-Cell Software Suite was used to perform sample demultiplexing, barcode processing, and single-cell 3′gene counting. Samples were first demultiplexed and then aligned to the mouse genome (mm10) using "cellranger mkfastq" with default parameters. Unique molecular identifier (UMI) counts were generated using "cellranger count". Further analysis was performed in R using the Seurat package. For in vivo and *ex vivo* samples, we performed an integrated analysis to identify and compare common cell types. Cells with fewer than 500 detected genes per cell and genes that were expressed by fewer than 5 cells were not included in the analysis. Prior to data integration, we performed a log-normalization and also identified the 2,000 most variable genes in each dataset. Subsequently, integration anchors were identified and both datasets were integrated to generate a new integrated matrix. The integrated matrix was then scaled to a mean of 0 and variance of 1 and the dimensionality of the data was reduced by principal component analysis (PCA) (30 principle components). Subsequently, a non-linear dimensional reduction was performed via uniform manifold approximation and projection (UMAP) using the first 20 principle components. Then, we used a a graph-based clustering approach to cluster cells. We constructed a K-nearest-neighbor (KNN) graph based on the euclidean distance in PCA space using the

"FindNeighbors" function and applied Louvain algorithm to iteratively group cells together by "FindClusters" function (resolution = 0.5). A total of fourteen clusters were identified in the integrated dataset.

Cell type identification based on high gene expression of the following genes relative to all cells: Cancer: Epcam; Proliferating Cancer: Epcam/Mki67; Fibroblast: Thy1/Dcn; Myofibroblast: Thy1/Dcn/Acta2; Endothelial: Pecam1/Cdh5; Neutrophils: S100a8/Retnlg; Myeloid: Ptprc/CD14; M2-like Macrophage: Ptprc/CD14/Mrc1/Cd163; Inflammatory macrophage: Ptprc/CD14/Il1b; Proliferating myeloid: Ptprc/CD14/Mki67; T-Cell/NK Cell: Ptprc/Thy1/CD3e/Nkg7; B Cell: Ptprc/CD19/CD79a.

*Statistical analyses.*

Statistical analyses were performed using GraphPad Prism. Data is presented from at least three biological replicates. One-way ANOVA and post-hoc Tukey's Test were used to assess statistically significant differences of mean expression values. Results were considered statistically significant for $p$ values $< 0.05$.

## Results

*Cancer cell transcriptome is dictated by culture conditions*

RNA sequencing was performed on 4T1 cells grown in different culture modalities to determine molecular phenotypes driven by the culture environment (Fig1). *In vitro* methodologies profiled included conventional 2D 4T1 monolayer culture on polystyrene tissue culture treated flasks (Fig1c), spheroids cultured in non-adherent well plates in culture media for 7 days following a 4-day initial spheroid formation (3DM) (Fig1d) or spheroids encapsulated in a gelatin-fibrin hydrogel (3DG) (Fig1e) for 7 days post spheroid formation. *In vivo* methodologies required generation of 4T1-BFP$^+$ cells to enable the isolation of cancer cells from the heterogenous tumor environment

using fluorescently activated cell sorting (FACS) (FigS1). Transcriptional profiles of cancer cells isolated from primary tumors of immunodeficient (NSG) mice and syngeneic, immune competent (BALB/c) mouse models were analyzed in this study. While malignant cells inoculated into the tissue of origin is ideal for reproducing native stromal environments, subcutaneous administration of tumor cells offers a more technically reproducible and simple approach to introducing cancer cells *in vivo*. Here we comprehensively examine the transcriptional effects imparted by localization of primary tumors in both orthotopic [mammary fat pad (MFP)] and subcutaneous [back flank (SQ)] sites (Fig1b).

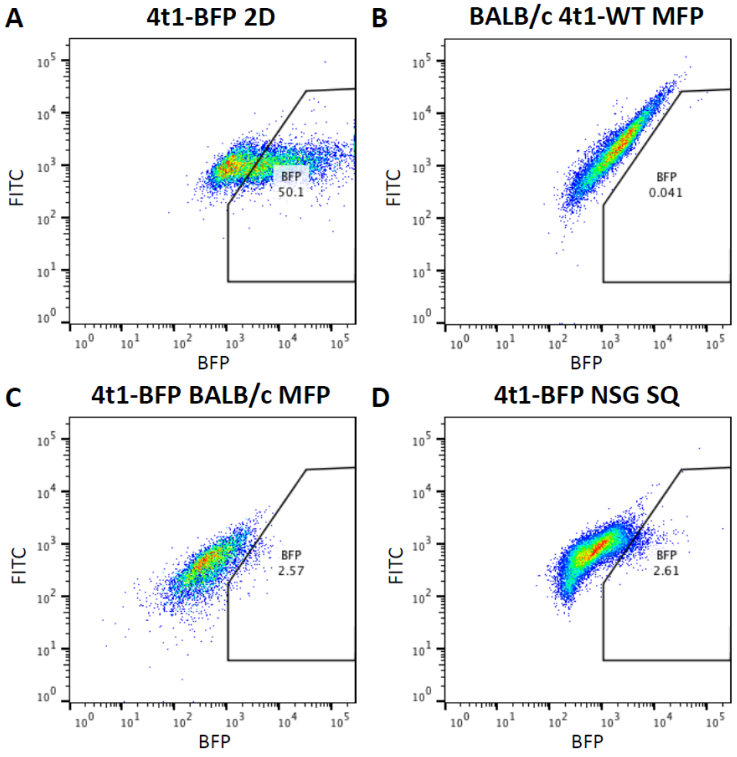


**Figure Supplemental 1. Purification of 4T1-BFP+ cells from BALB/c and NSG tumors.** Dot plots of BFP fluorescent intensity of 4T1-BFP+ cells in monolayer culture (**A**). *In vivo* gating of BFP+ tumor cells from a WT 4T1 BALB/c MFP (**B**), 4T1-BFP BALB/c MFP (**C**), or 4T1-BFP NSG SQ (**D**).

Conventionally, cancer cells are cultured in a monolayer (2D). For this reason, transcriptional profiles of alternate 4T1 culturing conditions were referenced to 2D culture to identify differentially expressed genes (DEGs) in each platform. The sorted Balb/c derived MFP (SBM) culture represents the most clinically relevant, due to its *in vivo* syngeneic environment and orthotopic site of injection. Henceforth, successful recapitulation of native cancer cell behavior will be in comparison to SBM samples. Histologically, *in vivo* 4T1-BFP$^{+}$ tumors had more densely packed cells than 4T1 cells cultured in spheroids (Fig1c-g) and labeled 4T1 cells were surrounded by other stromal cell types [Fig1g, 4T1 (green); actin (red); DAPI (blue)].

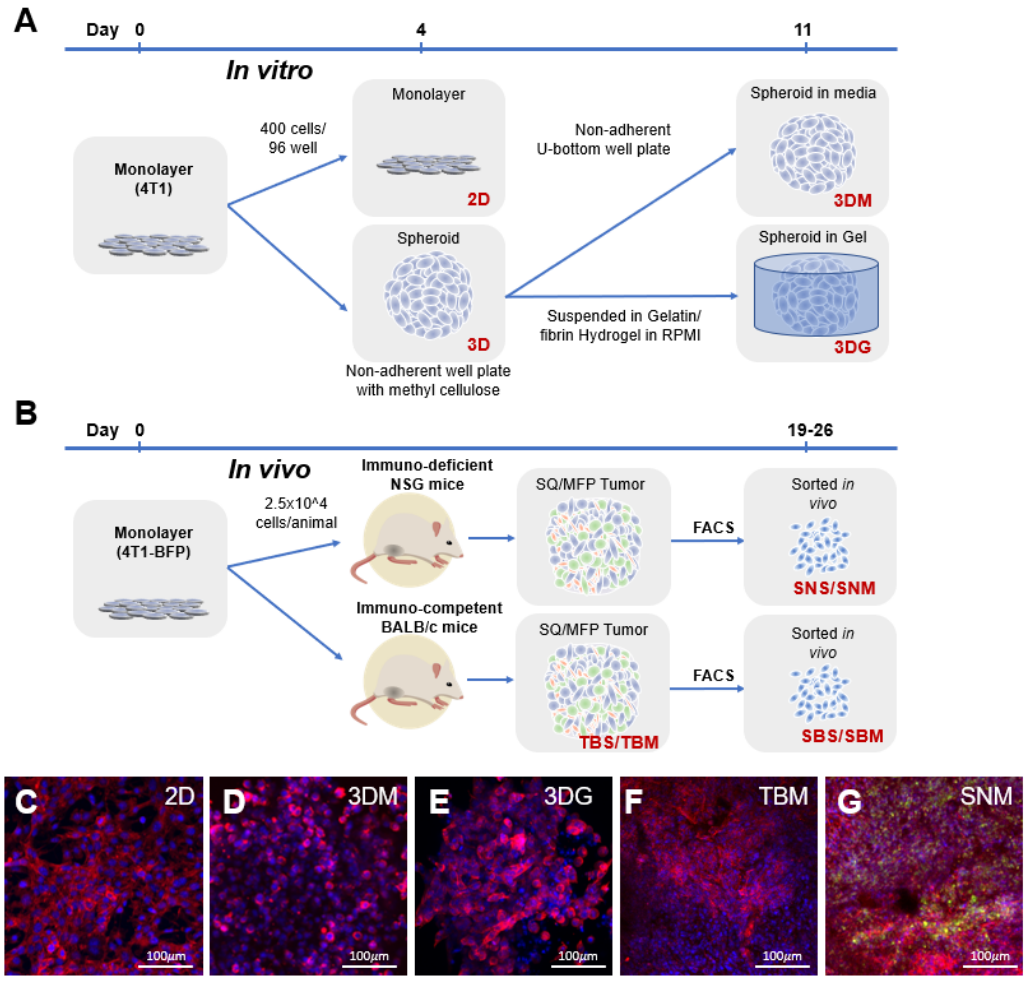

**Figure 1. Experimental Overview. (A)** 4T1 *in vitro* samples originated from low passage number, sub-confluent, monolayer cultured cells seeded at 400 cells/well in 96 wells into tissue culture treated flat bottom plates or non-adherent U-bottom plates. Following 4 days of culture, monolayer (**C**) RNA was collected, and spheroids were continued to be cultured in wells containing media (**D**) or cast into a gelatin/fibrin hydrogel (**E**) for an additional 7 days prior to RNA isolation. (**B**) *In vivo* tumor samples were generated by injection of sub-confluent, monolayer 4T1-BFP cultures into MFP or SQ locations in NSG or BALB/c mice. Tumors were isolated following a 19-26 day growth period yielding tumors ranging from 70-140mm$^3$. RNA samples were processed from bulk (**F**) or BFP$^+$ cancer cell populations isolated by fluorescently activated cell sorting (FACS) (**G**). Blue: Nuclear DAPI staining; Red: Phalloidin staining actin filaments; green: BFP expression.

4T1 MFP [whole tumor BALB/c mammary fat pad (TBM)] (Fig1f) and SQ [whole tumor BALB/c subcutaneous (TBS)] transcriptional profiles were most divergent from 2D cultured cells but showed high similarity to each other (Fig2a-c; Table S1). Whole tumor bulk RNA comparisons to 2D cells produced the highest number of DEGs, likely due to stromal cellularity (Fig2a). However, these genes did not correlate with changes exclusive to 4T1 cells, since 4T1-BFP$^+$ sorted from these tumors only shared 1251/2604 (48%) upregulated and 336/1385 (24%) down-regulated transcripts (Fig2e).

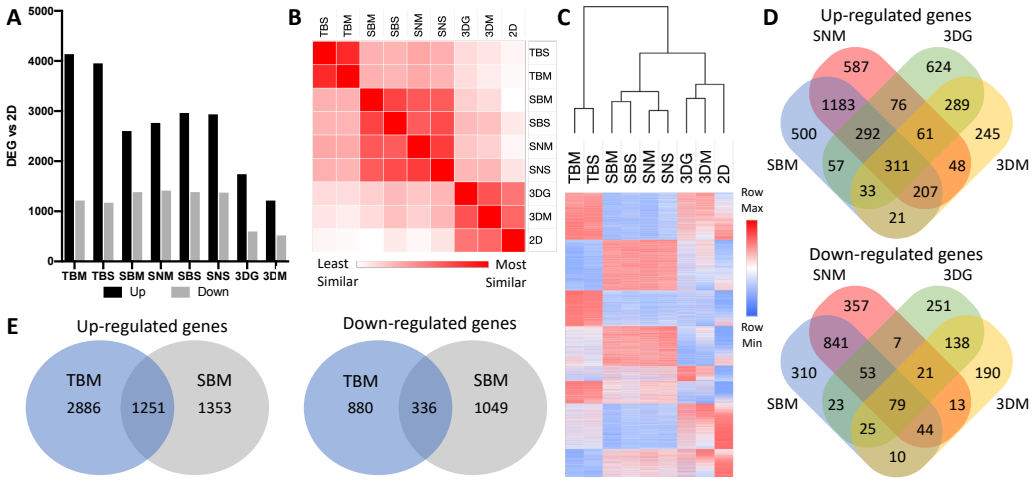


**Figure 2. Transcriptomic variability of cancer cells under different culturing conditions. (A)** Quantity of differentially expressed genes (DEGs) compared to 2D samples. DEGs were defined as greater than 2-fold change and FDR<0.05 (n≥4). Cultured condition abbreviations: TBM: whole Tumor from BALB/c Mammary fat pad; TBS: whole Tumor from

BALB/c Subcutaneous back flank; SBM: Sorted BALB/c Mammary fat pad; SBS: Sorted BALB/c Subcutaneous; SNM: Sorted NSG Mammary fat pad; SNS: Sorted NSG Subcutaneous; 3DG: 3D spheroids in hydroGel; 3DM: 3D spheroids in Media; 2D: 2D monolayer. (**B),** Similarity matrix based on whole transcriptome similarity of average expression values within each condition. Similarity differences calculated using Euclidean distance. (**C**) Heat map and dendrogram of whole transcriptome based of normalized logarithmic average expression values within each condition and hierarchal clustering of samples based on Euclidean distance. (**D)** Venn diagrams representing overlapping up- and down-regulated DEGs from 4T1 cultured from immunocompetent tumors, immunodeficient tumors, spheroids in gel, and spheroids in media compared to monolayer culture. (**E**) Venn diagrams representing overlapping up- and down-regulated DEGs from MFP BALB/c whole tumor vs MFP BALB/c sorted 4T1 compared to monolayer culture.

*In vivo* sorted BFP$^+$ 4T1 cells from BALB/c MFP (SBM) and SQ (SBS), NSG MFP (SNM) and SQ (SNS) tumors clustered most closely with themselves, however 3D spheroids induced a greater level of *in vivo*-like transcriptional level (Fig2b, c; Table S2,3). Interestingly, 4T1-BFP$^+$ cells derived from orthotopic MFP and SQ tumors were highly similar to each other in both immunocompetent and immunodeficient mice with minimal variability in the quantity and identity of genes differentially expressed compared to 2D (Table S2). MFP and SQ tumors shared 79% and 83% of DEGs in immune -competent and -deficient mice, respectively. As expected, immune-deficiency did drive unique gene expression changes within 4T1 cells, where only 1993/2604 up-regulated (75%) and 1017/1385 down-regulated (73%) DEGs were shared by 4T1-BFP$^+$ cells grown in BALB/c (SBM) and those grown in NSG mice (SNM) (Fig2d). Interestingly, 4T1-BFP$^+$ cells in syngeneic mice up-regulate a diverse set of genes associated with cellular processes indicative of differentiation and interactions with the surrounding microenvironment (Table 1). Furthermore, ECM organization, immune response, cell signaling, in addition to polarization and migration of cells were functional categories enriched in all *in vivo* conditions (Table 1). Relative to *in vivo*-derived cancer cells, cells cultured in monolayer promoted a set of cellular processes involved in multiple aspects of

cellular proliferation (Table 1, FigS2) such as DNA synthesis, RNA processing, protein translation, as well as cell cycle progression, suggesting that 2D cultured cells encourage proliferation.

**Table 1.** Ontologies associated with genes highly expressed in 2D vs cancer cells isolated from orthotopic and syngeneic 4T1 mouse tumors.

| **Key ontology terms associated with genes highly expressed in 2D compared to SBM** | | |
|---|---|---|
| **GO ID** | **Term** | **No. of genes** |
| *GO:1901605* | *alpha-amino acid metabolic process* | *34* |
| *GO:0007049* | *cell cycle* | *197* |
| *GO:0044770* | *cell cycle phase transition* | *67* |
| *GO:0051301* | *cell division* | *88* |
| *GO:0045333* | *cellular respiration* | *26* |
| *GO:0007059* | *chromosome segregation* | *60* |
| *GO:0006259* | *DNA metabolic process* | *110* |
| *GO:0006281* | *DNA repair* | *56* |
| *GO:0006260* | *DNA replication* | *54* |
| *GO:0032543* | *mitochondrial translation* | *30* |
| *GO:0007005* | *mitochondrion organization* | *101* |
| *GO:0034660* | *ncRNA metabolic process* | *128* |
| *GO:0000280* | *nuclear division* | *88* |
| *GO:0048285* | *organelle fission* | *91* |
| *GO:0009126* | *purine nucleoside monophosphate metabolic process* | *32* |
| *GO:0006220* | *pyrimidine nucleotide metabolic process* | *11* |
| *GO:0042254* | *ribosome biogenesis* | *97* |
| *GO:0016072* | *rRNA metabolic process* | *77* |
| *GO:0006360* | *transcription by RNA polymerase I* | *14* |
| *GO:0006412* | *translation* | *74* |
| *GO:0006399* | *tRNA metabolic process* | *45* |
| **Key ontology terms associated with genes highly expressed in SBM compared to 2D** | | |
| **GO ID** | **Term** | **No. of genes** |
| *GO:0001525* | *angiogenesis* | *141* |

| | | |
|---|---|---|
| *GO:0001775* | *cell activation* | *208* |
| *GO:0007155* | *cell adhesion* | *341* |
| *GO:0016477* | *cell migration* | *307* |
| *GO:0032963* | *collagen metabolic process* | *49* |
| *GO:0060429* | *epithelium development* | *243* |
| *GO:0030198* | *extracellular matrix organization* | *120* |
| *GO:0006955* | *immune response* | *349* |
| *GO:0000165* | *MAPK cascade* | *178* |
| *GO:0023056* | *positive regulation of signaling* | *321* |
| *GO:0012501* | *programmed cell death* | *357* |
| *GO:0045595* | *regulation of cell differentiation* | *358* |
| *GO:0042127* | *regulation of cell proliferation* | *348* |
| *GO:0034097* | *response to cytokine* | *210* |
| *GO:0070848* | *response to growth factor* | *154* |
| *GO:0034341* | *response to interferon-gamma* | *60* |
| *GO:0070482* | *response to oxygen levels* | *83* |
| *GO:1901700* | *response to oxygen-containing compound* | *314* |
| *GO:0048771* | *tissue remodeling* | *56* |
| *GO:0001944* | *vasculature development* | *191* |


**Supplemental Figure 2. Network visualization of enriched pathways.** Pathways enriched in DEGs from 2D culture vs. orthotopic SBM 4T1 culture (A). Pathways enriched in DEGs from orthotopic SBM vs 2D culture of 4T1 culture (B). Cytoscape was used to generate visualizations with pathways defined from REACTOME [36,38].

### *Culturing condition affects cancer cell behavior critical to cancer progression*

Cancer requires a successive acquisition and management of critical cell behaviors in order to promote disease progression. Here we further examined

differential expression of biological processes associated with tumor progression to understand the imparted behavioral impact from varying culturing conditions. Dysregulation of cell cycle progression is a hallmark of cancer initiation and a target for numerous chemotherapeutic treatments (145), however alteration in cell metabolism is also required for cancer progression and includes extracellular matrix remodeling (70), cell-cell communication *via* secreted cell signaling (146,147), as well as transitioning from an epithelial to a mesenchymal cell state also known as EMT (148).

Genes associated with proliferation and cell division were highly expressed in 2D but these transcripts were least abundant in 4T1 cells purified from *in vivo* tumors (Fig3a). This involved 88 genes down-regulated in SBM relative to 2D that are associated with cell cycle and includes several cyclin transcripts (*Ccna2*, *Ccnb1*, *Ccnd2*, *Ccne2*) (Fig3a, Table S4). Both 3DG and 3DM showed modest expression of cell cycle genes, whereas cells sorted from *in vivo* tumors significantly repressed this gene set (Fig3). Genes robustly expressed in monolayer also showed enrichment in biological processes that promote growth and cell division including DNA synthesis, RNA processing, and ribosomal translation. For example, cyclin dependent kinase substrates involved in mitotic functions (*Ccp110, Npm1, Cdc6, Cdc25a*) and DNA replication (*Fen1, Orc1, Orc2*) were significantly upregulated in 2D relative to *in vivo*. However, 22 cell cycle-associated genes including cyclin-dependent kinase inhibitor 1 a (*Cdkn1a*), a regulator of cell cycle progression, and members of the ubiquitin-proteasome system (*Ubb*, *Ubc, Psmb8*, *Psmb9*, *Psmb10*, *Psme1*, *Psme2*) were expressed at higher levels *in vivo* (Fig3a; Table S4). Specifically, immunoproteases (*Psmb8-10*) associated with proliferative human embryonic stem cells (149) were amongst the most highly expressed cell cycle genes *in vivo*, suggesting up-regulation of genes associated with stemness, *in vivo*. Cell cycle processes are not only regulated at the transcriptional level but involve tightly controlled translational and post-translational regulation. Up-

regulated levels of phosphorylated Cdk1 (a regulator of progression into mitosis) and phosphorylated Mcm2 (a regulator of S-phase progression) were observed in monolayer culture. Decreased expression of these cell cycle genes was identified in 3D cultured cells and very low expression was found in *in vivo* cultured cells (Fig3c-d).

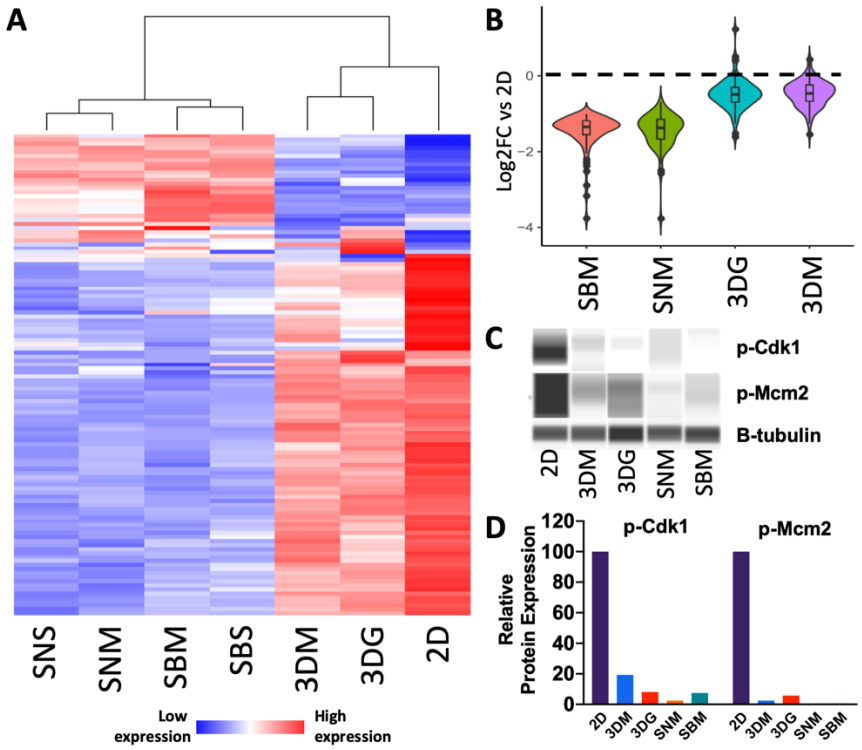


**Figure 3. Cell cycle progression genes are up-regulated in cells cultured in monolayer culture. (A)** Heat map of differentially expressed cell cycle genes (Table S4) relative to 2D culture depicting increased down-regulation as culturing complexity increases (n=4-5). **(B)** Violin plot depicting magnitude of down-regulation and distribution of SBM vs 2D up-regulated cell cycle progression genes across other culturing conditions relative to 2D culture. **(C)** Pseudogel representation of protein levels of phosphorylated cell cycle genes (Cdk1 and Mcm2) from 4T1 cells cultured across multiple conditions. **(D)** Quantification of protein levels relative to ß-tubulin.

Structuring and remodeling of the tumor ECM and surrounding tissue is an essential facet of tumor initiation, extravasation and intravasation that allow the disease to progress (70). 4T1 cells grown in monolayer had low expression of core matrix genes including collagens, *Eln, Bgn, Dcn, fibulins*

*and fibrillins* (Fig4a; Table S5); genes associated with ECM regulation (Fig4b; Table S6) and cell matrix adhesion (Fig4e; Table S7). In contrast, these genes were robustly expressed *in vivo* and in 3D culture, which expressed significantly higher levels of ECM-associated genes. Although ECM-related genes were up-regulated in all *in vivo* and 3D models, a large number of ECM genes showed the highest level of up-regulation in syngeneic mice (SBM), with decreased levels in the immune deficient animals (SNM) (Fig4c, d). Expression was further decreased under 3D culturing conditions (Fig4c, d). Spheroids cultured in hydrogel did encourage moderate up-regulation of both core matrix and ECM regulating genes above levels in spheroids cultured in media and thus expression levels were more similar to the *in vivo* conditioned cell behavior.

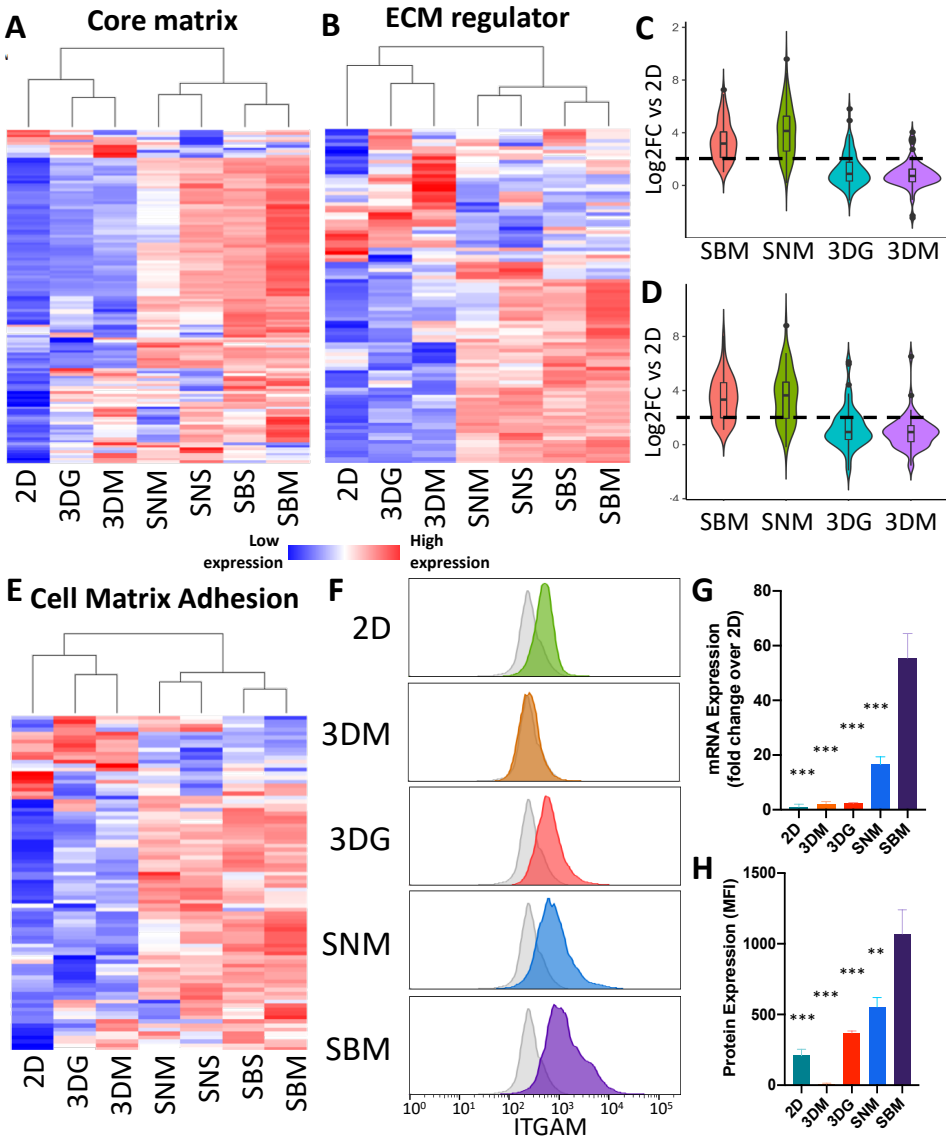


**Figure 4. Extracellular matrix organization genes are up-regulated in cells cultured in 3D and *in vivo* conditions.** Heat maps of differentially core matrix genes **(A)** (Table S5) and ECM regulator genes **(B)** (Table S6) relative to 2D culture. Expression values represented are average of 4-5 replicates. Violin plots depicting magnitude of up-regulation and distribution of SBM vs 2D upregulated core matrix genes **(C)** and ECM regulator genes **(D)** across other culturing conditions relative to 2D culture. Violin plot depicting magnitude of up-regulation and distribution of SBM vs 2D upregulated core matrix genes across other culturing conditions relative to 2D culture. **(E)** Heat map of differentially expressed cell matrix adhesion genes (Table S7) relative to 2D culture (n=4-5). **(F)** Histogram of representative *Itgam* abundance of single cancer cells cultured in different methods. Grey shaded plots represent unstained controls. **(G)** mRNA expression levels of *Itgam* in 4T1

cells under differing culturing condition. Expression levels normalized to 2D culture ± SEM. (n=4-5). (**H**) Bar graph of flow cytometric analysis of ITGAM protein expression showing up-regulation in 3DG and *in vivo* conditions. Protein expression values represent background (unstained control) subtracted median fluorescent intensity of cancer cells ± SEM; (n=4). (** p value<0.001; *** p value<0.0001 relative to SBM).

ECM regulators highly expressed *in vivo* included protease gene families [matrix metalloproteinases (*Mmp1a, Mmp2, Mmp3, Mmp12 and Mmp13*), cathepsins (*Ctsf, Ctsk, Ctso* and *Ctss*), and ADAMTS (*Adamts2, Adamts6, Adamts12, Adamts14*)] as well as ECM crosslinking genes (lysyl oxidases), many of which were also up-regulated in 3D cultures compared to 2D, but this up-regulation was more modest than in SBM samples (Table S6). Several *Mmps* (Mmp15, Mmp24) however, were found to be downregulated in 3D and *in vivo* tumors, relative to 2D culture. Two integrin genes (*Itgam* and *Itga4*) found to be differentially regulated were used to validate protein expression *via* flow cytometry. Itgam protein expression increased with culturing complexity where 2D cultured cells expressing the lowest amounts, while SBM expressed the greatest amount (Fig4f), correlating with transcriptional data (Fig4g) with the exception of the 3DM sample where the protein could not be detected (Fig4f, 4h). This deviation in Itgam protein levels from transcriptional expression suggest subsequent translational regulation.

Many of the behavioral changes of cancer cells including proliferation, motility, as well as immune interaction could be mapped back to activation of cell signaling pathways (146). Unsupervised clustering identified several cell-signaling pathways (RAS, TNF, PI3K-AKT, MAPK, Interferon and Interleukins) that were significantly up-regulated under *in vivo* conditions but showed a modest increase in 3D conditions (FigS2a, S3). Specifically, interferon alpha and beta (IFNα/ß) (Fig5a, Table S8), interferon gamma (IFNɣ, Table S9) (Fig5b), and signaling by interleukins (Fig5e, Table S10) were significantly up-regulated in cancer cells isolated from immune competent mice (SBM). This effect was significantly reduced in immunodeficient mice

(SNM) and only minimal up-regulation was measured in cancer cells cultured in 3D for both IFNα/β (Fig5c) and IFNγ (Fig5d) signaling. Surprisingly, both IFNα/β receptor subunits (IFNAR1 and IFNAR2) showed modest up-regulation (1.47±SD 0.165 and 1.84±SD 0.93 respectively) across all conditions; however significant up-regulation of downstream targets was observed in cancer cells isolated only from syngeneic tumors including IRF transcription factors (*Irf1*, *Irf2*, *Irf4*, *Irf7*, *Irf8*, *Irf9*) as well as interferon target genes (*Ifi27, Ifi35, Ifit1, Ifit3, Ifitm1, Ifitm3, Isg15, Isg20*).

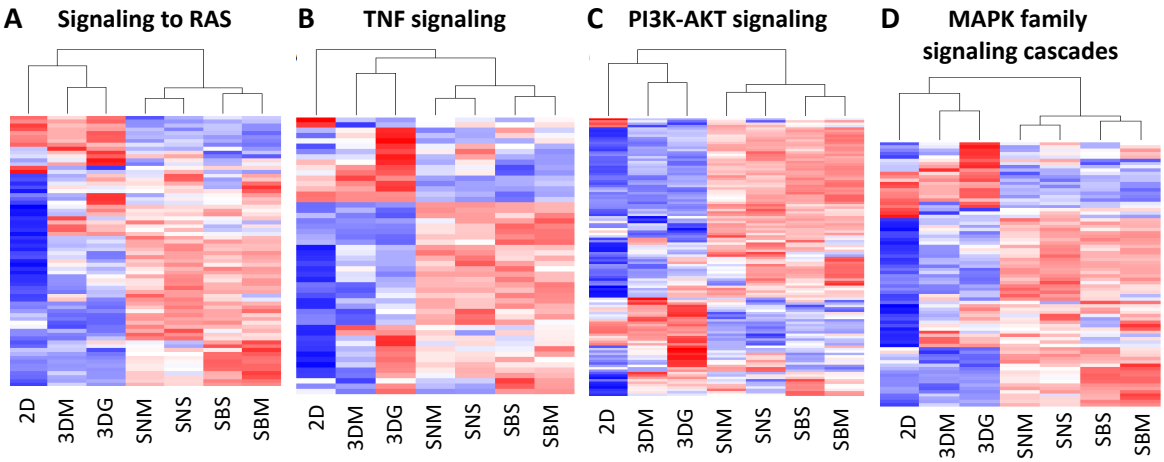


**Supplemental Figure 3. Heat maps of key cancer pathways.** Heat map of differentially signaling genes of Ras (A), tumor necrosis factor alpha (TNFα) (B), phosphoinositide-3 kinase (PI3K) (C), and mitogen-activated protein kinases (MAPK) (D) signaling pathways. Expression values represented are average of 4-5 replicates.

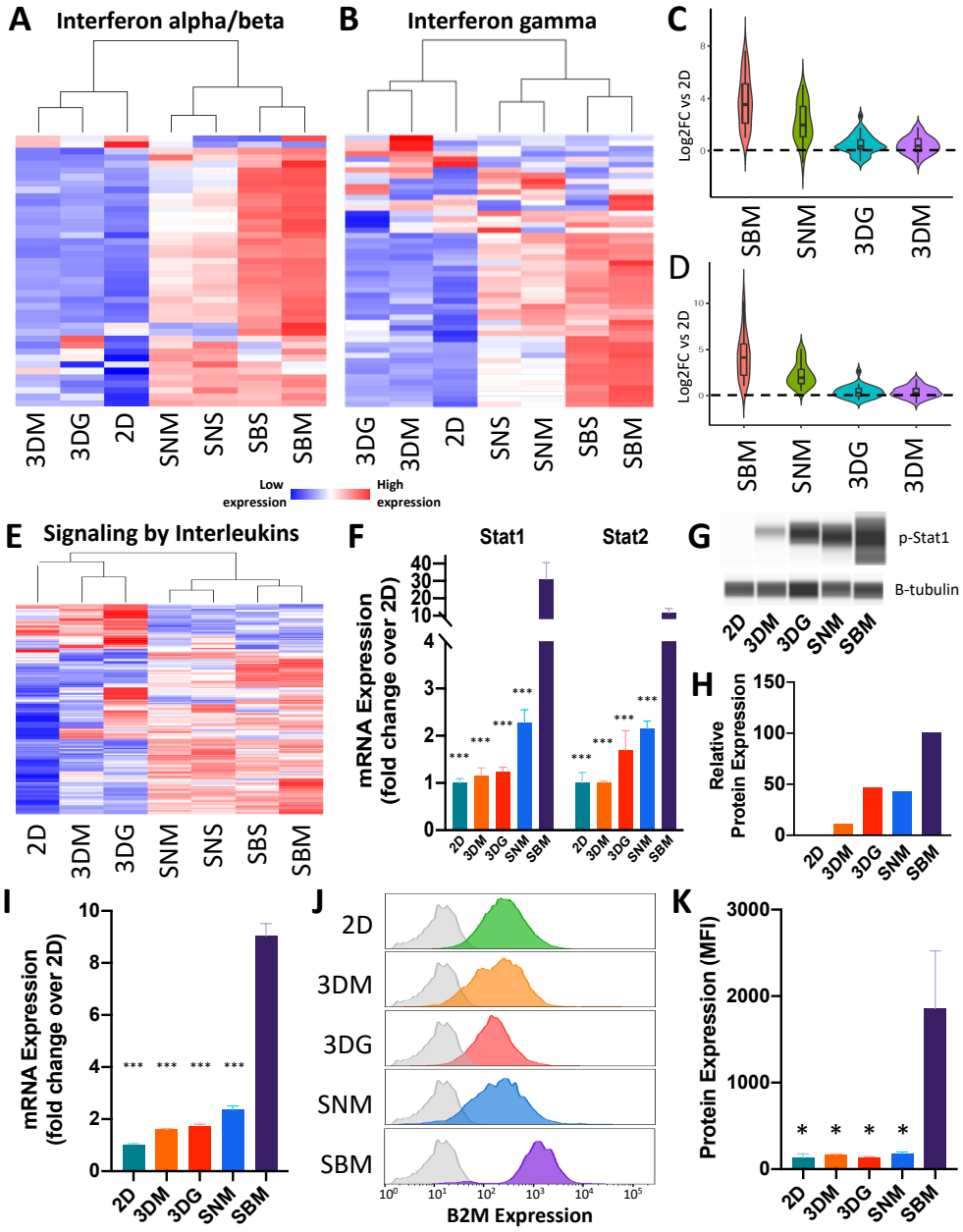


**Figure 5. Cell signaling is highly up-regulated under syngeneic culturing conditions. (A)** Heat map of differentially interferon alpha/beta signaling genes (Table S8) relative to 2D culture (n=4-5). **(B)** Heat map of differentially interferon gamma signaling genes (Table S9) relative to 2D culture (n=4-5). **(C)** Violin plot depicting magnitude of up-regulation and distribution of SBM vs 2D up-regulated interferon alpha/beta signaling genes across other culturing conditions relative to 2D culture. **(D)** Violin plot depicting magnitude of up-regulation and distribution of SBM vs 2D up-regulated interferon gamma signaling genes across other culturing conditions relative to 2D culture. **(E)** Heat map of differential signaling by interleukin genes (Table S10) relative to 2D culture (n=4-5). **(F)** mRNA

expression levels of *Stat1* and *Stat2* in 4T1 cells under different culturing conditions. Expression levels normalized to 2D culture ± SEM (n=4-5). **(G)** Pseudogel representation of protein levels of phosphorylated Stat1 from 4T1 cells cultured across multiple conditions. **(H)** Quantification of p-Stat1 protein levels relative to ß-tubulin. **(I)** mRNA expression levels of B2M in 4T1 cells under differing culturing conditions. Expression levels normalized to 2D culture ± SEM; n=4-5. **(J)** Histogram of representative Beta-2-microglobulin (B2M) abundance of single cancer cells cultured in different methods. Grey shaded plots represent unstained controls. **(K)** Bar graph of flow cytometric analysis of B2M protein expression showing up-regulation in BALB/c MFP. Protein expression values represent background (unstained control) subtracted median fluorescent intensity of cancer cells ± SEM (n=4). (* p value<0.05; *** p value<0.0001 relative to SBM).

IFNγ pathway genes also showed greatest expression in cancer cells cultured under syngeneic conditions with modest up-regulation in immunodeficient *in vivo* conditions and minimal up-regulation in 3D conditions, relative to 2D (Fig5b). Although IFNγ receptors were not up-regulated in SBS and SBM conditions, Beta-2-microglobulin (B2M), a downstream target of IFNγ signaling, was 9.03-fold up-regulated in BALB/c tumors relative to 2D cultures, a >3.5X increase above all other condition (Fig5i), suggesting that cancer cells significantly up-regulate the IFNγ pathway under syngeneic conditions. Quantification of protein levels analyzed *via* flow cytometry confirmed that B2M expression was promoted by a fully competent immune system, with minimal activation in NSG mice or 3D conditions (Fig5j-k). Consistent with interferon signaling, interleukin signaling associated genes were only weakly stimulated in 3D cultures, both in gel or in media, and underlie the necessity of stromal and immune cell signaling for recapitulation of *in vivo* cancer cell behavior.

STAT complexes serve as critical transcription factors mediating gene expression in response to both IFNα/ß and IFNγ signaling (150). Transcriptionally, both *Stat1* and *Stat2* were most highly expressed in syngeneic conditions (Fig5f) however phosphorylation leads to translocation of STAT complexes into the nucleus where they bind DNA and activate target

genes. To examine activation of both these signaling pathways, we quantified phosphorylated Stat1 (p-Stat1) levels as a metric of interferon signaling in 4T1 cells. Consistent with transcriptional levels, a significant increase in pStat1 levels was observed only in BALB/c derived cancer cells (Fig5h).

Critical pathways that indicate the transition from epithelial-to-mesenchymal phenotype (EMT) include suppression of proliferation *via* cell cycle progression, increased ECM remodeling, and stimulation of cell signaling (148). Recently, Pastushenko et al identified the existence of multiple cancer cell subpopulations associated with different EMT states being classified in distinct stages: from epithelial to completely mesenchymal states, passing through intermediate hybrid states which were described as early hybrid, hybrid, late hybrid, and mesenchymal states (151). To determine the cellular EMT states induced by various culturing conditions we first examined the expression levels of genes known to be associated with EMT (Fig6a). As expected, 4T1 monolayers expressed high levels of epithelial markers *Cdh1* and *Esrp* and low levels of mesenchymal markers *Mmp19* and *Vim.* In addition*,* 4T1 monolayers expressed low levels of EMT associated transcription factors *Snai1*, *Zeb1* and *Twist1*. In contrast, EMT markers *Krt14*, *Trp63*, and *Grhl2* which have been recently shown to correspond to an early hybrid state (152), were significantly up-regulated solely in *in vivo* conditions. However, late hybrid *Smad3* and mesenchymal marker *Mmp19* were significantly up-regulated in both 3D and *in vivo* conditions suggesting that tumors *in vivo* reside in more diverse EMT-hybrid states. Suppression of proliferation *via* cell cycle progression, increased ECM remodeling, and stimulation of cell signaling pathways, which are hallmarks of a transition from epithelial-to-mesenchymal phenotype (EMT) (148). To determine the cellular EMT states induced by various culturing conditions we first examined the expression levels of genes known to be associated with EMT (Fig6a) (151). As expected, 4T1 monolayers expressed high levels of epithelial markers *Cdh1* and *Esrp* and low levels of

mesenchymal markers *Mmp19* and *Vim.* In addition, 4T1 monolayers expressed low levels of EMT associated transcription factors *Snai1*, *Zeb1* and *Twist1*. In contrast, EMT markers *Krt14*, *Trp63*, and *Grhl2* which have been recently shown to correspond to an early hybrid state (151), were significantly up-regulated solely in *in vivo* experimental conditions. However, late hybrid *Smad3* and mesenchymal marker *Mmp19* were significantly up-regulated in both 3D and *in vivo* conditions suggesting that tumors *in vivo* reside in more diverse EMT-hybrid states under the culturing conditions described.

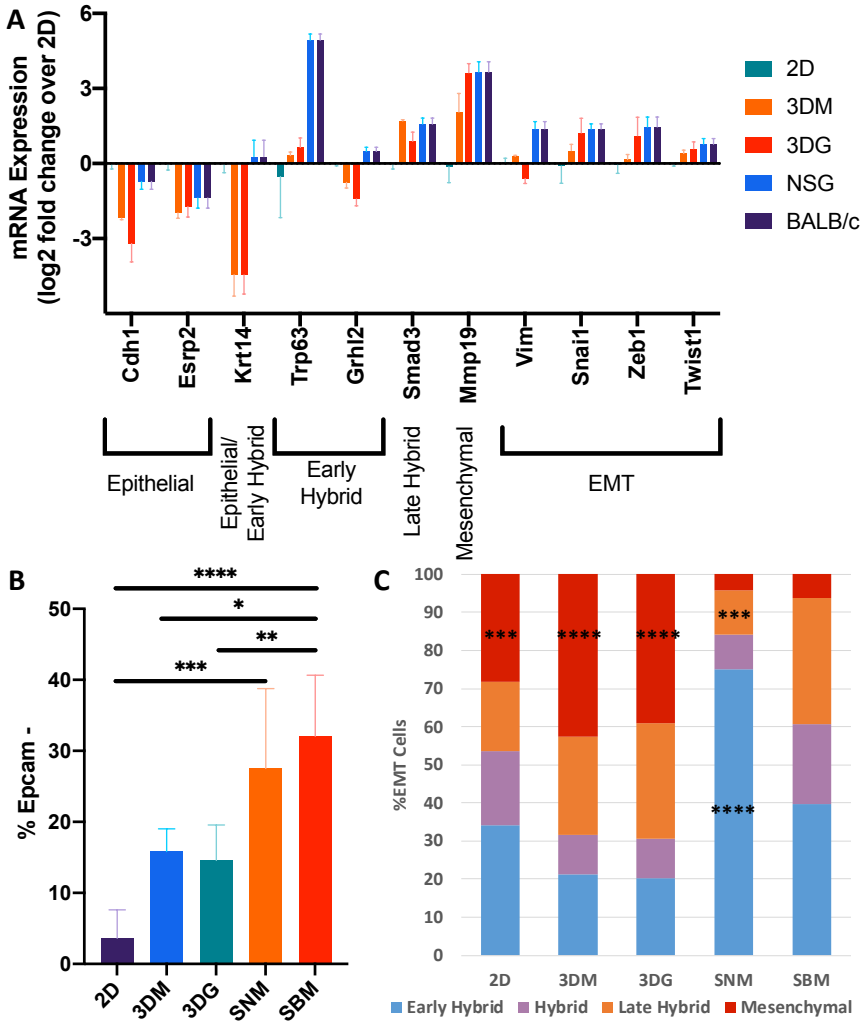


**Figure 6. 4T1 cells *in vivo* reside in multiple transitional EMT states. (A)** 4T1 log2 expression of EMT related genes under different culturing methods relative to 2D culture. Error bars ±SEM. **(B)**

Proportion of cells lacking Epcam expression based on flow cytometric analysis (n=4-7). Error bars ±SD (C) Distribution of EMT cells across hybrid EMT states induced by culturing method (n=4-7). * $p<0.05$, ** $p<0.0005$, *** $p<0.0005$, **** $p<0.0001$ relative to SBM.

Flow cytometric analysis was utilized to further probe the heterogeneity of EMT states induced by 2D and 3D culturing and gated based on previously described methods (151). Loss of epithelial phenotype was primarily examined through the loss of Epcam expression. Consistent with the transcriptional data, monolayers largely maintained epithelial status with only 3.6% of cells undergoing EMT. 3D cultured samples increased the frequency of cells undergoing EMT however, this increase was not statistically significant from monolayer culture. Additionally, there was no difference observed as a result of encapsulation into the hydrogel (15.8% in media and 14.6% in gel). *In vivo* conditions induced a significant increase in the abundance of these cells (27.5% SNM, 32.1% SBM) with no significant differences between immunodeficient and immunocompetent hosts (Fig6b).

Cells undergoing EMT were further analyzed for the frequency of hybrid states based on the presence of cell surface markers CD51, CD61, and CD106. Transitional hybrid EMT states were classified into progressively more mesenchymal subpopulations as follows: (1) early hybrid EMT (triple negative and CD106+), (2) hybrid EMT (CD51+, CD51+/CD106+), (3) late hybrid EMT (CD51+/CD61+), and (4) Mesenchymal (CD51+/CD61+/CD106+). *In vitro* culturing promoted a greater abundance of mesenchymal cells than *in vivo*. Additionally, *in vivo* cultured cells possessed an increased abundance of early and hybrid populations relative to *in vitro* samples. Stromal composition *in vivo* was associated with EMT distribution as shown by the increased abundance of early hybrid and decreased abundance in late hybrid EMT cells in immunodeficient tumors relative to syngeneic tumors. (Fig6c).

*Ex vivo tumoroids inclusive of stromal cells preserve in vivo behavior.*

As shown by altered cell signaling processes and EMT distribution at the RNA and protein level, the effects of stromal complexity undoubtedly affect cancer cell behavior; however *in vitro* research with cell lines is classically performed exclusive of stromal cells. In order to examine the contributions of stromal cells *in vitro*, we created *ex vivo* tumoroid cultures from tumor cell homogenates cultured for 5 days as a monolayer or spheroids prior to FACS sorting of cancer cells for transcriptomic analysis (Fig7a). Incorporation of stromal components increased 4T1 global transcriptomic similarity to syngeneic SBM conditions where *ex vivo* monolayer (EV2D) and spheroid (EV3D) had increased similarity to *in vivo* cultured compared to any other 4T1 *in vitro* method (Fig7b). Interestingly, in silico hierarchal clustering of 4T1 transcriptomes was capable of differentiating *in vitro* from *in vivo* conditions (Fig2c) however incorporation of tumoroid cultures aligned EV3D closer to *in vivo* conditions, while the EV2D more similar to the *in vitro* culturing (SFig 4).

Examination of ex vivo gene regulation of critical cancer processes previously profiled further support global transcriptome analysis that EV3D tumoroids best retain *in vivo* characteristics compared to EV2D or homogenous *in vitro* cultures in cell cycle, ECM, and cell signaling (Fig7c-e). EV2D samples had improved *in vivo* gene expression similarity in ECM and cell signaling genes however cell cycle genes reverted to a monolayer-like expression level after 5 days of ex vivo culture. The presence of stromal cells in tumoroid cultures also maintained high rates of cancer cells EMT diversity (Fig7f) regardless of 2D or 3D culture. However, ex vivo culturing rapidly encourage EMT cells into a more mesenchymal state and reduced the frequency of cells present in transitional EMT states as both tumoroid conditions yielded more EMT cells in a mesenchymal state (EV3D: 49%, EV2D: 35%) in similar abundance to 4T1 cultured in 3D alone. Late hybrid populations were also significantly lower (EV3D: 17%, EV2D: 7%) than in syngeneic tumors.

Surprisingly, EV2D maintained a higher rate of early hybrid EMT cells (48%) while EV3D frequency was reduced (22.5%) (Fig7g).

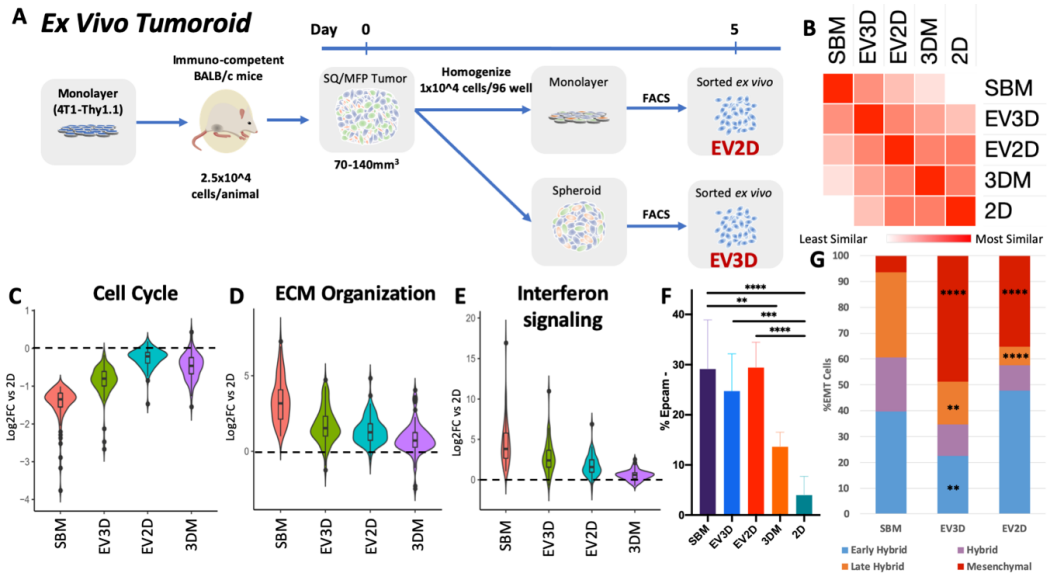


**Figure 7. *Ex vivo* tumoroid culture encourages *in vivo*-like cancer cell behavior. (A)** *Ex vivo* tumoroid culture experimental design. **(B)** Similarity matrix of 4T1 transcriptomic profiles across *in vivo*, *ex vivo*, and *in vitro* conditions. **(C)** Violin plot of magnitude of differential expression of cell cycle DEGs of SBM *vs* 2D across culturing conditions. **(D)** Violin plot of magnitude of differential expression of ECM organization DEGs of SBM *vs* 2D across culturing conditions. **(E)** Violin plot of magnitude of differential expression of interferon signaling DEGs of SBM vs 2D across culturing conditions. **(F)** Flow cytometric analysis of 4T1 cells undergoing EMT following 5 days of *ex vivo* culturing. **(G)** Abundance of hybrid EMT states following *ex vivo* culturing. Tumoroid conditions n=6 from 3 independent tumors. * $p$<0.05, ** $p$<0.0005, *** $p$<0.0005, **** $p$<0.0001 relative to SBM.

The inclusion of stromal heterogeneity into tumoroid cultures recapitulated aspects of syngeneic cancer cell behavior yet tumoroid cultures still evolved features associated with *in vitro* culturing of 4T1 cells alone. We hypothesized that this rapid change may be in part due to loss of specific stromal subpopulations. In order to investigate differences in tumor and tumoroid composition, scRNA-seq was utilized to compare cellular heterogeneity in 3D tumoroid cultures (Fig8a FigS4). Cancer cell populations more than doubled over the 5 days of *ex vivo* culture, increasing the ratio of tumor cells from 24.7% in the harvested tumor to 59.7% in the tumoroids

(Fig8b). The expansion of cancer cell populations *ex vivo* was validated via flow cytometry and observed in in both 2D and 3D conditions (FigS5). More specifically, *ex vivo* culturing encouraged the expansion of Epcam$^{+}$/Mki67$^{+}$ cancer cells from 7.4% to 30.1% of the total cells (Fig8c). Fibroblasts comprise 8.0% of the original tumor and *ex vivo* culturing expanded this population to 16.0% of the tumoroid. In particular, the myofibroblast [Thy1$^{+}$/Dcn$^{+}$/Acta2$^{+}$ (αSMA)] population which comprise 4.8% of all cells in a tumor increased to 15.9% of tumoroid cells (Fig8e). In contrast, endothelial cells (0.4%) were completely absent from the tumoroid cultures.

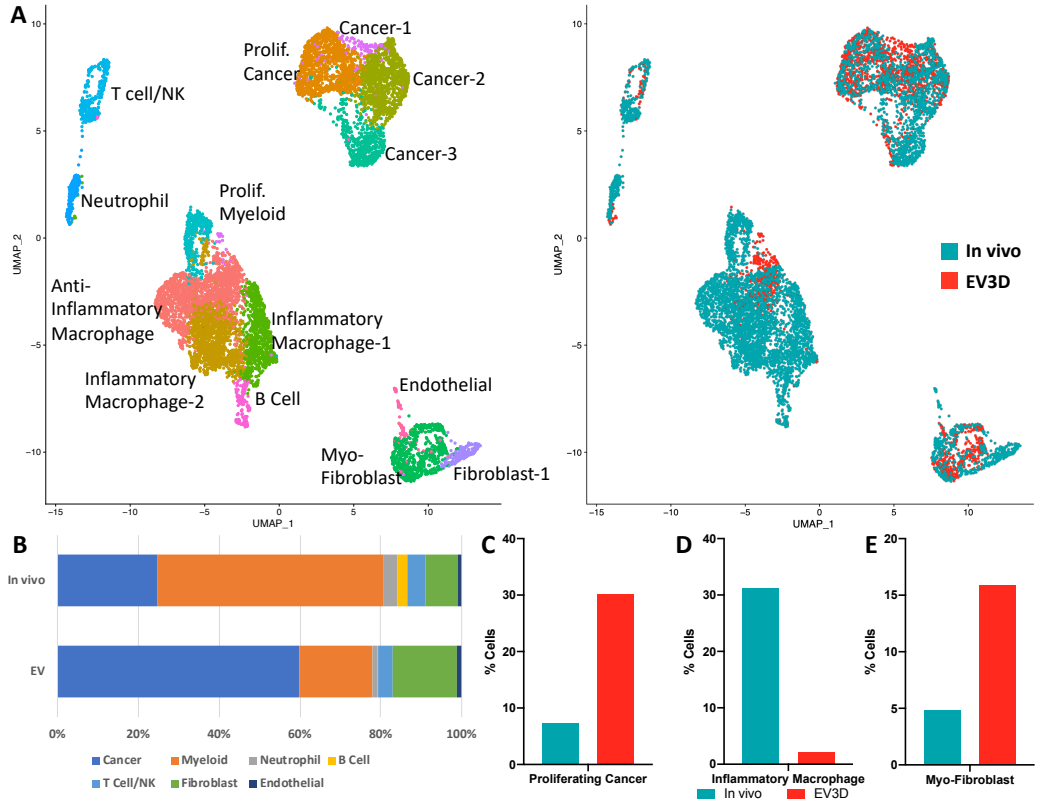


**Figure 8. Single cell RNA-seq analysis of 4T1 tumor and tumoroid cultures. (A)** Merged UMAP projection of identified cells from a syngeneic tumor (*in vivo*) and 5-day *ex vivo* tumoroid (EV3D) cultures. **(B)** Cell type abundance from original tumor and tumoroids. **(C)** Abundance of proliferating cancer cells (Epcam$^{+}$/Mki67$^{+}$) in tumor/tumoroid. **(D)** Abundance of inflammatory macrophages (Ptprc$^{+}$/CD14$^{+}$/Il1b$^{+}$) in tumor/tumoroid. **(E)** Abundance of myofibroblast (Thy1$^{+}$/Dcn$^{+}$/Acta2) n tumor/tumoroid.

4T1 syngeneic tumors were discovered to have high immune (Ptprc/CD45$^{+}$) infiltration with a high abundance of myeloid derived neutrophils (3.4%) and monocytes/macrophages (55.9%) (Fig8a). During *ex vivo* culture these populations were both reduced to 1.2% and 18.1%, respectively. Furthermore, the loss in monocyte/macrophage abundance was largely attributed to inflammatory macrophages (Ptprc$^{+}$/CD14$^{+}$/Il1b$^{+}$) that were reduced from 27.9% to 0.3% of the tumor, post *ex vivo* culturing (Fig8d), while anti-inflammatory and proliferating myeloid cells maintained comparable ratios in tumoroid cultures ~17.0% and ~3.4%, respectively. T-cell/Natural killer populations remained in similar proportions (~4%) following *ex vivo* culture as well as endothelial cells comprising ~1% of the cells in both conditions. Lastly, B-cell populations comprised 2.6% of cells *in vivo* yet decreased *ex vivo* to 0.3% in tumoroids (Fig8a).

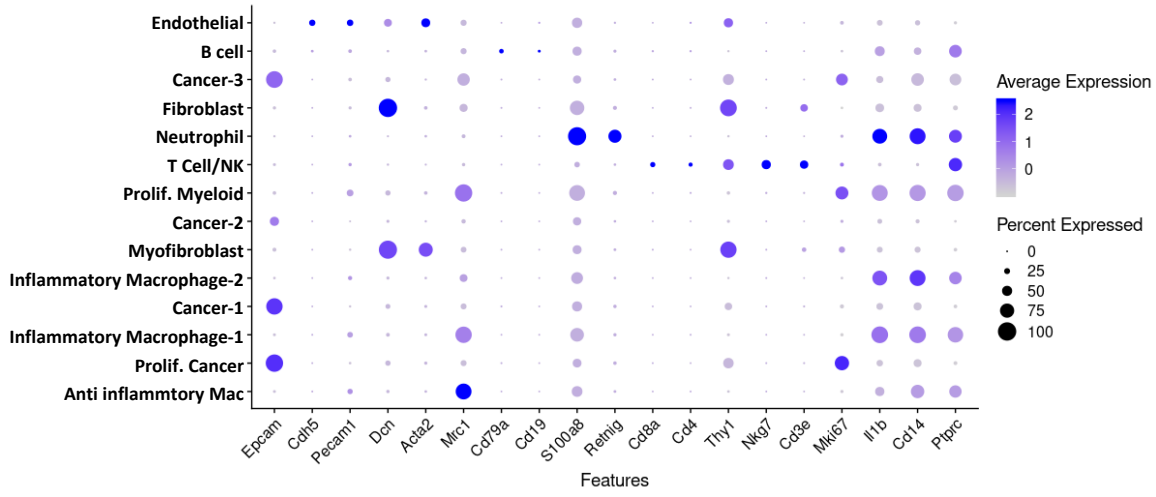


**Supplemental Figure 4. Dot blot of genes used to identify cell clusters.** Intensity of dot indicates average cell expression and size of dot represents percent expressed in cluster.

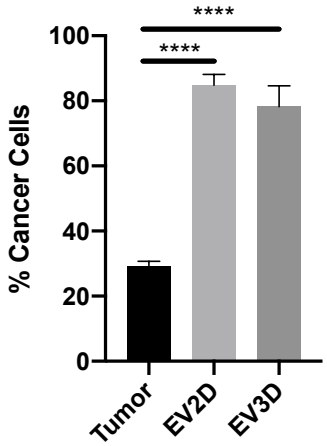

**Figure S5. Cancer cell expansion in *ex vivo* culture.** Abundance of 4t1-Thy1.1 expressing cells in tumor and 5-day *ex vivo* cultures analyzed via flow cytometry. n=3 ****p<0.0001

## Discussion

Our study demonstrates the importance of culture platform selection in pre-clinical and research applications. Comparisons of purified cancer cells from different *in vitro* conditions (2D, 3D in media or hydrogel) and *in vivo* (immune- deficient and -competent mice, orthotopic and subcutaneous) studies revealed that cancer cell phenotype is highly influenced by its microenvironment. Conventional transcriptomic analysis of whole tumor bulk RNA analysis can lead to erroneous interpretations of tumor biology; we found that only 39% of transcripts significantly changed in cancer cells purified from orthotopic immune-competent tumors (SBM) overlapped with genes significantly changed when whole tumor bulk RNA was performed (Fig2e). Furthermore, 2402 significantly changed SBM transcripts were distinct from TBM significant changes. These results suggest that bulk tumor RNA analysis overlooks a vast molecular space that can be potentially interrogated for contribution to cancer progression, invasion, metastasis, and response to therapy.

Upon examination of solely cancer cell transcriptional behavior, cellular processes prioritized were closely linked to functions promoted by different culturing condition. For example, cancer cells grown in monolayers favored rapid proliferation, and this behavior was corroborated molecularly by significant up-regulation of cell cycle progression genes in addition to metabolic processes that synthesize DNA, RNA, and proteins. 2D cultured cells also maintained a high level of cellular homogeneity where ~96% of 4T1 cells persisted in an epithelial cell state. Carcinomas of different tissue origin, including lung and gastric, have been documented to undergo EMT, as characterized by a loss in epithelial behaviors like cell polarity and cell-cell

adhesion (152) and a decreased proliferation in cells up-regulating EMT genes (153).

Unlike cancer cells cultured in monolayers, cancer cells in 3D down-regulate proliferative processes, while up-regulating genes involved in ECM organization and cell adhesion. Spheroids in gel showed minimal changes in gene expression profiles compared to spheroids in media alone, and some of the differences were in genes associated with migration and angiogenesis, suggesting that cancer cells suspended in hydrogel may experience a more hypoxic, nutrient deficient environment. Cancer cells heterogeneity also increased under these conditions where more cells lost epithelial landmarks and may have differentiated into various EMT state (15%). Recent studies have suggested that cancer cell within tumors acquire and maintain a diverse array of subpopulations that correspond to transitional hybrid E/M cell states, *in vivo* (151,152,154–156) opposing the classical understanding of EMT as a binary process where cancer cells are either epithelial or mesenchymal (157). While we did determine that all culturing approaches investigated possessed subpopulations of cancer cells in all previously described EMT states, *in vitro* cultures promoted a binary-like distribution where the majority of cells were found either in an epithelial or a fully mesenchymal cell state (97% of 2D and 91% of 3D).

Unlike cancer cells cultured *in vitro*, characterization of cancer cells from *in vivo* tumors has revealed a high degree of heterogeneity. Epithelial tumors have been shown to exhibit significant plasticity that allowed cancer cells to dynamically shift from epithelial to mesenchymal phenotypes and reside in a range of transitional states. In 2018, Pastushenko *et al.* highlighted the presence of EMT transition states in a genetic mouse model of squamous cell carcinoma, an epithelial malignancy, and through molecular characterization developed a cell sorting panel for early and late hybrid states to distinguish specific subpopulations actively undergoing EMT. Using the same FACS cell

sorting approach developed by Pastushenko *et al.* our experiments show that *in vivo* tumors initiated by 4T1 cells produced an EMT profile similar to that found in 10% of squamous cell carcinoma tumors (151). The main difference between *in vivo* cancer cell heterogeneity and that of *in vitro* or *ex vivo* cultures was the significant shift towards mesenchymal fate, *in vitro*, where only ~6% of a cancer cells in BALB/c tumor resided in a mesenchymal state, while 28-48% cancer cells were mesenchymal, in culture. It is important to note that *ex vivo* cultured tumoroids also rapidly transitioned to mesenchymal, expanding from 6% in the original tumor, to as much as 48% in the EV3D tumoroid. One potential contributor to this rapid shift to mesenchymal state may be the depletion of a stromal cell type that normally inhibits epithelial to mesenchymal transition. Since neutrophils, endothelial cells and inflammatory macrophage populations all seems to rapidly diminish in *ex vivo* cultured tumoroids, these cell types are likely to contribute to this phenotype.

The deviation of oxygen levels from physiological (~5% in normal tissue and <2% in tumors) to *in vitro* cultures (21%) may also play a critical role in recapitulation of *in vivo* cancer cell and tumoroid behavior (158). Reactive oxygen species that result from oxidative stress has been linked to numerous cancer types and phases of tumorigenesis resulting in the activation of inflammatory signaling (159). The underrepresentation of inflammatory cell populations discovered in this study may in turn be a response to a lack of oxidative stress imparted by culturing *in vitro*. Furthermore, cell signaling pathways upregulated in cancer cells under *in vivo* conditions (interferon, MAPK, TNF cytokine/interleukin) have previously been implicated in upregulation in response to oxidative stress response (159). Future *in vitro* tumor platforms should therefore be cognizant of oxidative stress levels and their downstream effects on cellular behavior and tissue dynamics.

It is important to note that NSG, similar to fully immune competent mice also had a low percentage of cancer cells residing in the mesenchymal state,

and NSG mice have normal functioning neutrophils. Therefore, a future testable hypothesis would be to investigate the role neutrophils may have in modulating EMT states. While we clearly find changes in EMT subpopulation ratios as culture conditions are changed, future experiments will have to validate the role these transition states may play in tumor progression and metastasis. Pastushenko *et al.* suggested that a hybrid EMT phenotype may be associated with increased tumor stemness, whereas a fully epithelial or fully mesenchymal phenotypes may be associated with loss of stem cell markers and tumorigenicity (150). While this may be the case for some tumor subtypes, additional experiments will have to conducted where hybrid EMT subpopulations would need to be further functionally characterized to determine which tumor behavior they promote.

Direct comparisons of tumors cultured in NSG and BALB/c mice allowed us to determine the impact a fully competent immune system has on the transcriptional program of cancer cells. A thorough understanding is critical for assessing the limitations of characterizing human tumors in PDX mice. As anticipated, we found that cancer cells purified from BALB/c tumors expressed very high levels of cytokines, growth factors and members of the INFα/ß and INFγ signaling pathways, hallmarks of an active interaction with the immune system. While PDX mice will continue to be invaluable resources for exploring therapeutic treatments that are independent of immune function, such as chemotherapies and cell cycle checkpoint inhibitors (160), therapies that engage the immune system to kill the tumor will require the development of *ex vivo* bioreactor type methodologies that will permit the incorporation of all immune components.

The alterations in cancer cell behavior under differing conditions presented in this study underlie the importance of proper culturing conditions pertaining to the application. While monolayer culturing yields the most non-native behavior of cancer cells, this model still maintains value due to its ease and

scalability of culture in applications targeting unaltered cancer driving pathways. Moreover, analysis and discovery of potential therapeutics targeting stromal interactions, ECM development, or cell signaling may yield erroneous results. Increased efforts to mimic the complexity of the native tumor microenvironment will be necessary to create useful models used for *ex vivo* therapeutic screening and novel drug development. 3D culturing and inclusion of stromal cell types do show increased similarity to *in vivo* cancer behavior. However, improvements upon *ex vivo* culture conditions that allow all stromal components to persist will greatly enhance our ability to conduct pre-clinical screens that may more closely recapitulate the biological responses of patients.

While cancer cell heterogeneity recapitulation will be a necessary method of assessing preclinical cancer model efficacy, it is important to note that we only surveyed *in vitro* cultures and *in vivo* tumors at a single time point. An ideal tumor model will be capable of reproducing the dynamics of cancer progression as it is likely that these populations will shift as the cultures/tumors progress, especially during metastasis. Future longitudinal surveys of tumor subpopulations will be required to functionally define the role of these EMT states during cancer progression and metastasis. Additionally, the location of these EMT subpopulations within the tumor microenvironment may be important factors in recapitulating native cancer cell behavior, and a thorough understanding of the tumor architecture will inform any future bioprinting approaches. Subsequent analysis of spatial organization or co-localization with fibroblasts, endothelial and immune cells and how microarchitecture contributes to EMT state will add further resolution to understanding tumor microenvironment effects on cancer cells and be able to educate future tumor model approaches to appropriate cellular compositions. Importantly, this study demonstrates the need for comparative studies which incorporate multiple culture platform types for characterizing preclinical cancer model efficacy.

For cancer drugs to fulfill their promise in clinical trials we need better screening platforms that reliably mimic responses in humans. Towards this goal, a better understanding of tumor heterogeneity and phenotypic plasticity is needed, as well as of *ex vivo* conditions that maintain this plasticity post resection. Recent *in vivo* work, in immune competent mice, demonstrated that the cancer EMT process is not binary but rather spans a range of intermediate states, and postulated that these cancer cellular phenotypes may specifically promote cancer progression, metastasis and drug resistance. Here we showed for the 1st time that that cancer EMT spectra is modulated by a fully competent immune system, such that tumors grown in immune deficient mice had most of the cancer cells in early hybrid state, while tumors in BALB/c mice had >50% of cancer cells in hybrid and late hybrid states. Most significant however, is the result that *in vitro* and *ex vivo* conditions rapidly promote a mesenchymal state, suggesting that any drug screens conducted on organoids may only reflect the phenotype of these cells, which *in vivo* account for less than 10% of all cancer EMT subtypes. Our study also shows for the 1st time that tumors cultured *ex vivo* rapidly become depleted of inflammatory macrophages and neutrophils, while the fibroblasts rapidly expand to include primarily the myofibroblast subtype. These results highlight the need to continue to improve 3D culturing conditions to preserve stromal components and EMT diversity, such that future drug screen can identify therapies that will stop cancer in its track.

Supplementary Materials: The following are available online at www.mdpi.com/xxx/s1, Supplementary tables are available at https://ucmerced.box.com/s/kpv314alyjrlf5kuslt0qs2kvpdlljwj

## Chapter 3. *Ex vivo* triple negative breast cancer tumor culturing optimization

### Abstract

Translation of pre-clinical findings into a clinical setting remains a huge hurdle hindering cancer research. Previous research has identified cell behavioral biases imparted because of differing preclinical approaches, yet recapitulation of the native tumor microenvironment remains elusive. This study aims to evaluate the retention of native cancer cell behavioral in a longitudinal study across 6 conventional preclinical cancer culturing approaches. Specifically, mouse mammary carcinoma (4T1) tumors were harvested from syngeneic, orthotopic mice and subsequently cultured using various methods over the course of 12 days. *Ex vivo* cultures were first assessed for retention of tumor cellular heterogeneity using endogenous Thy1.1 (CD90.1) expression via flow cytometry to distinguish 4T1 cancer cells from stromal derived cells. Cancer cells from each culturing technique were also evaluated for cellular states related to epithelial to mesenchymal transition (EMT) relative to the distribution at time of isolation. Subsequent analysis of EMT populations for transitional hybrid states based on CD51, CD61, and CD106 expression was conducted using flow cytometric analysis. Cancer cell populations were found to rapidly expand ~2 fold by 3 days in culture compared to the original tumor population. *In vitro* culturing was also found to promote mesenchymal EMT and discouraged hybrid and late hybrid states. Overall tumoroid cultures in media were found to best retain native cancer cell behaviors amongst culture conditions evaluated.

## Introduction

Pre-clinical tumor models serve as an invaluable tool for basic research and translation into clinical practice. Faithful recapitulation of tumor response to therapeutic screening *ex vivo* has potential to vastly improve treatment efficacy, identify and validate novel therapeutic targets, and reduce treatment time to minimize therapeutic side effects. The utility of pre-clinical tumor models and the impact cancer cell culturing conditions have on tumor behavior is not a novel concept. This idea can be traced back over 100 years ago when Rous et al. observed alterations in mouse tumor growth rates due to changes in the host diet (161). Within the last century, steady improvements in tumor modeling have resulted from an increased understanding of cancer behavior (162).

Furthermore, technological advances have played a pivotal role in development of novel therapies resulting improved cancer survival rates (85,163,164). Despite the evolution of pre-clinical cancer approaches, there remains a disparity when transitioning research successes to the clinic. A study examining novel cancer-targeting drugs identified that only 3.4% of therapies pass clinical trials and were approved for use in patient care underlying the necessity for further improvements in clinically relevant pre-clinical cancer models for diagnostic and discovery applications (165).

While all cancer cell models and culturing techniques have unique benefits and limitations, an optimal pre-clinical culturing system would accurately recapitulate the idiosyncrasies of the native tumor in a reliable and reproducible fashion. For example, immortalized human cancer cell lines grown *in vitro* have the distinct advantage of reproducibility, species similarity and ease of use, however, offer an extremely oversimplified view of the tumor landscape by only representing only the cancer cells and not stromal cells that

are known to play a critical role (166). Mouse models, on the other hand, such as i*n vivo* models of patient-derived xenografts (PDXs) have been employed on a multitude of cancer types and evolved into an indispensable tool to retain clinically relevant tumor genomic mutations and behavioral traits (167,168)

As demonstrated in Chapter 2, cancer cell behavior is heavily affected by culturing environment, spatial organization, and stromal complexity. Numerous studies have sought to address specific deficiencies of classical cancer culturing approaches with success yet integration of these optimizations into more universal protocols has proven more challenging (169,170)

Conventional primary cancer cell culturing has largely based culturing techniques on encouraging proliferation and attachment of cancer cells in an epithelial or stem cell like phenotype in monoculture. One such media developed by the Hans Clevers lab, WENR media, contains supplementation of standard cell culture media with recombinant Wnt3a and EGF for proliferative stimulation and noggin, and R-spondin-1 to retain stem like behavior (171–173) Other media formulations exist for specific cancer subtypes based on recapitulation of the native TME (for example added estrogen for breast cancer or androgen for prostate cancer) yet these custom cocktails of growth factors are designed to support monoculture and not retention of native *in vivo* tumor behavior so would not be ideal in a preclinical use of stromal targeted or phenotypic targeted therapies (174). Other modifications utilized in next generation tumor culture models contain optimization of ECM components, addition of fluidic control of nutrients, and spatial organization through bioprinting technologies (175). Additionally, adding complexity to these cancer monocultures has shown limited utility due to the difficulty in recreating the native tumor complexity and maintenance of

the TME heterogeneity. Optimal *in vitro* tumor models therefor have proven to be an elusive goal and remains an outstanding concern for pre-clinical cancer models.

*Ex vivo* culturing has gained further attention as a possible approach to enable a more personalized approach to clinical cancer care. Current approaches range in complexity from monolayer and spheroid cultures to retention of tumor fragments as organoids or tumoroids (176). Specifically, culturing patient derived tumoroids has become an emerging technique that has provided promising results in the last decade as an improved pre-clinical model capable of replicating clinical response to chemotherapeutic therapies across a multitude of cancer types. This technology aims to retain tumor complexity and clinical cancer behavior through passage and *ex vivo* growth of primary tumor fragments. Short falls in predictive response have also been reported using this technology yet deconvolution of the causes of the alternative response rates *in vitro* remain elusive.

EMT of cancer cells during tumor progression has been implicated in tumor initiation, growth, invasion, metastasis, colonization, and resistance to therapy. In building a successful *in vitro* tumor model, it is critical to recapitulate *in vivo* cancer cell heterogeneity inclusive of both cell types and transition state present. This study investigates the EMT hybrid states of mouse triple negative breast cancer cells during *ex vivo* culturing across multiple platforms.

The cellular composition of tumors is highly variable among patients (177–179) Differential cell composition has a large impact on cancer cell behavior *via* modulations of ECM components, cell signaling, and nutrient accessibility and in turn creates microenvironments unique to each tumor. In order for *in vitro*

preclinical models to faithfully recapitulate tumor behavior, careful optimization of culture conditions is critical. In building a successful *in vitro* tumor model, it is critical to recapitulate *in vivo* cancer cell heterogeneity inclusive of both cell types and the cancer transition states present.

Therefore, research presented in this chapter aims to identify strengths and weaknesses of existing methodologies at maintaining *in vivo* cancer cell properties. To accomplish this goal, syngeneic murine mammary carcinoma (4T1) cells were utilized as a model of TNBC tumors. Tumors were harvested for *ex vivo* culture utilizing three commonly used culturing techniques (single cell suspensions, spheroids, tumoroids) with and without a supplemented hydrogel ECM to perform a longitudinal study of culture approach induced alterations in cancer abundance and behavior when all tumor populations are cultured *ex vivo*. The findings resulting from this analysis provides the framework for future improvements in creation of an optimal *ex vivo* tumor that retains *in vivo* like behavior for pre-clinical cancer testing.

## Materials and Methods

### *Cell culturing and allograft generation*

4T1-Thy1.1 cell line was graciously provided as a gift from Dr. Julian Lum (143) and was used in allograft and *in vitro* experiments. 4T1 cells were cultured in RPMI Medium 1640 containing 10% FBS with 100,000 U/L of penicillin and 100 mg/L of streptomycin at 37 °C with 5% $CO_2$. Female BALB/c mice at 8-10 weeks of age (Jackson Laboratories, Bar Harbor, ME, USA) were injected with $1 \times 10^5$ 4t1-Thy1.1 cells and tumors were collected at 500 $mm^3$. Moribund behavior was evaluated regularly throughout the tumor bearing period. All animal experimental procedures were completed under an approved Institutional Animal Care and Use Committee (IACUC) protocol at Lawrence

Livermore National Laboratory (LLNL) and conforming to the National Institute of Health (NIH) guide for the care and use of laboratory animals.

*Tumor single cell isolation and enrichment*

Single-cell suspensions of tumor cells were prepared by passing the tumor through a syringe without a needle. If designated for physical homogenization only, isolate was size selected using 70 and 100 uM cell strainers ("tumoroid) or further manually dissociated to collect single cells deemed for "single cell suspension" groups and plated accordingly. Samples designated for enzymatic homogenization were further digested for 1 h with shaking at 37 °C in 100 μg/mL DNase I (Roche, Basel, Switzerland; catalog no. 11284932001), 300 U/mL collagenase/100 U/mL hyaluronidase (Stemcell Technologies, Vancouver, Canada; catalog no. 07912), 0.6 U/mL Dispase II (Roche, Basel, Switzerland; catalog no. 4942078001) in DMEM/D12 with 10% FBS (Gibco, Waltham, MA, USA). All digests were filtered through a 100 μm cell strainer prior to debris removal per manufacturer's guidelines (Miltenyi Biotec, Bergisch Gladbach, Germany; catalog no. 130-109-398) and resuspended in BD FACS Pre-Sort Buffer (BD, Franklin Lakes, NJ, USA; catalog no. 563503).

*Ex vivo cell culture*

Following homogenization by either physical or enzymatic methods as previously described, $1x10^4$ cells were then plated into each well of a 96-well flat bottom cell culture plate (with or without 50% hydrogel) for the "single cell" experimental group and into a U-bottom 96-well plate with a hydrophilic, biologically inert, and non-degradable ultra-low attachment surface coating (Greiner, Germany) in 150 μL of complete RPMI (with our without hydrogel) for the "spheroid" experimental group for subsequent analysis. Tumoroids were plated onto non-adherent 24-well polystyrene plates at a density of approximately 10 tumoroids/well with or without 50% hydrogel in RPMI media

for downstream assays, with one replicate representative of 10 spheroids/well. Cultures were imaged using brightfield at days 3, 7, 12 of *ex vivo* growth at 10x magnification on a Leica DMI6000B microscope.

*Flow Cytometry and epithelial to mesenchymal transition (EMT) analysis*

Dissociation of monolayer, spheroid and tumoroid cultures were accomplished using Accutase (Stemcell Technologies) until single cell suspensions were achieved. Prior to Accutase treatment, spheroids and tumoroids were released from hydrogels by first mincing gels into ~1mm fragments followed by incubation in Collagenase 1 (Gibco 17100-017, 2mg/ml) in complete media shaking at 37 ◦ C for 1-1.5 hours or until gel is completely dissolved. Cell Sorting was performed using either a FACSMelody (BD Biosciences) or FACSAria Fusion (BD Biosciences) instrument. 4T1 cancer cells were identified via flow cytometry using endogenous Thy1.1 expression detectable by a CD90.2 antibody (Miltenyi Biotec, 130-102-637). Cultures were collected for analysis EMT status at days 3, 7 and 12 of ex vivo growth. Protein expression of EMT markers was quantified using Biolegend antibodies FITC anti-mouse CD326 (Ep-CAM) (118207), PE anti-mouse CD51 (104105), Fluor® 647 anti-mouse/rat CD61 (104313), PerCP/Cy5.5 anti-mouse CD106 (105715) were used at a 1:100 dilution prior to analysis on a BD FACSMelody cell sorter.

*Statistical analyses*

Statistical analyses were performed using GraphPad Prism. Data is presented from at least three biological replicates. One-way ANOVA and post-hoc Tukey's Test were used to assess statistically significant differences of mean expression values. Results were considered statistically significant for $p$ values $< 0.05$.

## Results

Building upon the flow cytometric based analysis used in Chapter 2 for discriminating culture induced cancer phenotypic changes, the work presented here will focus on retention of cancer behavior *ex vivo* inclusive of stromal cellular heterogeneity. Findings from Chapter 2 confirmed results from numerous published studies, that inclusion of stromal contributions is a clear necessity for any pre-clinical model to accurately examine cancer cell behavior or drug response. The separation of solely cancer cells from a primary tumor from a patient will likely result in incomplete and/or biased enrichment of cancer cells. As a result, this work focused on primary tumor ex *vivo* cultures, inclusive of stromal and cancer cell populations. In order to address heterogeneity originating from differences in the tumor architecture and ECM contributions, tumor fragments (tumoroids; comparable to patient derived organoids) will also be examined in this study. Furthermore, cancer cell population shifts as determined by EMT status resulting from length of time grown in an *ex vivo* environment was also assessed.

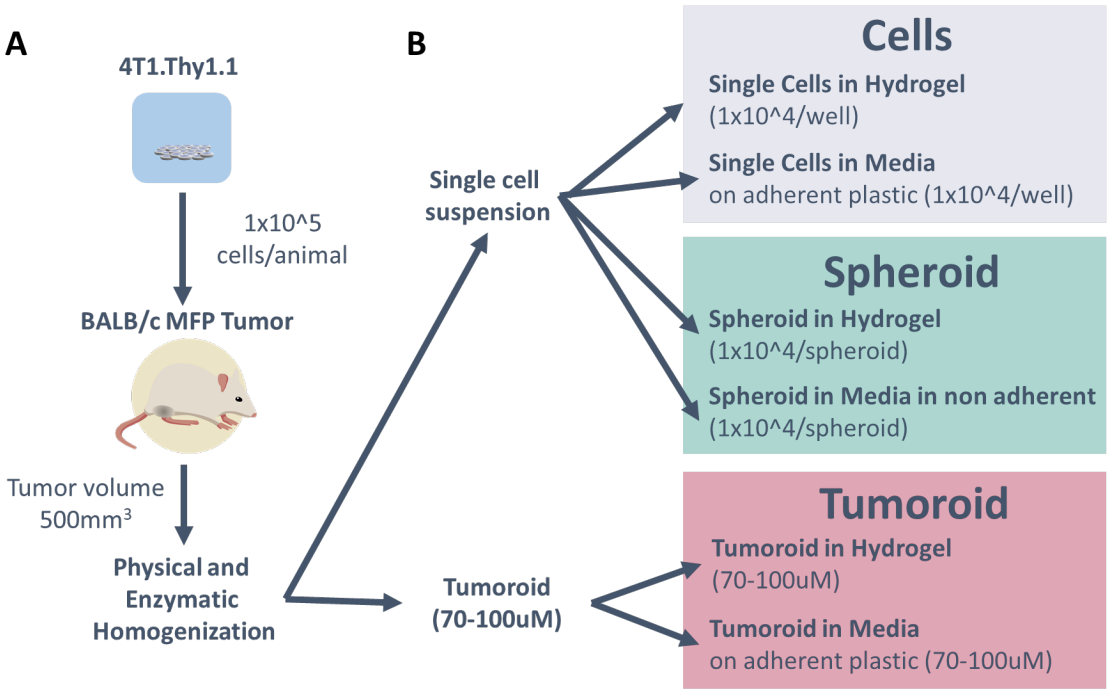


**Figure 1. 4T1 *ex vivo* culture comparative analysis experimental overview.** Tumor derived cells were isolated from 4T1 syngeneic MFP tumors (A). Upon tumor homogenization, *ex vivo* cultures were grown for up to 12 days in differing conditions (Cells, Spheroid, or Tumoroid) and environments (media only or hydrogel/media) (B).

Transgenic 4T1 cells constitutively expressing Thy1.1 were utilized for this study to easily denote and separate cancer cells ($Thy1.1^{+}$) from stromal cells ($Thy1.1^{-}$) in the tumor. $1x10^5$ 4T1-Thy1.1 cells were injected into the mammary fat pad of 10-week-old BALB/c mice (Fig1A). Upon initiation and subsequent growth of tumor to approximately $500mm^3$, tumors were excised and homogenized using both physical and enzymatic dissociation methods. The homogenate was then separated into two fractions for downstream *ex vivo* analysis as a tumoroid or as a single cell suspension (Fig 1a). Additionally, cancer cells derived from the primary tumor were also analyzed at time of digestion prior to any subsequent *ex vivo* culturing as an initial point of reference for cancer cell abundance and EMT state between different tumors.

Tumoroids, or fragments of tumor size selected to be 70-100 μm in diameter were first analyzed. These fragments retain the cellular composition as well as spatial configuration and ECM of the native tumor. The second fraction collected was further homogenized down to a single cell suspension for culturing as either a monolayer or in spheroid configuration. The effects of culturing in a hydrogel (Matrigel) suspension as opposed to solely in cell culture media was also examined under the three culturing platforms (Fig 1b). Matrigel is a commonly used basement membrane extracellular matrix derived from Engelbreth-Holm-Swarm (EHS) mouse sarcoma cells resembling the extracellular matrix found in many tissues and containing numerous components present in tumors (180).

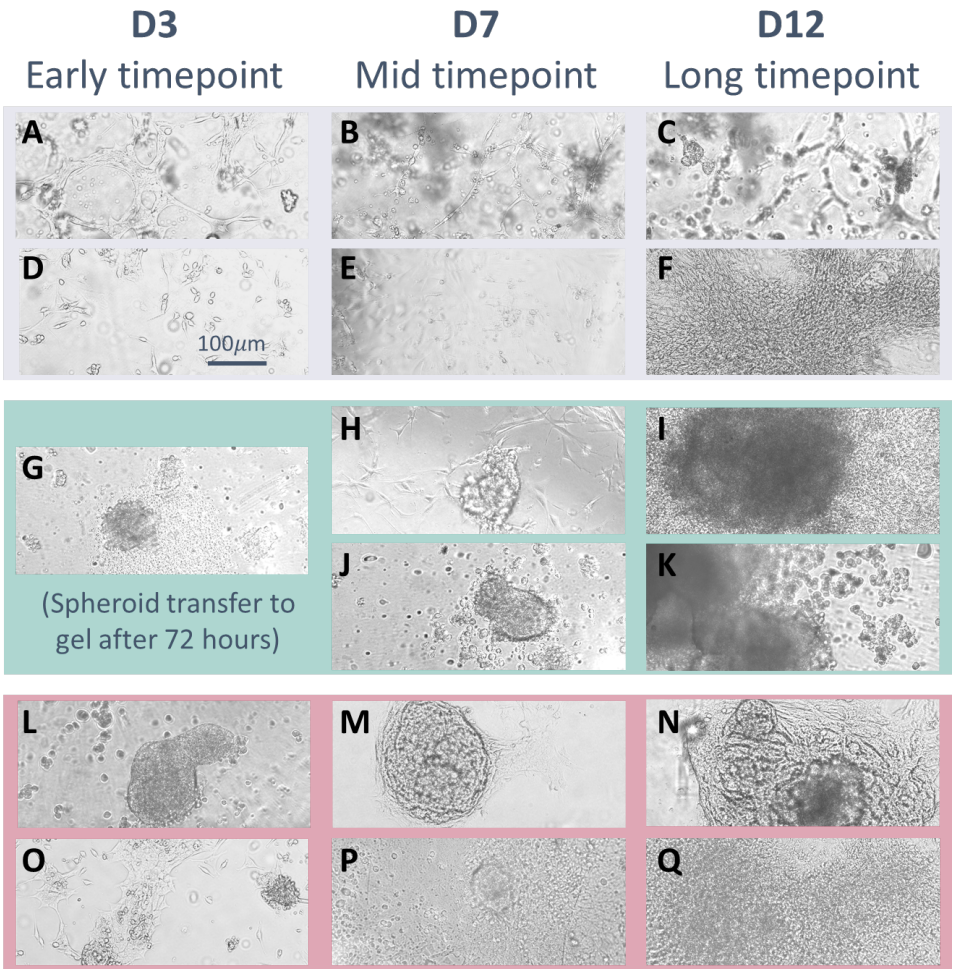


**Figure 2. *Ex vivo* culture morphology.** Imaging of *ex vivo* cultures derived from single cell suspensions (A-F), as *in vitro* formed spheroids (G-K) or as tumoroid fragments (L-Q) at an early (3 days post tumor excision), middle (7 days post tumor excision), or long timepoint (12 days post tumor excision). Culture pictures were collected at 10X magnification.

*Tumor culture morphology in ex vivo conditions*

Culturing time and method were shown to affect the distribution and cellular morphology of the tumor cells. The cell suspensions plated onto a cell culture treated polystyrene substrate adhered readily after 3 days in *ex vivo* culture with some cells proliferating as noted by clonal clusters of cells observed (Fig 2d). As the monolayer cultures progressed *ex vivo*, proliferation continued through Day 7 as a sub-confluent layer (Fig 2e) however remained confluent in the culturing well with densely packed cell layers throughout by Day 12 of *ex*

*vivo* culture (Fig 2f). Upon culture of cells suspended in hydrogel, tumor cells orient into network-like structures early (Fig 2a) and continue to proliferate throughout the depth of the gel through Day 7 of *ex vivo* culture (Fig 2b). By the final late timepoint, small spheroid-like aggregates of cells were observed in addition to the network morphology previously observed (Fig 2c).

Spheroid cultures were also derived from single cell tumor suspensions, yet tumor cells are initially placed into U-bottom spheroid culturing plates then allowed to localize together and form cell to cell adhesions for 72 hours prior to either extended culture in the spheroid place in cell culture media or embedding into hydrogel resulting in spheroid of approximately 100 μm in diameter (Fig 2g). Spheroids suspended in hydrogel resulted in some cell attachment to the culturing surface despite the non-adherent surface coating by 7 days in culture (Fig 2h) and further proliferation was observed for both the spheroid (based on increasing diameter to approximately 350 μm) and the attached cells which form a dense confluent layer at the late time point (Fig 2i). Extended culture in spheroid plates prevented the attachment to the culture vessel in both the mid and late time points however satellite cells were observed in the gel by day 7 in *ex vivo* culture which then proliferate into small spheroid cultures by the 12-day late timepoint. It is unclear if these cells have migrated out of the spheroid or are an artifact of the embedding process into the hydrogel. Additionally, spheroids in gel produced larger spheroids than the comparable media only conditions at both late timepoints with an increase in diameter at day 7 to approximately 150 μm and exceed 500 μm in diameter at the terminal timepoint (Fig 3j, 3k). It was also noted that more distinct edges of the spheroid cultures were observed upon suspension in hydrogel. This phenotype may be related to the pressure induced by the surrounding gel consistent with prior cancer spheroid comparisons noting similar phenomena and correlated with a more *in vivo*-like phenotype (181).

Tumoroid cultures also suffered from adherence in *ex vivo* culture with a majority of tumoroid derived cells attaching and culturing as a monolayer by day 3 (Fig 2O). 3-dimensional clusters of cells were noted early and continued throughout the duration of the culture however the adherent cells readily proliferated and became confluent in the culture wells by day 7 in culture (Fig 2p, q). Tumoroids suspended in hydrogel were able to minimize adherence to the culture surface at day 3 of *ex vivo* culture yet was observed at later timepoints (Fig 2l-n). Tumoroids initially size selected for 70-100 μm range expanded in the hydrogel environment to approximately 150 μm at the early timepoint growing to approximately 250 μm at day 7 and greater than 500 μm at the 12-day late timepoint.

*Heterogeneous ex vivo culture cancer expansion was increased in hydrogel*

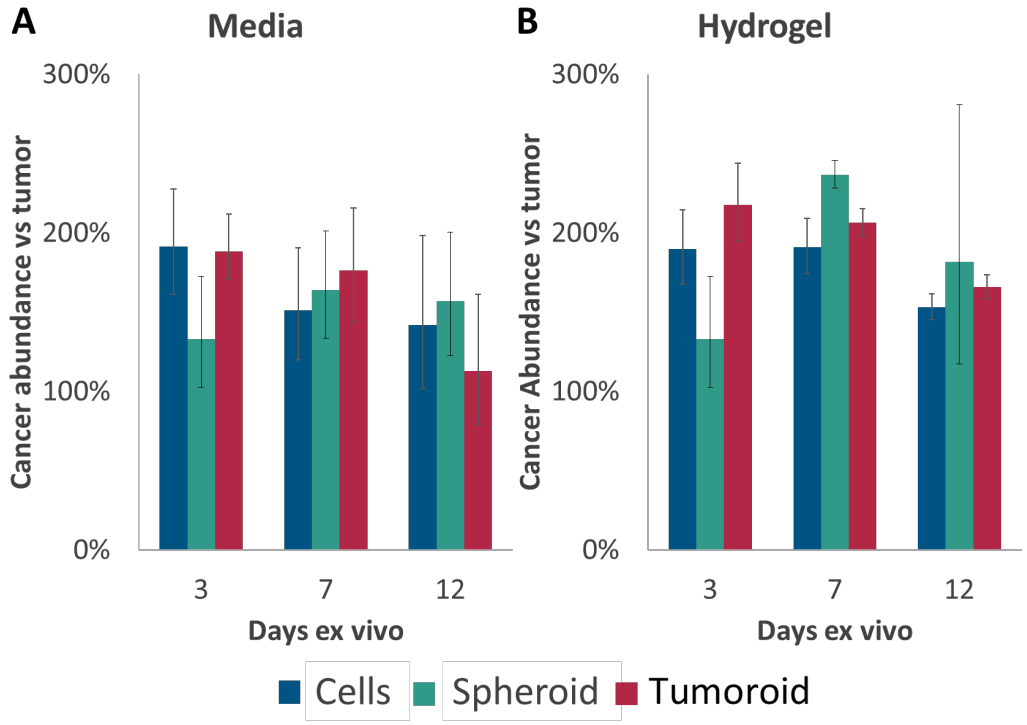


**Figure 3. Cancer cell abundance changes throughout *ex vivo* culture.** Relative cancer cell abundance in heterogenous tumor cell cultures under differing *ex vivo* conditions quantitated via flow cytometric analysis utilizing the transgenic Thy1.1 expression system to denote cancer vs stromal cell populations. Each culture is normalized to the initial cancer frequency determined at time of dissection. n=6

4T1 cells expressing transgenic *Thy1.1* were isolated and relative abundance quantitated to examine the maintenance of proper cancer to stromal cell ratios during *ex vivo* culture using flow cytometry (Fig 3a, b). Cancer cells rapidly expand in *ex vivo* cultures relative to other cell types in cells and tumoroid conditions. In single cell and tumoroid cultures, cancer cells were twice the concentration compared to tumors by 3 days *ex vivo* yet do not continue to expand in later timepoints. The environmental substrate single cells were cultured in did not affect the increase of cancer abundance at the early timepoint resulting in 91% more cancer cells relative to the tumor abundance in media and a 90% increase in hydrogel. This abundance was reduced in subsequent timepoints with decreasing cancer cell abundance of 151% and

142% of the initial tumor ratio observed in mid and late timepoints in media, respectively. In hydrogel conditions, cell suspensions maintained a high ratio of cancer cells at 7 days of *ex vivo* culture (191%) and decreases by 12 days in culture (153%). Comparable to cell suspension cultures, tumoroid cultures also showed rapid expansion under *ex vivo* conditions with cancer cell abundance peaking at the early timepoint (188% in media, 218% in hydrogel) with declining abundance as cultures mature (176% at day 7 and 113% at day 12 in media; 206% at day 7 and 166% at day 12 in hydrogel). Interestingly the hydrogel environment stimulated increased expansion of cancer cells relative to media only in both cell and tumoroid suspensions and slightly promoted expansion of cancer cells at late timepoints.

Spheroid cultures showed a delayed increase in cancer abundance. During initial tumor formation minimal increase (133%) of cancer cells abundance in the culture was found at day 3 prior to culturing in media or hydrogel for the remainder of the *ex vivo* culturing. As noted in cell suspension and tumoroid cultures, the hydrogel environment stimulated increased abundance of cancer cells in the tumor population relative to media only conditions. Increases in cancer abundance peaked at 7 days *ex vivo* in hydrogel (237% initial cancer concentrations) then slightly diminished (181%) by 12 days in culture. Spheroids in media maintained native cancer abundance in culture better with only modest increases at 7 days (164%) and 12 days (157%) in *ex vivo* culture.

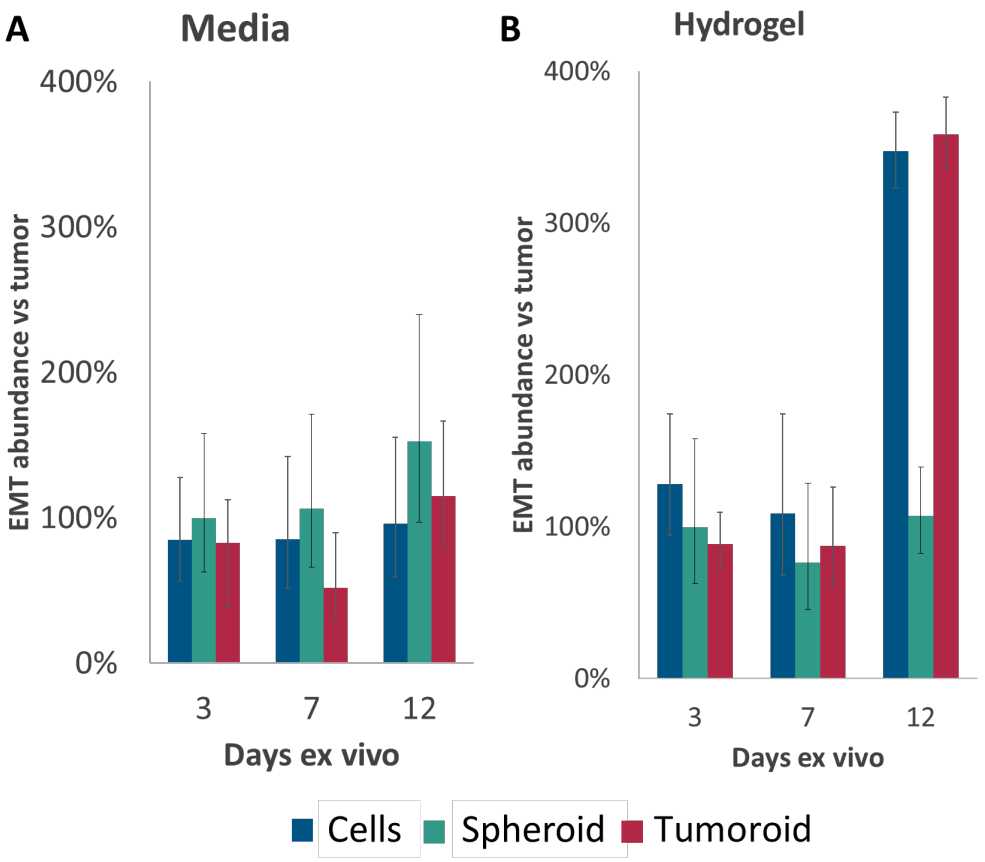


**Figure 4. *Ex vivo* effects on cancer cell EMT**. 4T1 cells were able to retain comparable rates of cancer cells undergoing EMT (Thy1.1+/Epcam-) up to 7 days in *ex vivo* culture in all culturing conditions and 12 days in media only conditions. Yet significant increases in EMT cancer cells were observed by day 12 of culturing in single cell and tumoroid cultures in hydrogel. Each culture is normalized to the initial EMT frequency determined at time of dissection. n=6

*Epithelial to mesenchymal transition changes induced by ex vivo cultures.*

As shown in Chapter 2, the epithelial to mesenchymal transition (EMT) is a process critical to cancer progression and can be dramatically altered based on altered stromal contributions and culturing environment. Loss of EPCAM expression was utilized to determine if cancer cells have lost their epithelial phenotype and initiated the EMT process. *In vivo* cultured cancer cells significantly upregulate the abundance of cells undergoing EMT relative to *in vitro* culture comprising ~30% of the cancer cell population in tumors (182). Upon *ex vivo* culture with all tumor residing cells, EMT abundance was

maintained in cultures in media only across all forms of cell culturing at all timepoints (Fig 4a). Non-significant decrease in tumoroid cultures at the middle timepoint and an increase in spheroid cultures at the late 12-day timepoint was observed in media conditions. Cultures embedded in hydrogel were also able to maintain consistent abundance of 4T1 cells undergoing EMT consistently through 7 days of culture (Fig 4b). While spheroid cultures continued the stability of cells undergoing EMT *ex vivo* up to 12 days, cell and tumoroid cultures saw a dramatic increase in rate of cancer cells undergoing EMT (347% and 349%, respectively).

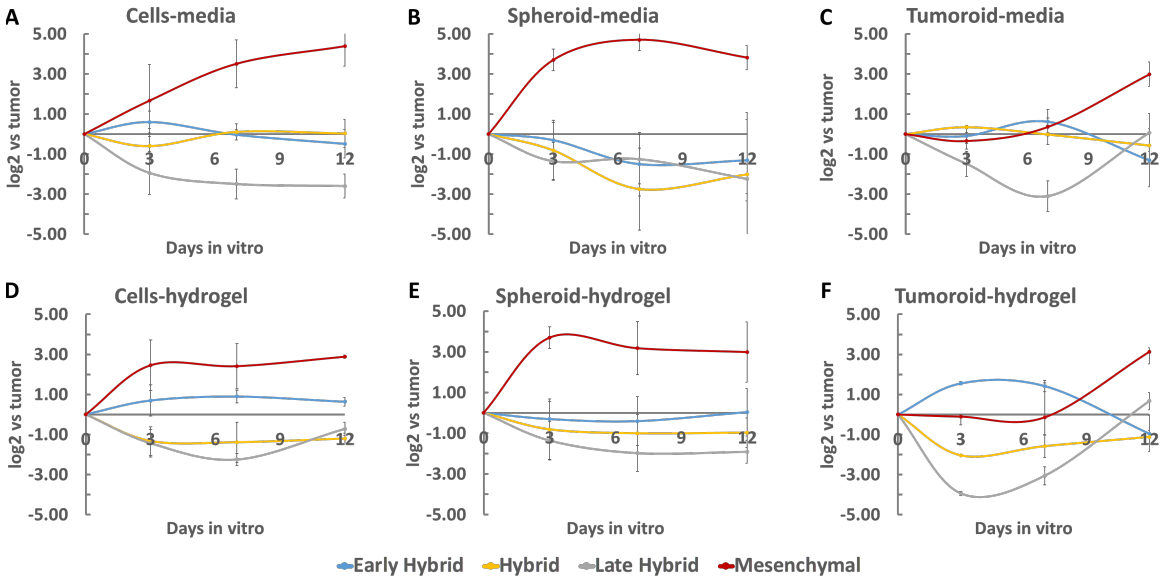


**Figure 5 Transitional EMT state shifts during *ex vivo* culture**. Cancer cells undergoing EMT were assessed for hybrid EMT states using expression of CD51, CD61, CD106. Transitional hybrid EMT states were classified into progressively more mesenchymal subpopulations as follows: early hybrid EMT (triple negative and CD106+), hybrid EMT (CD51+, CD51+/CD106+), late hybrid EMT (CD51+/CD61+), and Mesenchymal (CD51+/CD61+/CD106+). Each culture is presented as log2 fold change relative to the initial subtype frequency determined at time of dissection. n=6

Characterization of hybrid EMT states was additionally performed on cancer cells lacking Epcam expression. Culturing technique appears to be a key determinant in EMT population shifts as similar trends in emerging or declining hybrid states were observed in each of the three culturing platforms

with only minor differences when grown in media or hydrogel. A hydrogel extracellular matrix surrounding tumor cells does mitigate EMT state shifts in 2D and 3D as shown by the decreased change in EMT states throughout the 12-week *ex vivo* culture (Fig 5a, b, d, e). However, tumoroid culture had increased differentiation under hydrogel conditions relative to media alone (Fig 5c, f).

Mesenchymal populations increase in all conditions but the shift toward fully mesenchymal behavior is most robustly during spheroid formation in the first 3 days of culture. Cell suspensions appear to have a consistent increase in mesenchymal abundance over time and tumoroid cultures appear to retain mesenchymal state comparable to the tumor for the first 7 days of culture before increasing at the late timepoint. While early hybrid states were the most unchanged in frequency across all conditions relative to other EMT states. Hybrid and late hybrid states showed a slight reduction in abundance in all conditions yet increase in late tumoroid cultures was observed to return to within 2-fold difference of the initial tumor ratio.

## Discussion

The longitudinal examination of cancer cell behavior in *ex vivo* culture presented here further illustrates the impact the EMT has on cellular phenotypes and underlies the importance of optimizations of future tumor culturing methodologies. This work has identified that early effects of *in vitro* culturing promote the rapid expansion of cancer cells in mixed cultures within 3 days of tumor excision however this expansion was slowed after the initial expansion over the course of 12 days of *ex vivo* culture. Despite the increase of cancer cell abundance observed *ex vivo*, the distribution of cancer cells undergoing EMT only moderately increased promoting a shift away from

hybrid and late hybrid cell states toward a fully mesenchymal behavior throughout the duration of *ex vivo* culture.

Cancer cell behaviors specific to culturing technique were discovered but the previously mentioned trends were generally conserved across culturing condition and may represent behaviors induced by *in vitro* culturing aspects (oxygen levels, carbon dioxide levels, serum/media composition, temperature variability, etc) standard to all tested conditions rather than the variable culturing substrates utilized. EMT subtype shifts were found to be culture technique specific as tumor cells cultured from single cell suspensions displayed an increasing abundance of mesenchymal cells over the *ex vivo* culture while spheroid cultures rapidly shifted EMT states to mesenchymal during early spheroid formation then had minimal shifts in subsequent timepoints. Tumoroid culture, specifically when cultured on non-adherent culturing vessels in media, was best able to maintain the EMT subtype distribution of the primary tumor with minimal shifting populations observed up to 7 days in culture.

The effects of embedding tumor derived cells in an ECM hydrogel also were found to effect cancer cells *ex vivo* by slightly promoting increased cancer cell abundance in culture when compared to media only and significant increases in abundance of EMT cancer cells at the late timepoint in both cell and tumoroid conditions. Furthermore, the cell and spheroid conditions in hydrogel slightly mitigated the shifts in EMT states *ex vivo* yet amplified the shifts in tumoroid cultures. Based on this analysis, the tumoroid in media condition provides the best preservation of cancer cell behavior throughout the 12-day *ex vivo* culturing experiment based on the analysis utilized in this study. In this condition, cancer cell abundance does still initially increase however the ratio declines to close to initial levels by the late timepoint. This condition also

has minimal shift in cells undergoing EMT during *ex vivo* culture. Furthermore, this condition did show a slight reduction in late hybrid populations at the 7-day timepoint, but this culturing method was able to best resist increasing mesenchymal populations and retain early and late hybrid abundances in culture. These findings suggest that maintenance of the native spatial orientation of cells and ECM content, retained from incomplete digestion of tumor samples, is helpful in maintaining native cancer behavior. While cancer cells represent the only malignant cell type in a tumor and the target of most therapeutic options, the stromal cells supporting their behavior also play a vital role in tumor behavior (183–185). The cellular heterogeneity comprising tumors will also need to be characterized to understand how *ex vivo* culture encourages or discourages stromal cell modulation. Data provided in this study solely identifies the expanding cancer populations however it remains unknown which populations decrease over *ex vivo* culture. Chapter 2 provides insight stromal population shifts in spheroid culture at 5 days in culture by utilizing single cell RNA sequencing technologies (expansion of fibroblasts and reduction in myeloid derived cells) however longitudinal analysis comparable to these analyses will identify population shifts over time in culture that will require culture condition manipulations to offset.

Further work will focus on further improving tumoroid culture in media. This will be accomplished through alterations in media composition (supplementation, pre-cultured media, serum content, etc), time point optimization to define or prolong clinical relevance, and drug screening validation to *in vivo* response. Additionally, species specific differences in cell behavior and cellular sub-types will also need to be examined when transferring mouse model-based systems to human samples. Based on observations of spheroid culture, optimal size selection of tumoroids should be examined since diffusive properties of 3-dimensional cultures have been

reported to create a hypoxic and nutrient limited core that may alter the tumoroid homeostasis (186). Additionally, potential incorporation of complexity like vasculature and modulation in nutrient kinetics comparable to that of a human metabolism has been previously demonstrated and may also benefit pre-clinical tumoroid cultures as well (186).

Furthermore, validation of clinical response using patient samples will also be critical in development of preclinical *ex vivo* tumor culture models for drug discovery or prognostic applications in personalized treatment. Despite the complexity involved in development of improved culturing platforms, an optimized high-throughput *ex vivo* system capable of maintaining clinical behavior for basic research, translational research, and screening personalized therapies will be an invaluable tool for cancer research and human health.

# Chapter 4. IL-17A increases doxorubicin efficacy in triple negative breast cancer


## Abstract

Triple negative breast cancer is an especially difficult subtype to treat due to its lack of targetable receptors and intertumoral heterogeneity. Standard of care therapies typically include anthracyclines like doxorubicin (DOX) for non-specific neoadjuvant chemotherapy, however resistance to this therapy has been observed clinically, yet mechanisms for resistance are not fully elucidated. This work utilizes a 4T1 syngeneic mouse model of TNBC that presents a differential response to a 7-day DOX treatment regimen. Single-cell RNA sequencing identified an increase in T cell abundance in tumors that were responsive to DOX treatment compared to resistant tumors that continued tumor growth uninhibited and validated through flow cytometric analysis. Furthermore, T cells residing in DOX sensitive tumors have increased abundance of CD4 T helper cells (514%), γδ T cells (322%), and activated CD8 T cells (2000%) compared to resistant tumors. Additionally, transcriptional profiles of tumor infiltrated T cells revealed decreased exhaustion, increased chemokine/cytokine expression, and increased activation and cytotoxic activity in T cells in DOX responsive tumors. Furthermore, IL-17A was identified (secreted by γδ T cells) to be more abundant in sensitive tumor microenvironment. IL-17A was then found to directly increase sensitivity of TNBC cells in combination with DOX treatment with possible indirect effects through mechanisms of chronic T cell activation and cytokine response that may prove to be responsible for the exhausted T cell phenotype observed. Increased presence of IL-17A abundance in DOX sensitive TNBC tumors has a direct effect on cancer cell responsiveness and chronic stimulation of tumor infiltrated T cells leading to increased chemotherapeutic efficacy. The identification of IL17A as a synergistic cytokine to chemosensitivity in TNBC may offer an avenue to combat chemoresistance in breast cancer and potentially other cancer type.

## Introduction

Due to the late stage of diagnosis, aggressiveness, and lack of targetable receptors driving the disease, TNBC is especially challenging to treat with very few effective therapies available. TNBC is insensitive to hormone therapy and typical treatments are limited to a combination of surgery, radiation, and systemic chemotherapy depending on genetic drivers and disease progression status. Late stage TNBC patients are faced with very poor prognosis with just a 15% to 20% response rate and a median progression-free survival of 4.2 months (53,54). Regardless of BC status, systemic non-specific cytotoxic chemotherapy remains the recommended therapeutic option with no clinically significant difference in efficacy when utilized in a neoadjuvant (prior to surgical intervention) or an adjuvant (post-surgery) administration (55). Neoadjuvant administration of chemotherapy is preferred as it allows for assessment of treatment efficacy and optimization of therapy on the primary tumor in an effort to predict post-operative treatment response in case of residual disease.

In TNBC, standard chemotherapeutic therapy is comprised of an anthracycline (doxorubicin, daunorubicin, epirubicin) and a taxane (paclitaxel, docetaxel) in sequence to avoid excessive toxicity (56). Anthracyclines have numerous mechanisms of actions to eradicate BC including inhibition of topoisomerase II, DNA intercalation, and generation of reactive oxygen species (187). Taxane based chemotherapies function through stabilization of microtubule assemblies thus blocking mitotic progression and chronic activation of the spindle assembly checkpoint followed by induction of apoptosis (57). This combinatorial therapy does have limitations to specific TNBC subtypes. For example, BC containing p53 mutations have shown increased resistance to anthracyclines (58) as well as multidrug chemotherapy

resistance imparted by upregulation of ATP-binding cassette transporters in TNBC (59).

Despite these standard chemotherapeutic options, TNBC remains a difficult to treat BC subtype associated with poor prognosis and as a result alternative therapeutic regiments are continuously being explored and utilized in TNBC subtypes. For example, the use of docetaxel and cyclophosphamide has proven to be an effective therapy for cases where anthracyclines need to be avoided. Adding a platinum-based agent (cisplatin, oxaliplatin) to standard chemotherapeutics has also shown increased efficacy on TNBC due to the high prevalence of DNA repair pathway defects (60,61). The dependence of TNBC containing BRCA mutations on DNA repair function are additionally being exploited using poly (ADP-ribose) polymerase (PARP) inhibitors (Olaparib) as a promising neoadjuvant (62). Augmentation of dosing scheduling and concentration is also an attractive option to increase efficacy of treatment for TNBC due its more aggressive and highly proliferative nature however dose dense strategies have yet to show consistent advantages for progression free survival or long-term outcomes (63). No single therapy has proven universally effective for TNBC which may be linked to the disease heterogeneity with therapeutic innovation focused on more personalized approaches to identify TNBC subtype dependencies and treatment escalation regiments (6).

In addition to cancer heterogeneity complicating efficacy, the lack of cellular specificity from the standard of care anthracycline adjuvant therapy presents a myriad of non-cancer cell responses that can result in systemic side effects in addition to both pro and anti-tumor effects. The most well characterized systemic effect induced by doxorubicin (DOX) treatment is induction of cardiomyopathy in which heart cells interact with DOX to induce acute cardiotoxicity in approximately 11% (187). Systemic inflammation is another side effect of DOX treatment which has been linked to the systemic

release of endotoxin driven by upregulated TLR4 response in macrophages (188).

Previous studies have demonstrated non-cancer effects of DOX therapy on stromal cells in the tumor microenvironment (TME) as well resulted in modulation of tumor response. For example, neutrophil exposure to anthracycline drugs results in the suppression of extracellular traps of DNA-protein complexes which may affect the cytotoxic and inflammatory response in tumors in response to DOX (189). Additionally, regulation of neutrophil phenotypes (specifically down regulation of CD133 and CD309 via co-administration of berberine) has been shown to increase cancer cell sensitivity to DOX (berberine). Other myeloid lineages have also been implicated in altering chemotherapeutic efficacy specifically in myeloid derived suppressor cells (MDSCs) where DOX activates the proliferation of MDSC and antitumor activity (190). In the TME, macrophages will decrease the localized response of doxorubicin due to the uptake of drug away from cancer cells yet can potentiate the anti-cancer effects of DOX through activation and release of active DOX into cancer cells (191). This stromal response has additional promise as stromal modulating treatment in combination with alternative anticancer therapies. In fact, the immunomodulatory effects of DOX treatment increases adoptive T-cell transfer therapy in BC when administered before immunotherapy (192). In urinary cancer patients treated with DOX, CD86 expression is upregulated in B cells that then enhance CD4+ T cell anti-cancer activity (193).

IL-17 is a proinflammatory cytokine that has previously been linked to numerous tumor behaviors. Its secretion is limited to T helper 17 cells and innate lymphocytes (γδ T cells, natural killer (NK) cells and innate lymphoid cells) (194) yet the receptor is broadly expressed across numerous cell types. In multiple types of cancer, IL-17 has been implicated in tumor progression and

associated with poor prognosis in breast cancer (195) however previous studies have identified both pro and anti-tumor function in the TME. Chronic IL-17 expression leads to a protumor microenvironment through modulation of stromal cell types that increase angiogenesis and antitumor immunity (195). Upon exposure to chemotherapeutic administration, IL-17 has been implicated to improve efficacy. Decreased efficacy of anthracyclines and oxaliplatin was observed in mouse fibrosarcoma allografts into IL-17A knockout mice. This phenotype was rescued upon adoptive transfer of γδ T cells capable of IL-17 production (196). In breast adenocarcinomas a similar correlation was observed in which optimal DOX therapeutic efficacy was found to require IL-17 in mice (197). Correlation with increased efficacy was also observed in gastric cancer patients (198). IL-17's proinflammatory role in combination with chemotherapy has been implied to aide in recruitment of antitumor cytotoxic T cells however specific mechanisms of action remain unknown (196).

This study aimed to examine the altered stromal composition and behavior of cells residing in the TNBC TME to determine molecular and cellular drivers of DOX treatment response. To properly recapitulate clinical relevance, 4T1 murine syngeneic tumors in the mammary fat pad of BALB/c mice were utilized in this work. This allograft model was discovered to possess a range of responses to a 7-day dosing regimen with DOX. Further examination of sensitive versus resistant tumors correlates inhibition of tumor growth during treatment with an increase in the absolute number of T cells in the TME. T cell subtypes increased in cytokine secretion and decreased exhaustion were found to be more abundant in DOX sensitive tumors as well. Specifically, γδ IL-17+ CD8 T cells were identified as differentially abundant in chemoresponsive tumors and may induce effects on numerous cell types in the TME. *In vitro* analysis of IL-17's effect directly on cancer cells showed anti-tumor effects by increasing tumor responsiveness to DOX upon co-

administration with recombinant IL-17A. In response to IL-17A and DOX, 4T1 cells increased cytokine signaling and cell cycle disfunction while decreasing DOX induced stimulation of immune response genes which may contribute T cell exhaustion.

## Materials and Methods

*Cell culturing and allograft generation*

4T1-Thy1.1 cell line was graciously provided as a gift from Dr. Julian Lum (143) and was used in allograft and *in vitro* experiments. 4T1 cells were cultured in RPMI Medium 1640 containing 10% FBS with 100,000 U/L of penicillin and 100 mg/L of streptomycin at 37 °C with 5% $CO_2$. Female mice (8-10 weeks old) NOD.*Cg-Prkdc*$^{scid}$*Il2rg*$^{tm1Wjl}$/SzJ (NSG) or BALB/c mice (Jackson Laboratories, Bar Harbor, ME, USA) were injected $1 \times 10^5$ 4t1-Thy1.1 cells and tumors were established to 70–140 $mm^3$ prior to intravenous Doxorubicin (Sigma Aldrich, St. Louis, MO, USA) administration. Doxorubicin was introduced via intravenous (IV) tail vein injection at 5mg/kg for 3 doses 3-days apart. All mice were weighed, and tumor measurements collected using manual palpation and caliper measurements prior and during the chemotherapeutic regimen until the terminal timepoint 2 days following the final DOX injection. Tumor volume calculations were determined using the following formula: volume= length x (width)*2 x ½ (199). Moribund behavior was evaluated regularly throughout the tumor bearing period. All animal experimental procedures were completed under an approved Institutional Animal Care and Use Committee (IACUC) protocol at Lawrence Livermore National Laboratory (LLNL) and conforming to the National Institute of Health (NIH) guide for the care and use of laboratory animals.

*Tumor Single cell isolation and enrichment*

Single-cell suspensions of tumor cells were prepared by passing the tumor through a syringe without a needle followed by a 1 h digest with shaking at 37 °C in 100 μg/mL DNase I (Roche, Basel, Switzerland; Cat # 11284932001), 300 U/mL collagenase/100 U/mL hyaluronidase (Stemcell Technologies, Vancouver, Canada; Cat # 07912), 0.6 U/mL Dispase II (Roche, Basel, Switzerland; Cat # 4942078001) in DMEM/D12 with 1% FBS (Gibco, Waltham, MA, USA). Red blood cell lysis was then performed using ACK Lysing Buffer (Gibco, Waltham, MA, USA) per manufacturers recommendation. Digests were next filtered through a 100 μm cell strainer prior to debris removal (Miltenyi Biotec, Bergisch Gladbach, Germany; Cat # 130-109-398) and resuspended in BD FACS Pre-Sort Buffer (BD, Franklin Lakes, NJ, USA; Cat # 563503).

*Single-cell sequencing and data analysis*

Tumor growth, digestion, and isolation of cell suspensions were prepared as previously described for tumor digests and tumoroids were dissociated as previously described. Then, 2 subsequent washes in sterile PBS + 0.04% non-acetylated BSA were performed to further remove debris from final suspension. Immune and cancer cell depletions were performed for T cell specific reactions using Pan T Cell Isolation Kit II, mouse (Miltenyi Biotec, Bergisch Gladbach, Germany; Cat # 130-095-130) in combination with CD90.1 MicroBeads, mouse and rat (Miltenyi Biotec, Bergisch Gladbach, Germany; catalog no. 130-121-273) per manufacturers protocols prior to were cell depletion using LS columns (Miltenyi Biotec, Bergisch Gladbach, Germany; Cat # 130-042-401). Sequenced T cell populations were derived from 3 independent syngeneic 4T1 tumors in BALB/c mice as previously described pooled into a single sequencing population. Cell pellets were resuspended in PBS with 0.04% non-acetylated BSA prior to single-cell sequencing preparation using Chromium Single-cell 3′ GEM, Library & Gel Bead Kit v3

(10× Genomics, Pleasanton CA, USA Cat # 1000075) on a 10× Genomics Chromium Controller following manufacturers protocol.

Sequencing data was demultiplexed, quality controlled, and analyzed using Cell Ranger (10× Genomics, Pleasanton CA, USA) and Seurat (144). Data analysis, expression values, and representative plots were generated using Loupe Cell Browser (10× Genomics) and Seurat (153). The Cell Ranger Single-Cell Software Suite was used to perform sample demultiplexing, barcode processing, and single-cell 3′gene counting. Samples were first demultiplexed and then aligned to the mouse genome (mm10) using "cellranger mkfastq" with default parameters. Unique molecular identifier counts were generated using "cellranger count". Further analysis was performed using Loupe (10X Genomics, Pleasanton CA, USA).

*Flow cytometry*

Cell preparations for tumor cells was derived from cell suspensions as previously described then resuspended in FACS buffer (PBS with 2% FBS). Bone marrow preparations were performed from isolated femurs. Femoral epiphyses were removed from the bone then the marrow cavity is flushed with a 28-gauge needles with 2 mL of PBS. The bone marrow derived cell suspensions are then centrifuged at 500G for 10 minutes followed by red blood cell lysis then resuspended in FACS buffer as previously described prior to cytometric analysis. Splenocytes were prepared from isolated spleens that were forced through a 40-um cell strainer. Cells were washed with PBS and pelleted by centrifugation at 500g for 10 min. Red blood cell lysis was then performed and resuspended in FACS buffer as previously described prior to cytometric analysis.

Cell suspensions were stained with the following antibodies for 30 minutes on ice prior to cell staining: BioLegend (San Diego, CA, USA): CD45 (1:100; Cat # 103116, 157613), CD3ε (1:50; Cat # 100312), CD4 (1:100; Cat # 100414,

100406), CD8b (1:100, Cat# 126622, 126609), CD279 (PD-1) (1:100, Cat # 135213), IL-17A (1:100, Cat # 506922), TCR γ/δ (1:100, Cat # 118107; Miltenyi Biotec (Miltenyi Biotec, Bergisch Gladbach, Germany): CD90.1 (1:10, Cat # 130-102-637). Viability dyes Zombie Violet™ Fixable Viability Kit (BioLegend, San Diego, CA, USA), Zombie Aqua™ Fixable Viability Kit (BioLegend, San Diego, CA, USA), or eBioscience Fixable Viability Dye eFluor506 (Invitrogen, Waltham, MA, USA) were utilized to discriminate live/dead cells. Following staining, cell populations were washed 2 times with FACS buffer prior to 20-minute fixation using Cytofix Buffer (BD Biosciences, San Jose, CA; USA) then resuspension in FACS buffer for analysis.

For cytokine detection, tumor derived cells were cultured in RPMI supplemented with 10% FBS, 50ng/ml PMA Sigma, St. Louis, MO, USA, Cat# P-8139, 1ug/ml Ionomycin (Sigma, St. Louis, MO, USA, Cat# I-0634), and GolgiPlug (BD Biosciences, San Jose, CA; USA) at 37°C with 5% $CO_2$ for 4 hours followed by extracellular staining then fixation as described previously. Intracellular staining was accomplished using Intracellular Staining Permeabilization Wash Buffer (BioLegend, San Diego, CA, USA) for permeabilization, staining buffe, and subsequent washes followed by resuspension in FACS buffer for downstream analysis. Flow cytometric analysis was performed using FACSMelody (BD Biosciences, San Jose, CA; USA), BD LSR II (BD Biosciences, San Jose, CA; USA), FACSAria Fusion (BD Biosciences, San Jose, CA; USA) instrument.

Immunofluorescent staining

Tumor samples were collected at the day of harvest, snap frozen in liquid nitrogen and stored at -80°C. Frozen tumors were embedded in O.C.T. compound (Fisher Healthcare, Waltham, MA, USA) and sectioned at 10 μm slices. Slices were then placed onto Superfrost Plus microscope slides (Fisher

Scientific, Waltham, MA, USA) and stored at -80$^{o}$C until the staining was done. To stain sections, slides were warmed to room temperature and then sections were immersed in PBS with 4% formaldehyde for 15 minutes. Slides were then immersed in PBS with 0.1% Tween 20 and 10% goat serum for one hour at room temperature. Primary antibody IL-17-A (Abcam, Cambridge, MA, USA, ab79056, (1:250)) was incubated overnight at 4$^{0}$C. Samples slides were then incubated at room temperature for 1 hour with the secondary antibody goat anti rabbit (Thermo Fisher Scientific, Waltham, MA, USA; A-11037 (1:1000)). Negative control slides were incubated with secondary antibody-only. Stained slides were mounted with Prolong Gold with DAPI (Molecular Probes, Eugene, OR, USA). Slides were imaged using a Leica DM5000 microscope. ImagePro Plus V7.0 Software and a QIClick CCD camera (QImaging, Surrey, BC, Canada) were used for imaging and photo editing.

*Western blot*

Tumor samples lysed in RadioImmunoPrecipitation Assay (RIPA) buffer followed by centrifuging at 14,000 rcf for 5 min. The supernatants were collected and analyzed using the Jess automated Western blotting system (ProteinSimple, San Jose, CA, USA). Jess reagents (biotinylated molecular weight marker, streptavidin-HRP fluorescent standards, sample buffer, DTT, stacking matrix, separation matrix, running buffer, wash buffer, matrix removal buffer, fluorescent labeled secondary antibodies, antibody diluent, and capillaries) were purchased from the manufacturer and used according to the manufacturer's standard protocol. Antibodies were diluted with ProteinSimple antibody diluent at the following dilutions: anti IL-17-A (1:50, Abcam, Cambridge, MA, USA, ab79056, and GAPDH (1:100, Licor, Catalog no. 926-42216). Target protein concentration is quantitated using Compass for SW 4.0 software (https://www.proteinsimple.com/compass/downloads/). The expression of each target protein is normalized to the expression of GAPDH.

*Ex vivo culturing and in vitro doxorubicin and IL-17A administration.*

Single cell suspensions were from primary syngeneic tumors were performed as previously described. CD90.1 MicroBeads, mouse and rat (Miltenyi Biotec, Bergisch Gladbach, Germany; catalog no. 130-121-273) were used for cell isolation using LS columns. Subsequent elution of cells of the cell isolation columns were then *ex vivo* 4T1 cultured overnight. Cancer cell populations from 3 syngeneic tumors derived from unique mice were utilized for *ex vivo* 4T1 DOX response experiments for each tumor phenotype.

Doxorubicin (200ng/ml, Sigma Aldrich, St. Louis, MO, USA)) and/or Recombinant Mouse IL-17A Protein (25ng/mL, R&D Systems, Minneapolis, MN, USA) was administered for 48 hours prior to cell quantitation using Cell Titer-Glo 2.0 (Promega, Madison, WI) according to manufacturer's protocols then read for luminescent signal on a Modulus II Microplate Multimode Reader. Raw reads were first background (media without cells) subtracted then normalized to untreated cells for cell quantitation. 3 independent experiments were performed for *in vitro* DOX viability assays.

*Bulk RNA sequencing and analysis*

4T1-Thy1.1 cells were cultured to 25% confluency in a 12 well culture plate Total RNA was isolated using RNeasy mini spin columns (Qiagen). Sequencing library preparation was performed using QuantSeq 3' mRNA-Seq Library Prep Kit FWD for Illumina (Vienna, Austria; catalog no. 015.96) according to manufacturer's protocols. and single end 75 base pair sequencing was performed using an Illumina NextSeq 500. Sequencing data quality was checked using FastQC software (https://www.bioinformatics.babraham.ac.uk/projects/fastqc/). Reads were mapped to the mouse genome (mm10) using STAR (version 2.6) (136)and read counts per gene were determined using "featureCounts" from Rsubread

package (version 1.30.5; https://bioconductor.org/packages/release/bioc/html/Rsubread.html). Only genes with ≥10 reads in at least 3 samples were selected for analysis. Subsequently, a between-sample normalization was performed using EDASeq (version 2.16.0) (137). RUVseq (version 1.16.0) was used to estimate the factors of unwanted variation (138). Differentially expressed genes were identified using edgeR (version 3.22.3), controlling for factors of unwanted variation (139). A gene was significantly differentially expressed when its false discovery rate adjusted *p*-value was <0.05 and fold change was >2. Gene set enrichment analysis was performed using GenePattern with Reactome pathway ontologies (200).

*Statistical analyses*

Statistical analyses were performed using GraphPad Prism. Data is presented from at least three biological replicates. One-way ANOVA and post-hoc Tukey's Test or Student's t-test were used to assess statistically significant differences of mean expression values. Results were considered statistically significant for $p$ values < 0.05. IC50 curves were generated using a nonlinear regression curve fit analysis.

## Results

*TNBC tumors exhibit a range of responses in mouse allografts driven by stromal complexity.*

In order to faithfully recapitulate the TNBC microenvironment, syngeneic allografts with 4T1 cells injected into the mammary fat pad of BALB/c mice were utilized for this study. Upon reaching approximately 100mm$^3$ in volume, tumor bearing mice were given a clinically comparable doxorubicin treatment regimen with three doses administered over the course

of 7 days. Tumor growth rates were collected throughout the chemotherapeutic treatment via caliper-based measurements of palpable tumors. Two days following the final dose, tumors were measured and isolated for downstream analysis (Fig1a).

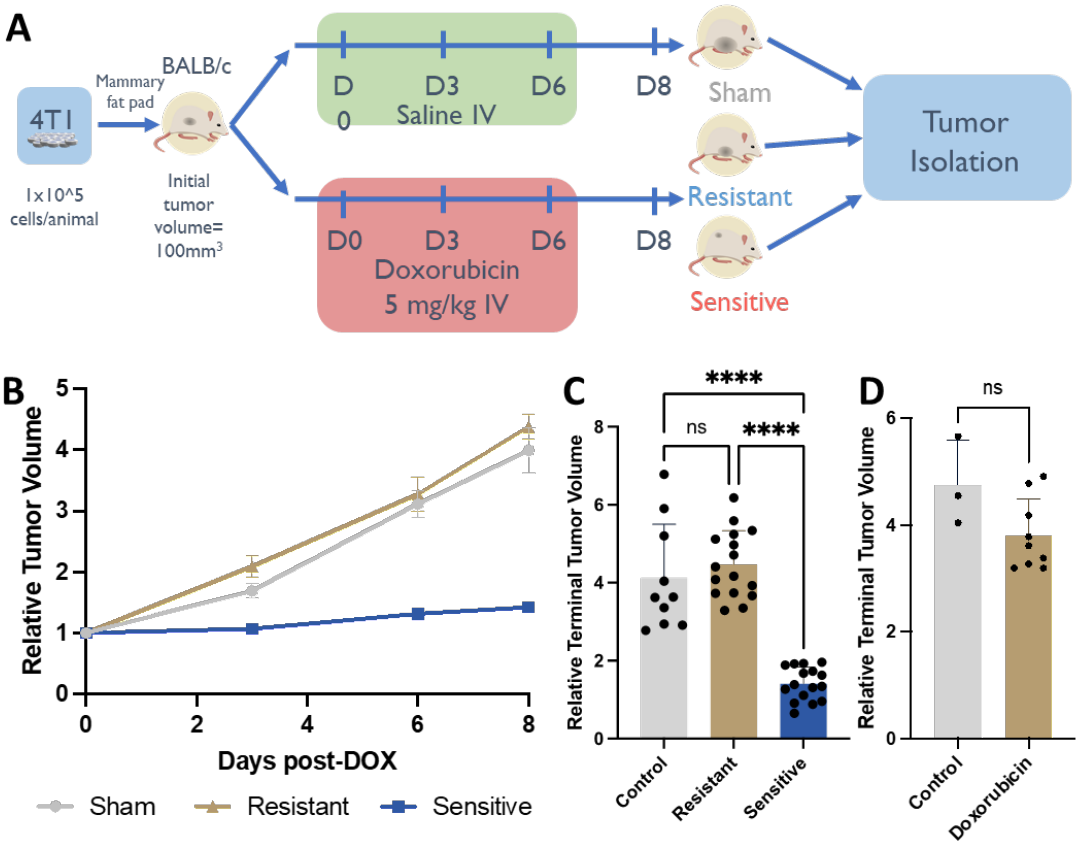


**Figure 1. Syngeneic 4T1 tumors differentially respond to doxorubicin treatment.** A) Doxorubicin treated BALB/c 4T1 mammary fat pad tumor experimental design. B) Syngeneic tumor growth rates of tumors in response to doxorubicin. Relative tumor volume was normalized to initial volume and calculated from caliper measurements throughout DOX treatment. C) Relative terminal tumor volume at Day 8 post DOX initiation from saline injected controls or DOX treated tumors in immunocompetent BALB/c mice binned into resistant or sensitive populations. n=10-16. D) Relative terminal tumor volume at Day 8 post DOX initiation from saline injected controls or DOX treated tumors in immunodeficient NSG mice. n=3-9. **** $p < 0.0001$

In control tumors, growth continues without chemotherapeutic administration resulting in a terminal tumor volume increase to 399% of the initial recorded size on day 8 post injection (Fig1c). Interestingly, 4T1 TNBC tumors exhibit a diverse response to doxorubicin treatment (Fig1b). DOX treated tumors can be classified as resistant or sensitive tumors based on relative growth rates throughout the chemotherapeutic treatment. Sensitive tumors showed a consistent inhibition of growth throughout the chemotherapeutic regimen yielding tumors that were significantly smaller (142% terminal tumor volume) than control tumors. Conversely resistant tumors continued to grow comparable to untreated tumors (438% terminal tumor volume) and were also significantly different than the sensitive cohort. This polarized response to DOX treatment failed to be recapitulated in immunocompromised (NSG) mice; these mice lack mature B, natural killer (NK), and T cells in addition to functionally defective dendritic cells and macrophages (201,202). All NSG-DOX dosed tumors exhibiting a drug response to chemotherapeutic that resembled drug resistant DOX response in Balb/c mice, where no significant differences in growth rates were observed between treated and undosed control tumors (Fig1d). The lack of sensitivity to DOX in mice lacking functional immune cells suggests that the stromal complexity is an important facet of tumor chemosensitivity.

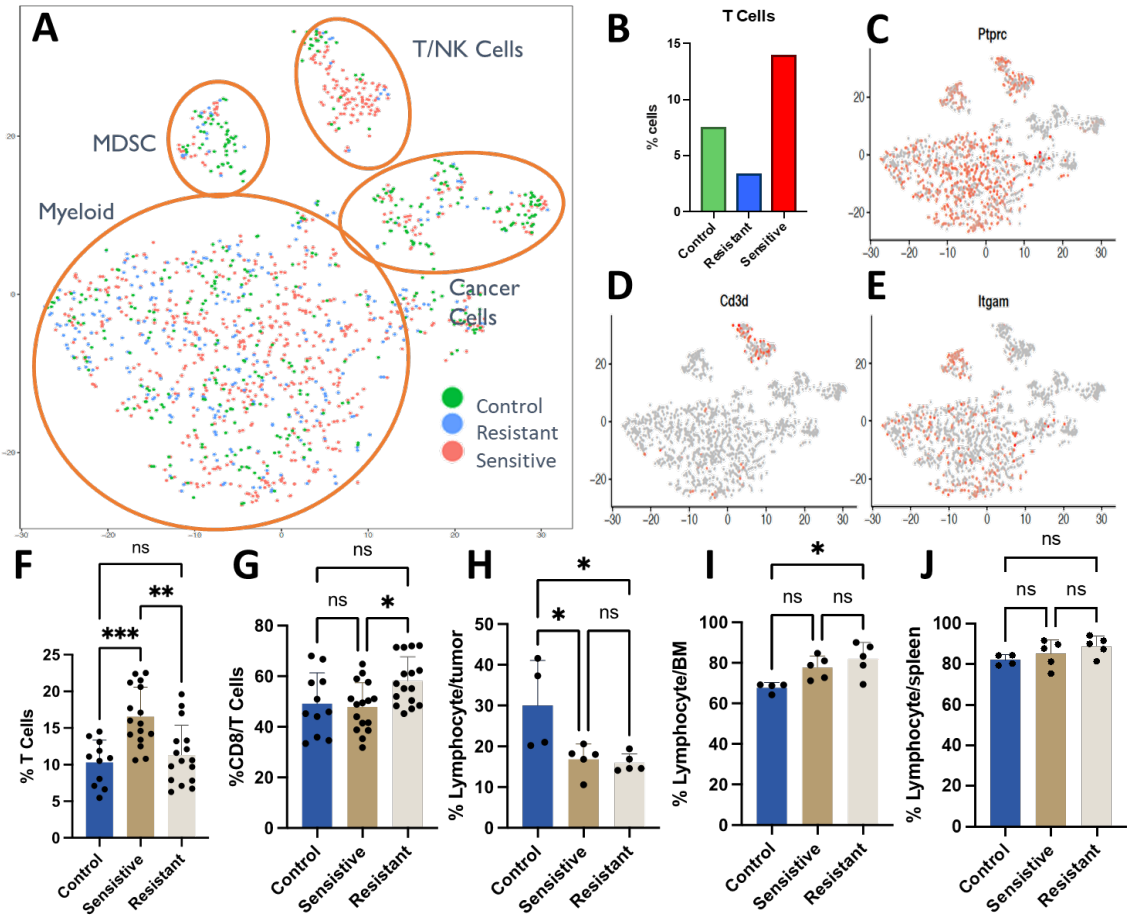


**Figure 2. Single cell sequencing of tumors following doxorubicin administration.** A) t-SNE projection representing all tumor cells following doxorubicin treatment. Colors depict cells derived from tumors of different treatment/response. B) T cell (*Ptprc* (CD45)+ *CD3d*+) relative abundance derived from single cell RNAseq data. C-E) Feature plots of identifying immune clusters. F) Flow cytometric quantification of T cell (CD3ε+) abundance in syngeneic 4T1 tumors. G) Flow cytometric quantification of cytotoxic T cell (CD8+CD3ε+) abundance in syngeneic 4T1 tumors. H) Flow cytometric quantification of immune (*Ptprc* (CD45)+) abundance in syngeneic 4T1 tumors. I) Flow cytometric quantification of immune (*Ptprc* (CD45)+) abundance in bone marrow of tumor bearing mice. J) Flow cytometric quantification of immune (*Ptprc* (CD45)+) abundance in spleens of tumor bearing mice.

## *Increased abundance of tumor infiltrating T-cells in doxorubicin sensitive tumors.*

Single cell RNA sequencing was performed on representative tumors from each category to further investigate alterations in the abundance of the stromal cells. Unsupervised hierarchical clustering of cell types based on

transcriptional profiles identifies cancer, T cell, myeloid derived suppressor cells (MDSC), and myeloid populations as represented in a tSNE projection (Fig2a, 2c-2e). Specifically, the number of T/NK cells were found to be increased in sensitive tumors relative to untreated and drug-sensitive tumors (Fig2b). Single cell RNA-seq data was further validated using flow cytometric analysis (Fig 2f). Sensitive tumors were comprised of 16.55% $CD3e^+$ T cells in the primary tumors which is significantly increased relative to saline injected sham control tumors (10.29%) or tumors unresponsive to treatment (11.33%). We also observed an increase in the number of CD8+ T cells within the tumor T cell population of drug resistant primary tumors, compared to the drug-sensitive tumors (58.1%, 47.8% respectively).

Responsiveness to doxorubicin did not induce tumor infiltration of all immune populations. In fact, DOX treatment induces a decreased abundance in total tumor infiltrating lymphocytes regardless of tumor response. Significant increases in CD45+ immune cells were observed in saline treated tumors (30.0% of tumor cells) compared to both sensitive and resistant tumors (16.85%, 15.92% respectively) (Fig2h). Furthermore, the increase in lymphocyte abundance was exclusive to the TME as both the bone marrow (Fig 2i) and spleen (Fig 2j) were found to be largely unchanged with a slight increase in abundance only observed in the bone marrow in mice bearing resistant tumors compared to control tumor bearing mice.

*Altered T cell composition in chemoresistant tumors.*

While T cell abundance was confirmed, the functionality and behavior of these infiltrated lymphocytes was further examined using targeted single cell RNA-sequencing focused on tumor residing T cell populations. 5,065 *Ptprc* (CD45) and *CD3e* expressing T cells were identified from pooled resistant and sensitive tumors. In silico dimensional reduction of the transcriptional profiles

of each cell produced 10 clusters of cells denoting different subtypes of T-cell as visualized in a tSNE plot (Fig 3a, Sfig 1). Cluster identification was performed using published gene markers of T cell subtypes (Fig3c). No single population was uniquely identified in sensitive or resistant tumors however, biases toward specific subtypes were discovered depending on chemosensitivity (Fig3b).

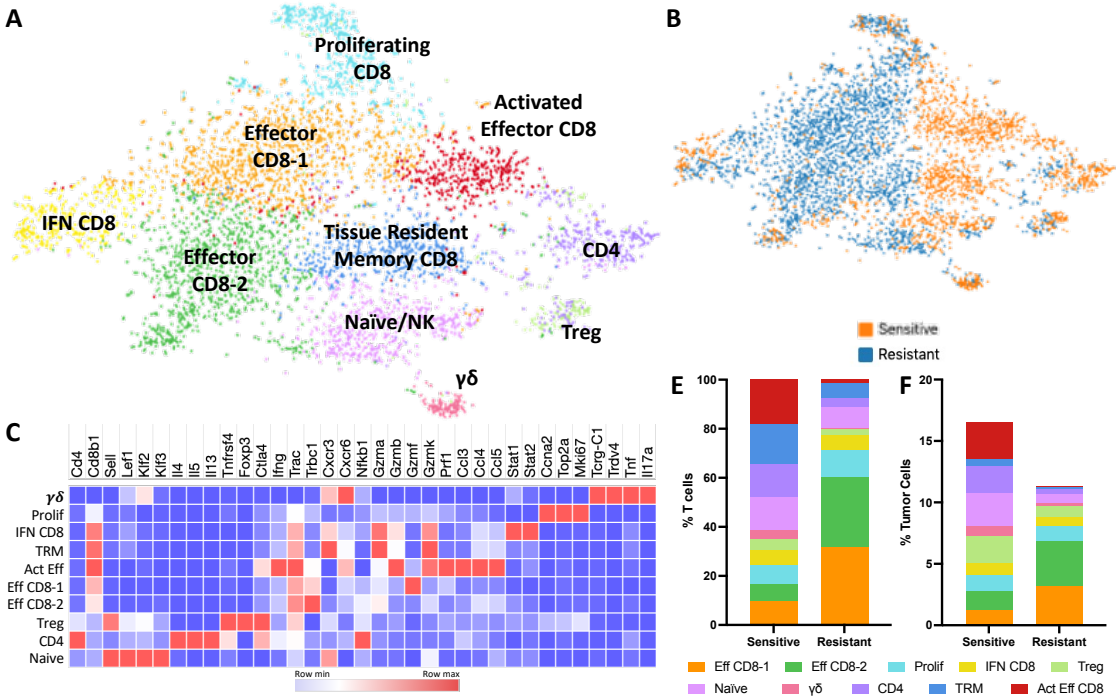


**Figure 3 Single cell sequencing of tumor infiltrating T cells.** A) t-SNE projection of tumor infiltrated T-cells. 10 populations identified via transcriptional profiles are denoted by color. B) t-SNE projection with colors denoting tumor response to DOX. C) Heat map showing relative gene expression for genes of interest per cell in each cell cluster. E) Distribution of T cell subtypes in sensitive and resistant tumors. F) Relative abundance of T cells in sensitive and resistant tumors.

Naïve T cells expressing genes associated with immature T cells and quiescence (*Klf2*, *Klf3*, *Sell* (CD62L), *Lef1*(203,204)) were found to be relatively unchanged (<2 fold change in relative abundance in relation to all T cells) between sensitive or resistant tumors (Fig3c, 3e). Proliferating T cell were a population characterized by expression of Mki67 (Ki-67) and cell cycle

progression genes (*Top2a*, *Ccna2*). Interferon stimulated CD8 T cells expressing high levels of Jak/Stat signaling pathway activation genes (i.e., *Stat1*, *Stat2*) and interferon response genes (*Ifit1*, *Ifit2*, *Ifit3*) were also identified as a consistent population regardless of tumor DOX response.

CD8 T cells were more abundant in resistant (85.2% of T cells) than in sensitive tumors (64.1%). Tumor infiltrated CD8 T cells were further subclassified into 5 subtypes. 2 subtypes, Effector CD8-1 and Effector CD8-2, expressing classical cytotoxic T cell markers (*Ifng*, *Gzma*, *Gzmb*, *Prf1*), were highly abundant in resistant tumors comprising 61.1% of all tumor infiltrating T cells compared to only 16.8% of sensitive tumor T cells.

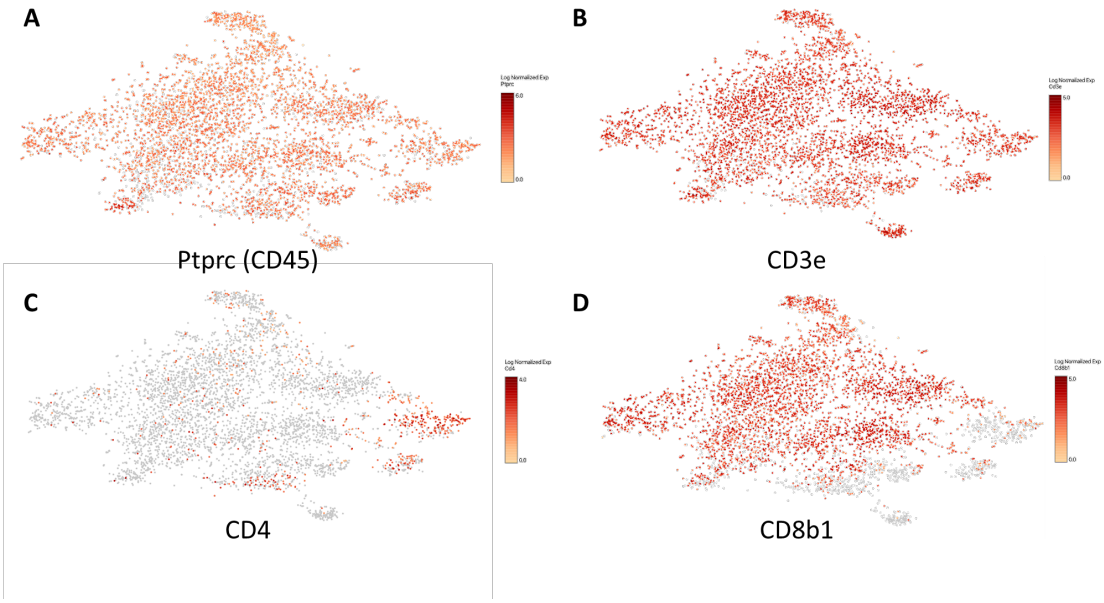


**Supplemental Figure 1. Feature plots denoting T cell gene expression.** t-SNE plots denoting cellular expression of A) Ptprc (CD45 expression), B) CD3ε, C) CD4, and D) CD8b1 in tumor infiltrated T cell poulations.

Sensitive tumors had higher numbers of CD4 T helper cells, regulatory T cells (Tregs), γδ T cells, and CD8 tissue resident memory T cells than resistant

tumors. CD4 T cell populations expressing *CD4* and several cytokines (*IL4*, *IL5*, *IL13*) increased by 350% from 3.8% in resistant tumors to 13.3% in sensitive tumors. Tregs, denoted by increased expression of *Foxp3*, *Ctla4*, and *Tnfrsf4* (CD134), represented 4.5% of sensitive tumor T cells compared to half as many (2.1%) in the resistant populations. γδ T cells expressing gamma and delta T cell receptors (Tcrg-C1 and Trdv4) in addition to *TNFa* and IL-17A were a minor population of T cells yet accounted for a 475% increase in abundance in sensitive tumors (Resistant: 0.8%; Sensitive 3.0%). Cxcr3+ tissue resident memory T cells and activated effector CD8 T cells, denoted by increased levels of activation and cytotoxic genes (*Ifng*, *Czmb*, *Gzmk*, *Prf1*) were the predominant CD8 subtype in sensitive tumors comprising 34.5% of sensitive T cells.

Upon normalization to total tumor cells based on previous cytometric analysis of T cell abundances, increases in naïve, Treg, tissue resident memory CD8, CD4, γδ, and activated effector T cell abundances were amplified. Specifically, γδ T cells were increased 694% and activated effector T cells increased by 2053% in abundance in sensitive vs resistant tumors (Fig3f).

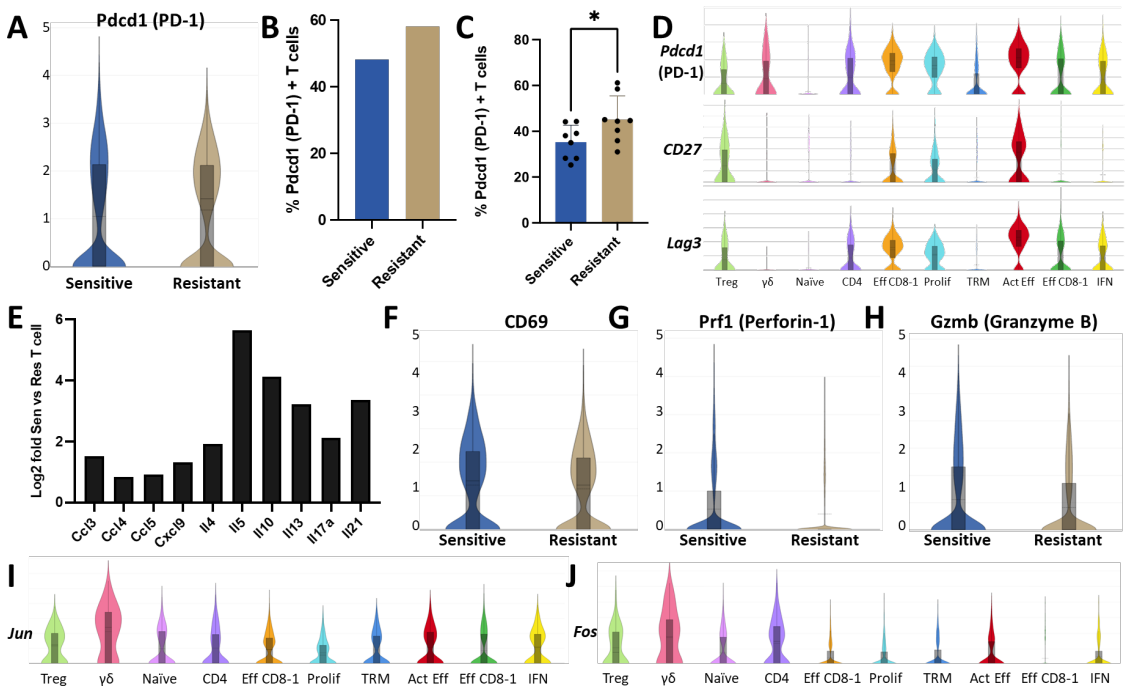


**Figure 4. T cell behavior in response to doxorubicin sensitivity**. A) Violin plots denoting expression of *Pdcd1* per T cell in sensitive or resistant tumors. B) Percentage of tumor residing T cells expressing *Pdcd1* as quantified in single cell RNA sequencing data. *C) Pdcd1+* T cells quantified from tumor infiltrated T cells following doxorubicin treatment using flow cytometric analysis. D) Single cell expression levels of T cell exhaustion marker genes segregated by cell type depicted as violin plots. E) Fold upregulation of chemokine and cytokine genes in sensitive vs resistant T cell populations inferred from single cell RNA sequencing data. F-H) Activation gene markers (*CD69*) and cytotoxic genes (*Prf1, Gzmb*) associated with T cell activity expression in sensitive or resistant tumors depicted as violin plots. I-J) Dimeric transcription factors comprising the AP-1 transcription factor indicative of T cell activation expression segregated by cell types identified in single cell transcriptomic data.

## *T cells populations from doxorubicin sensitive tumors are less exhausted and release higher cytokine levels than resistant tumors.*

Because the increased numbers of T cell subsets in chemosensitive tumors may not necessarily translate into an increase in activation, further analysis of the single cell transcriptomic data was performed to examine critical T-cell behavior in the TME. Chronic antigen stimulation is a well-documented phenomenon in tumors activation resulting in an exhausted phenotype characteristic of decreased effector function, proliferation, and

cytokine production and can be identified through over expression of *Pdcd1* (PD-1) (205,206). T cells from DOX resistant tumors expressed higher levels of *Pdcd1* per cell with a median normalized expression 14.4% greater than the sensitive tumors (Fig4a). Additionally, a 10% increase in the frequency of *Pdcd1*$^{+}$ exhausted T cells was observed in the resistant tumors (Resistant: 58%, Sensitive: 48%). Increased expression of other exhaustion related genes *Tox* and *Lag3* were also found in T cells from Dox resistant tumors (207). Cytometric analysis of tumor infiltrated T cells identified decreased PD-1+ T cells compared to the single-cell transcriptional data however a significant increase in abundance was confirmed in resistant tumors (Fig4c). *Pdcd1, CD27, and Lag3* have previously been utilized as exhaustion markers (208). Elevated expression of exhaustion markers was observed in activated effector CD8, effector CD8-1, effector CD8-2, CD4, and proliferating cell populations (Fig4d). Of particular importance is the exhaustion of Effector 1 and 2 populations as these populations comprise most T cells in resistant tumors.

As expected for less exhaustion, chemokine and cytokine genes were found to be elevated in sensitive tumors (Fig4e). CD4, *γδ,* and activated effector CD8 cells were the primary populations responsible for cytokine production and correlate to overrepresented T cell subtypes in sensitive tumors. Furthermore, T cells from sensitive tumors exhibit increased mean and median expression of *CD69*, an activation marker (209) (Fig 4f). Effector proteins associated with cytoxic activity, *Gzmb* and *Prf1,* were also found to be increased in the sensitive T cell population (Fig4g, 4h). Additionally, expression levels of *Jun* and *Fos,* transcription factors critical to T cell activation (210), were elevated in the cytokine producing CD4 and *γδ* populations.

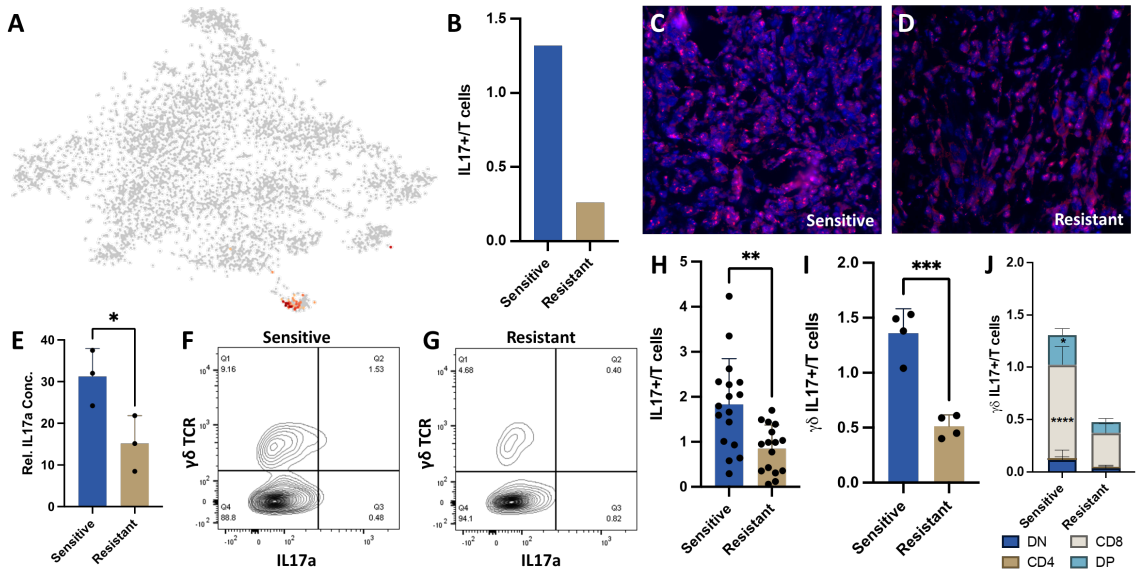


**Figure 5. Increased γδ IL-17+ T cells in the doxorubicin sensitive tumor microenvironment.** A) *IL17a* expression is restricted to γδ T cells. B) Ratio of IL17+ cells in sensitive and resistant tumors extrapolated from single cell RNA sequencing data. C-D) Representative immunohistochemistry images of 4T1 tumor sections from sensitive and resistant tumors following doxorubicin therapy. E) Protein abundance quantification in tumors normalized to GAPDH expression. n=3 F-G) Representative flow cytometry plots identifying γδ IL-17+ T cells in T cell populations. H) Quantitation of IL17+ T cells from DOX sensitive and resistant tumors. I) Quantitation of γδ IL17+ T cells from DOX sensitive and resistant tumors. n=4. J) Distribution of γδ IL17+ T cells identifying expanded CD8 and double positive (CD4+CD8+) cells in sensitive tumors. n=4. * $p \leq 0.05$, ** $p \leq 0.01$, *** $p \leq 0.001$

## *Sensitive tumors contain increased CD8 γδ IL-17+ T cells in the tumor microenvironment.*

Due to the increased cytokine production and activation of cytokine secreting T cell populations in tumors responsive to chemotherapeutic treatment, we next sought to further examine the impact of cytokines on cancer cells. Specifically, *IL-17A* expressing T cells were found to be more abundant in DOX sensitive than in resistant tumors. IL-17A is a proinflammatory cytokine with known pro and anti-tumor effects (211–214). Further transcriptional characterization of *IL-17A* expressing T cells revealed that they are not derived from αβ CD4 T cells but from γδ IL-17+ T cells (Fig5a). This T-

cell sub-population comprised 1.32% of all T cells in sensitive tumors and 0.26% of all T-cells in resistant tumors (Fig5b). While this population only represents a minor portion of the tumor infiltrating lymphocytes, single cell RNA-seq on syngeneic 4T1 tumors revealed that IL-17 is uniquely expressed and secreted from these specialized T cells into the tumor microenvironment yet numerous cell types in the tumor microenvironment can bind this cytokine by expressing its receptor (*IL-17ra*) underlying the potential impact of IL-17A in the tumor microenvironment (Sfig 2). Furthermore, despite the minimal quantity of cells, histological analysis of representative sensitive and resistant tumors confirmed detectable levels of IL-17A throughout the tumor with increased abundance in DOX-sensitive tumors (Fig 5c, 5d). Additional protein quantification was performed via Western Blot analysis further confirmed the increased abundance from homogenized tumor samples with sensitive tumors possessing 257% more IL-17A than resistant tumors (Fig5e).

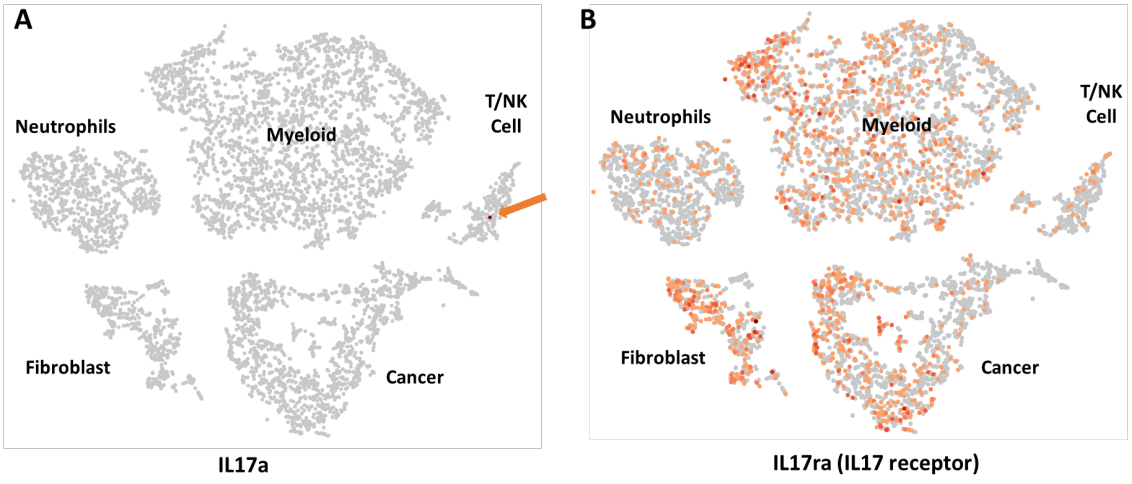


**Supplemental Figure 2. tSNE projection of 4T1 syngeneic tumor cells**. A) IL-17A expression restricted to IL-17+ T cells (arrowhead). B) IL-17 receptor (IL-17ra) is widely expressed across several cell types.

Flow cytometry analysis of tumor infiltrating T cells confirmed a significantly higher number of IL-17A expressing T cells in sensitive tumors compared to resistant tumors (1.83%, 0.85% respectively, *p-value*=0.0016) (Fig

5f-5h) with γδ T cells constituting the majority of the IL-17 expressing cells (1.36%, 0.51% respectively) regardless of tumor chemotherapeutic response (Fig5I). Interestingly, CD8+ T cells were identified as the most abundant and significantly increased population in sensitive tumors ($p<0.0001$). CD4+CD8+ double positive T cells population were also found to be significantly increased in chemosensitive tumors relative to resistant ($p=0.0218$) while double negative and CD4 T cells were not found to be significantly altered in abundance (Fig5j).

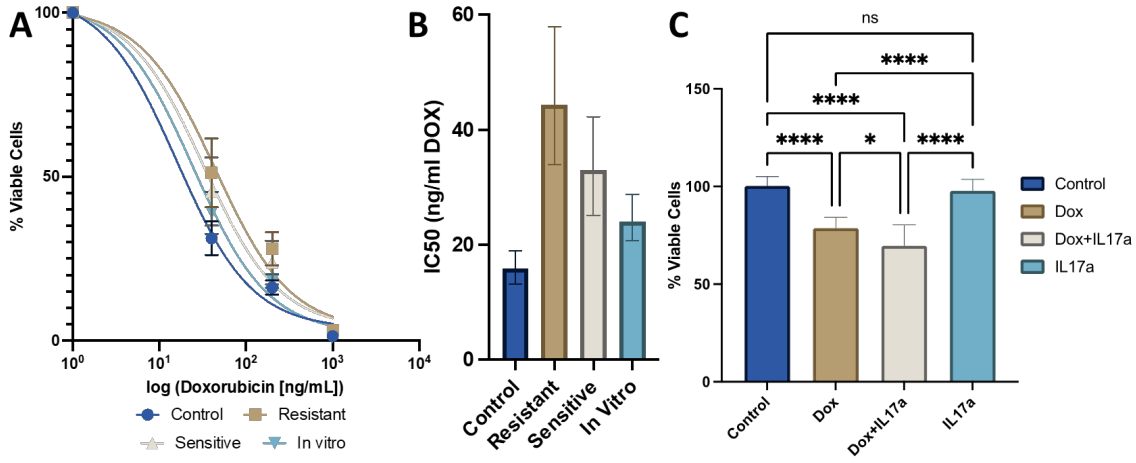


**Figure 6. IL-17A co-administration with doxorubicin directly affects chemotherapeutic efficacy in cancer cells.** A) Ex vivo doxorubicin sensitivity from 4T1-Thy1.1 cells isolated from primary tumors or from in vitro culture. n=12 from three tumor from independent mice. B) IC50 values extrapolated from dose response curves with error bars represent 95% CI. C) Relative viability of 4T1-thy1.1 cells cultured in the presence of DOX and/or IL-17A for 48 hours. n=9-11

*IL-17A increases doxorubicin sensitivity of TNBC cells.*

Cancer cells are among the numerous cell types expressing the IL-17 receptor (Sfig 1). In turn, the role of IL-17A on chemotherapeutic response directly on 4T1 TNBC cells was investigated through utilization of *in vitro* methodologies. Cancer resistance evolution driven by genomic mutations has

been thoroughly reported as a long-term mechanism for alternative response to chemotherapeutic (215–217) however we hypothesize that due to the short duration of treatment and clonal nature of the 4T1-Thy1.1 cell line that this evolution is an unlikely cause of the differential responses observed in DOX treated tumors. *Ex vivo* cytotoxicity assays on isolated 4T1 cells derived from DOX treated tumors were performed to examine intrinsic alterations in chemotherapeutic response conferred from the *in vivo* manipulations. An IC50 curve was generated from 4T1 cells derived from the parental cell line, saline injected control, DOX sensitive, or DOX resistant tumors were administered a range of DOX dosages for 48 hours in culture to generate an IC50 values for each subline. Interestingly, control tumors yielded a significantly decreased IC50 value (15.89ng/mL) compared to *in vitro* (24.50ng/mL) or DOX treated (Resistant: 44.32ng/mL; Sensitive: 32.67ng/mL) tumor 4T1 cells (Fig 6a, 6b). *In vivo* DOX treatment, regardless of response, increased cancer cell resistance above the parental controls. Only resistant sublines were significantly more resistant to DOX than the original line however resistant and sensitive sublines were not found to be significantly different thus suggesting the tumor behavior is not largely driven by a cancer resistance evolution.

Due to the lack of genomic mutations driving the differential DOX response, contributions of IL-17A to DOX chemosensitivity with treatment was next analyzed to evaluate alternate mechanisms driving tumor response. The

inhibitory effects of DOX were significantly enhanced with inclusion of IL-17A to the culture media (Fig6c).

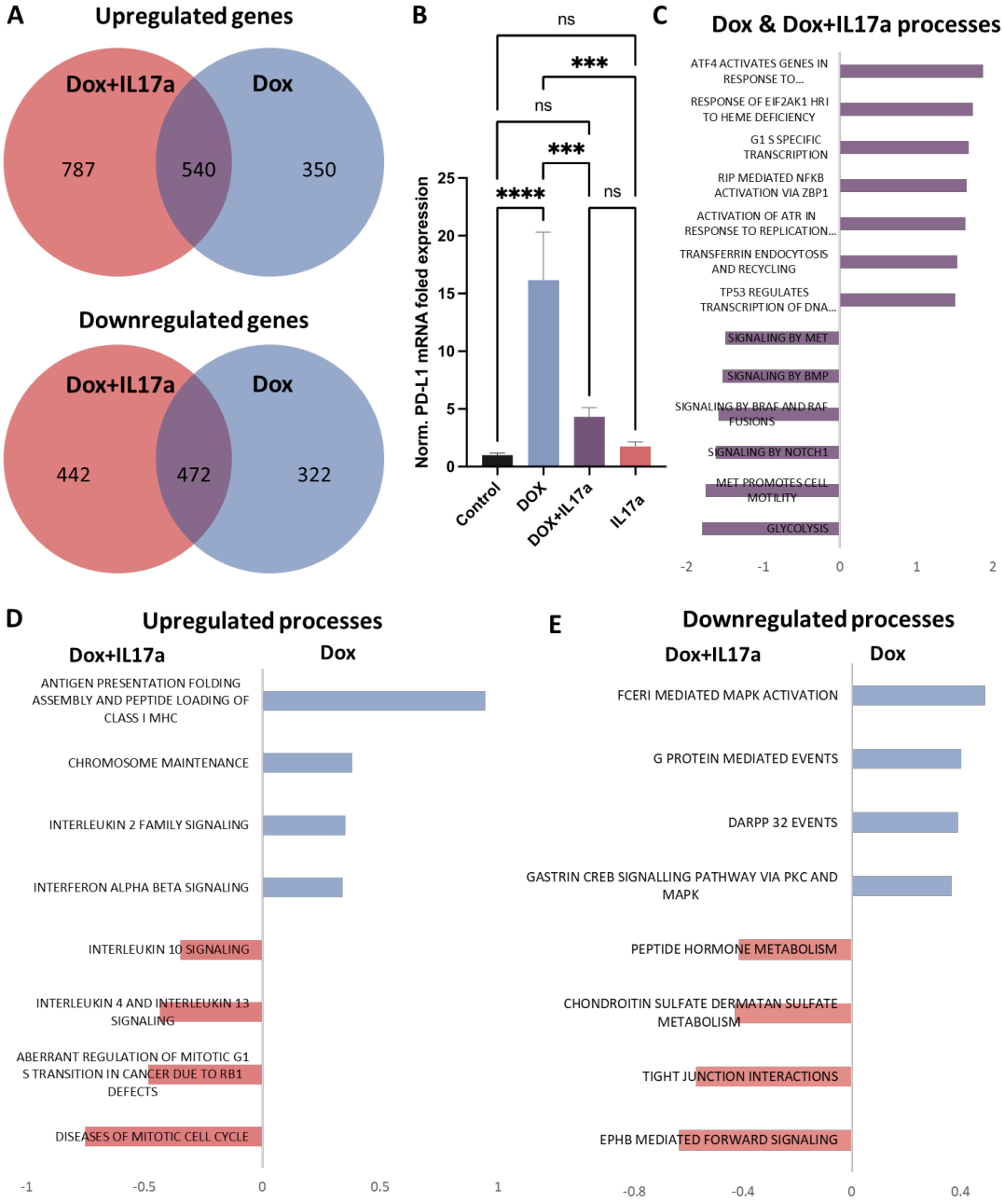


***Figure 7. Transcriptomic analysis of 4T1 cells in response to doxorubicin and IL-17A.*** A) Venn diagrams depicting overlapping differentially expressed genes from 4T1 cells exposed to DOX +/- IL-17A for 48 hours. B) Normalized gene expression of CD274 (PD-L1) across *in vitro* conditions. C) GSEA analysis of enriched Reactome pathways in common to DOX treated cells

regardless of IL-17A. C) Upregulated pathways with differential enrichment. D) Downregulated pathways with differential enrichment. n=3-4

*IL-17A mitigates PD-L1 induces cytokine signaling, cell cycle dysregulation, and mitigates interferon activation in TNBC cells.*

Bulk RNA sequencing was performed on 4T1 cells exposed to doxorubicin or doxorubicin co-administered with IL-17A. Doxorubicin alone upregulated 890 genes and downregulated 794 genes while the addition of IL-17A to doxorubicin treatment yielded 1327 upregulated genes and 914 genes relative to untreated controls. 540 upregulated and 472 downregulated genes that were consistent across doxorubicin treatments regardless of IL-17 inclusion (Fig6a). PD-1 ligand (*CD274*, PD-L1) was upregulated upon doxorubicin treatment consistent to prior studies (218). The addition of recombinant IL-17A to the culture media during DOX exposure abrogated the *CD274* upregulation. Expression levels were found to be significantly different relative to DOX only treatment but not control cells. IL-17A was not found to significantly alter *CD274* gene expression levels when administered alone when compared to control or combinatorial conditions (Fig7b).

In line with prior studies, gene set enrichment analysis of the transcriptional profiles identified that doxorubicin elicits enrichment in genes associated with cellular stress response pathways (ATF4, EIF2AK1, NFKB, ATR, P53) (219–221) while downregulating proliferative pathways (BMP, MET) (222,223) regardless of IL-17A coadministration. Cell to cell signaling (*Braf* and *Notch*) and glycolysis (224) were also found to consistently downregulated in response to doxorubicin with or without IL-17A presence (Fig6c). Furthermore, differential normalized enrichment scores for specific biological processes were discovered to be affected by the coadministration of IL-17A with doxorubicin. Specifically, cell cycle disfunction in progression from G1 to S phase in the cell cycle were also found to be highly upregulated in IL-

17A coadministration and increased immune recruiting cytokine (IL4, 10, and 13) signaling was also promoted. IL-17A mitigated pathways of immune activation that are upregulated because of DOX treatment including inhibition of MHC1 antigen presentation, IL2 signaling, and interferon a/b signaling were mitigated because of (Fig6d). Consistent with previous studies (3–5), mitogen-activated protein kinase (MAPK) activation was found to be increased in 4T1 cells treated with IL-17 and doxorubicin relative to doxorubicin alone (Fig6e).

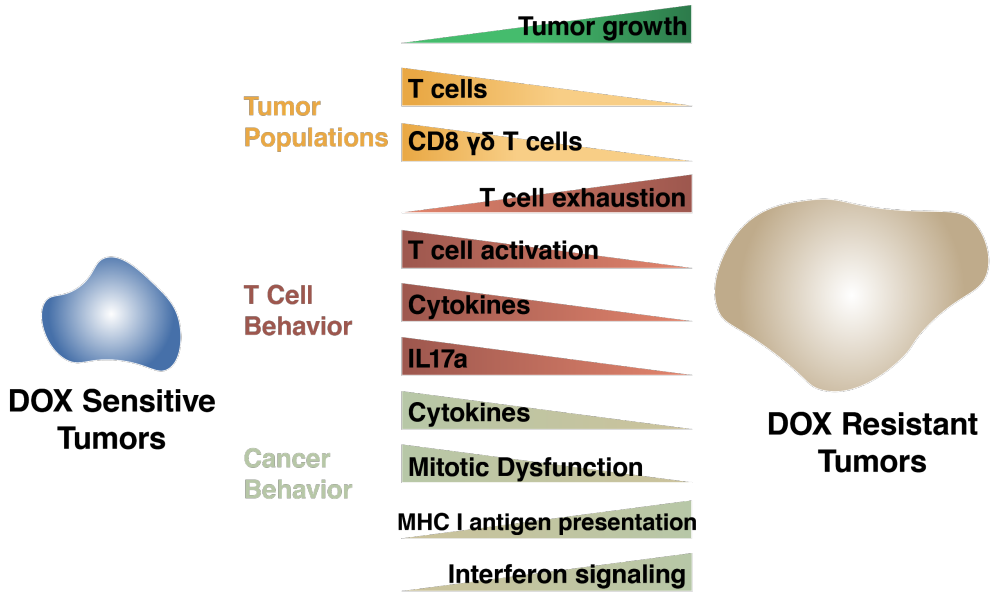


*Figure 8. Summary schematic.*

## Discussion

This study demonstrated the importance of stromal composition to chemotherapeutic efficacy (Fig 8). Single cell transcriptomics and flow cytometric analysis identified increased T cell abundance correlated with tumors sensitive to DOX treatment relative to resistant tumors. Upon deeper transcriptomic characterization of tumor infiltrated T cell populations alterations in the activity, behavior, and subtypes of T cells were found to also

be strongly correlated to chemotherapeutic response. Furthermore, IL-17A secreted by T cells was found to play a direct role on cancer cell sensitivity to DOX however transcriptional alterations in the as a result of IL-17A in cancer cells also likely contribute to signaling cascades inducing T cell exhaustion and T cell recruitment and activation.

Despite the overall increase in T cells in sensitive tumors, the TME of resistant tumors possess an increased effector CD8 abundance however these T cells exhibit increased exhaustion gene expression (*Pdcd1, Cd27, Lag3*) linked to decreased effector function and failure to eliminate cancer cells (208). This cellular state manifests from the chronic stimulation of antigen in tumors. Interestingly, cells exposed to doxorubicin alone induced increased several processes contributing to this phenotype such as antigen presentation, interferon signaling, and increased *CD274* (PD-L1) expression. The upregulation of these processes was significantly mitigated upon coadministration of IL-17A suggesting anti-exhaustion inducing effects derived from cancer cells. The increased cytotoxic gene expression (upregulated *Prf1* and *Gzmb*) in T cells found in chemosensitive tumors further substantiates the increased anti-cancer activity of IL-17A+ DOX sensitive tumors.

In addition to increased activity of cytotoxic effector T cells in DOX sensitive, elevated chemokine and cytokine secretion was inferred from the increased abundance of CD4 T helper cell and γδ T cell populations. Chemokines (Ccl3, Ccl4, Ccl5, Cxcl9) have demonstrated roles in increasing T cell infiltration into the TME (225,226). Furthermore, CC chemokines have also been correlated to improved prognosis in breast cancer patients (226). These potent chemotactic molecules may contribute to the increased infiltration of T cells into the DOX sensitive TME increasing the furthering the anti-cancer effects through increased quantity of active T cells. Single cell

RNA-seq further identified increases in *Il-4*, *IL-5*, *IL-10, Il-13, IL-17A,* and *Il-21* transcripts. These cytokines have a wide range of demonstrated functions in the TME (227). Specifically, IL-4 and IL-13 have demonstrated induction of cancer apoptosis as well as anti-inflammatory and innate immune activation functions (228,229). IL-10 also shares immunosuppressive function in addition to proven roles in antiangiogenic function in tumors and a correlation with improved prognosis in breast cancer (230–232). These functions suggest that the sensitive TME may be stimulated for increased anti-cancer function while modulating the infiltration from pro-tumor stromal cell populations. Despite the anti-tumor functions described previously, cytokine function in the context of DOX treatment will require further studies to fully elucidate the effects these cytokines have in the TME.

Interestingly IL-21 has demonstrated roles in stimulation of IL-17 production which was also found to be upregulated in sensitive tumors (208). Surprisingly, the IL-17A production was largely identified to be secreted from γδ not Th17 T cells in 4T1 tumors. Specifically, sensitive tumors expand the γδ CD8+IL-17A+ T cell population resulting in an increased IL-17a levels. This potent cytokine has potentially wide-spanning effects on numerous cell types found in a tumor and has a direct effect on increasing DOX efficacy in cancer cells. The presence of IL-17A has been examined in multiple cancer types and has arisen as an attractive biomarker of cancer (233,234). Studies on the impact of IL-17A in the TME have yielded both pro and antitumor functions. This phenomenon may be driven by the unique TME compositions found in different cancer types. IL-17 in developing tumors was found to have a negative correlation with survival, enhanced tumor development, or poor prognosis in numerous tumor types including breast cancer, head and neck, ovarian, prostate and colorectal cancer (233–236)) yet anti-tumor benefits have also been identified in and esophageal squamous cell carcinoma (237,238).

Contrasting anti and protumor effects have also been reported within the same tumor type as seen in melanoma (239,240) and lung cancer (241,242) suggesting that TME heterogeneity independent of tissue of origin may also play a contributing role in IL-17 response. This study observed no observable alterations in proliferation when 4T1 TNBC cells was exposed to IL-17 alone. IL-17A increased anti-cancer phenotypes observed *in vitro* only upon coadministration with DOX suggesting an alternate function in the presence of chemotherapeutics. The increased tumor responsiveness to chemotherapeutics in the presence of IL-17 has been previously reported in a range of cancer types (196–198,243). The data provided here supports the benefit of IL-17 in the TME upon anthracycline administration in syngeneic TNBC tumors and functionally characterizes this correlation to direct and indirect effects on cancer elimination.

The findings presented here suggest possible therapeutic benefits to IL-17A coadministration or stimulation in conjunction with anthracycline treatment regimens. Several outstanding concerns will need to be addressed prior to clinical implementation due to the pleiotropic pro and anti-tumor effects noted previously. Furthermore, the long-term effects of the presence of these IL-17A producing cells in TNBC following DOX treatment will require to further analysis for establishment of therapeutic efficacy as numerous studies have identified IL-17 protumor effects in development and progression of cancers which may outweigh the benefits during chemotherapeutic administration.

The source of γδ IL-17a+ T cell populations was not identified in this study. Future therapeutic avenues utilizing γδ IL-17A+ T cells will require identification of differentiation or recruitment into the TME. Recruitment appears to be a viable therapeutic option as intratumoral adoptive cell transfer of γδ T cells during doxorubicin administration has been demonstrated to

rescue the efficacy of chemotherapeutics in IL-17A knockout mice. However, subpopulations of γδ T cells may need to be selected for as T cells lacking IL-17A were unable to recover the sensitive phenotype (196). Additionally, the molecular cues triggering the presence of these beneficial T cells within the course of doxorubicin treatment will allow for more therapeutic targets. The merits of recombinant IL-17a coadministration DOX may also provide therapeutic benefits yet bioavailability, targeting, and stability of this molecule will need to be optimized to evaluate utility. Overall, this data strongly supports the contribution of IL-17A directly on cancer cells and in generating a TME with increased T cell infiltration and cytotoxic activity upon exposure to DOX in TNBC.

## Chapter 5. Comparative molecular characterization of breast cancer exosomes of differing aggressiveness and subtype


### Abstract

Cancer derived exosomes represent an enticing analyte to examine cancer behavior in a non-invasive, non-destructive fashion with applications in clinical diagnostics and pre-clinical research. Exosomes from three human breast epithelial MCF10A or breast cancer cell lines MCF7 a weakly aggressive, ER+, luminal BC; MDA-MB-231 a highly aggressive TNBC were isolated from cell culture media and analyzed for size, quantity, and protein and transcriptional cargo after 2 days in culture. Size and quantity of extracellular vesicles identified that MCF7 cells produced less heterogenous vesicles of smaller diameter, yet increased quantity compared to other cell lines. Transcriptional characterization of exosomal cargo was performed using small RNA sequencing technology identifying numerous coding and non-coding RNA species present in exosomes. Despite remarkably conserved distribution of RNA subtypes across all cell lines, unique profiles of small RNAs were observed in gene abundance identifying that exosomal content from BC cell lines share greater similarity to each other as opposed to normal epithelia. Further analysis of miRNA cargo showed comparable similarity across cell lines and functional enrichment analysis performed on differential pools of miRNAs predicts numerous cancer progressing biological functions could be potentially impacted by exosomal miRNA. Proteomic analysis identified that MCF7 exosomes had the most unique protein profile with increased protein abundance observed relative to other cell lines examined. The utility of this type of analysis in a clinical setting was validated as 4 putative biomarkers (hsa-mir-375, hsa-mir-138-1, FBP1, HLA-A) generated from this survey matched clinical tumor data. This work provides a valuable proof of concept that cancer cell lines of different subtype and behaviors can be discriminated preclinically and has demonstrated translatability to clinical significance.

## Introduction

Breast cancer (BC) is a frequent cancer in women, with an estimated 1.7 million diagnosed worldwide every year (124). Therapeutic approaches, such as surgery, chemotherapy, radiation, hormone therapy, and targeted therapy, have reduced the mortality rates associated with BC; however, therapeutic failures remain common and BC persists as a major cause of cancer-associated death in vulnerable individuals (244). Regular screening and mammograms have vastly improved early detection increasing progression free survival in recent decades (245,246) however these screening approaches are largely based on results from trials conducted over 20 years ago (247). Since the advent of these screening techniques, the understanding of breast cancer oncogenic drivers and the underlying mechanisms fueling its malignant nature have vastly improved and underscore the inherent intertumor heterogeneity of this disease. Therefore, the further subdivision of cancer subtypes and identification of individual tumor behavior are critical to advance the precision of cancer prognosis, diagnosis, and therapy (248).

Intercellular communication is fundamental to many biological processes from embryonic development to wound healing to cancer, and research has shown that cell-to-cell transfer of extracellular vesicles (EVs) is a critical biological mechanism by which cells exchange information [4]. EVs include all membrane-bound particles released by cells; the current distinguishing criteria for diverse EV populations (*e.g.*, exosomes, microvesicles, apoptotic bodies) are based on size, density, and subcellular origin [4, 5]. EVs carry molecules, such as proteins, DNA, and RNAs, that can change cellular behavior or function when taken up by recipient cells [6]. Many cell types, including tumors, secrete EVs into their microenvironment. Exosomes are a subtype of EVs of particular interest as these are produced via the endocytic pathway with specific cargo (biologically active molecules

contained within exosomes) as opposed to other EV species which bud directly from the plasma membrane and contain non-specific macromolecules from the cytoplasm which may not necessarily correlate with their function (249). Furthermore, the lipid bilayer membrane of exosomes safely packages molecular cargo, such as RNA and proteins, that would otherwise be subject to proteolysis, RNases, and other degrading enzymes (250) Exosomes are small in size (30–150 nm), and have been shown to be highly stable, and can be isolated and analyzed following freeze/thaw with retention in biological activity (251).

Because cancer cells release EVs into their microenvironment and EVs travel through body fluids to distant sites, cancer-derived exosomes (CDE) have been extensively studied to determine their role in promoting metastasis, drug resistance, escape from immune system recognition and other processes involved in disease progression (252,253). In fact, it is now established that in some cases, specific cancer-derived exosomes correlate with cancer-associated biological properties and functions (254–256). Not only can EVs influence the fate of another cell and govern a variety of disease properties, but the specific type of cargo packaged in EVs can dictate the molecular response of the recipient cell (257). Exosomes derived from human breast cancer cell lines have been previously surveyed and some microRNAs (miRNA) and protein biomarkers have been identified to relate to metastatic potential (258).

EVs also have shown great potential as diagnostic and therapeutic tools for cancer. Given that these EVs have been found in a wide range of biofluids including blood serum, urine, cerebrospinal fluid, breast milk, bile, semen, saliva, and sputum; all contain thousands to billions of exosomes per microliter of sample; therefore, they have potential to be further studied and used for non-invasive diagnostics of disease (259). As such, CDEs have been shown to be informative cell-free vesicles representative of their cell of origin and have

been used as cell-free biomarkers. Biomarkers from exosomal cargo of protein-coding or non-protein coding origin correlate with clinical disease progression and have previously indicated success as a non-invasive metrics of tumor status. Additionally, preclinical findings focused on CDE in cancer have been successfully translated into clinical relevance with numerous studies correlating in vitro and animal studies to clinical impacts (260–262).

In this study, I isolated and characterized exosomes derived from three different breast cancer cell lines: MCF-10a (normal epithelia), MCF-7 (weakly metastatic, breast cancer of luminal origin) and MDA-MB-231 (highly metastatic, TNBC). Using RNA sequencing and mass spectrometry I identified a panel of proteomic and RNA-based biomarkers found in CDEs that may be indicative of disease subtype and metastatic character. These findings were also correlated to publicly available clinical data providing a valuable proof of concept that cancer behaviors and discrimination of subtype in vitro has clinical significance and may provide a non-destructive analyte in a preclinical setting.

## Methods

### *Cell culture and exosome isolation*

Human breast cancer cell lines MDA-MB-231, MCF-7, and MCF-10a (ATCC, Manassas, VA, USA) were cultured as subconfluent monolayers in DMEM/F12 media (Gibco, Waltham, MA, USA) supplemented with 10% FBS (Gibco, Waltham, MA, USA) and 1% penicillin/streptomycin (Gibco, Waltham, MA, USA) on standard tissue culture dishes coated in a humidified incubator at 37°C and 5%$CO_2$. Exosomes were isolated from ~2.0x$10^7$ sub-confluent cells cultured in serum-free media for 48 hours using ExoQuick-TC kits (Systems Biosciences, Palo Alto, CA), per manufacturer guidelines. Briefly, 10 mL of exosome enriched media was centrifuged at 3,000g for 15 min. This was

followed by the addition of 5 mL of isolation reagent, vortexing for 5 min, and overnight incubation at 4 °C. After 12 h of incubation, the sample was centrifuged at 1,500g on a Sigma 13190 refrigerated centrifuge for 30 min. The supernatant was discarded, and the pellet was resuspended in 250 µL of resuspension buffer. 3 biological replicates were collected for each cell line.

*Nanoparticle Tracking Analysis*

NTA was recorded on a NanoSight LM10 (Malvern Panalytical, Wesborough, MA, USA) instrument with illumination at 488 nm. Following dilution of purified EVs (1:1000) in triple-filtered PBS, samples were introduced by perfusion pump. For a typical experiment, three 60 s videos were recorded, with 30 s of sample flow between replicates. Concentration was confirmed to be in the acceptable range for NTA analysis (3–20 × $10^8$ particles/mL), or else diluted/concentrated appropriately and re-analyzed.

*Exosomal RNA sequencing and data analysis.*

Small RNA sequencing libraries were constructed using the NEB Next small RNA library kit according to the manufacturer's protocol then sequenced on an Illumina Nextseq550 instrument. Read quality from RNA-seq raw data was first assessed using FastQC (263). Sequence data was aligned to the human genome (hg19) using TopHat2 and STAR (264). Subsequently, gene-wise readcounts were calculated using 'featureCounts' from Rsubread package. Then, the count data was normalized using TMM normalization method, and differentially expressed genes were identified using 'limma' (265) and 'voom' (266). Genes that were >2 fold up- or down-regulated with an FDR corrected p-value<0.05 were considered significantly differentially expressed.

*Protein Isolation*

Purified exosomes were resuspended in 50% RIPA buffer v/v (ThermoFisher Scientific) and protein concentration was measured by BCA assay (Thermo Scientific, USA). All protein samples were subjected to clean-up / reduction / alkylation / tryptic proteolysis by using suspension-trap (ProtiFi, Inc.) devices. S-Trap is a powerful Filter-Aided Sample Preparation method that consists in trapping acid aggregated proteins in a quartz filter prior to enzymatic proteolysis. Proteins were resuspended in 50 µL SDS solubilization buffer consisting of 5% SDS, 50 mM TEAB, pH 7.55. Disulfide bonds were reduced with dithiothreitol and alkylated (in the dark) with iodoacetamide in 50mM TEAB buffer. Digestion constituted of a first addition of trypsin 1:100 enzyme: protein (wt/wt) for 4 hours at 37 °C, followed by a boost addition of trypsin using same wt/wt ratios for overnight digestion at 37 °C. To stop the digestion, the reaction mixture was acidified with 1% trifluoroacetic acid. The eluted tryptic peptides were dried in a vacuum centrifuge and re-constituted in water with 2% acetonitrile.

*Liquid chromatography tandem mass spectrometry*

Peptides were directly loaded onto an Ionopticks (Parkville, Victoria, Australia) 75 um x 25 cm 1.6um C18 Aurora column with Captive Spray emitter. Peptides were separated using a Bruker nanoElute UHPLC at 400 nl/min. Solvent A composition was 0.1% formic acid in water, Solvent B was 0.1% formic acid in acetonitrile. Gradient conditions were 0 to 60 min (2%B to 14%B), 60 min to 90 min (14% to 24%B), 90 to 100 min (24% to 34%B), 100 to 110 min (34% to 95%B), 110 to 120 (95%). Eluting peptides were then further separated using TIMS (trapped ion mobility spectrometry) on a Bruker timsTOF Pro mass spectrometer. Mass spectrometry data was acquired using the dda PASEF method (267) The acquisition scheme used was 100 ms accumulation, 100 ms PASEF ramp (at 100% duty cycle) with up to 10 PASEF MS/MS scans per topN acquisition cycle. The capillary voltage was set at

1700V, Capillary gas temp 200C. The target value was set at 20,000 a.u. with the intensity threshold set at 500 a.u. The m/z range surveyed was between 100 to 1700. Precursor ions for PASEF-MS/MS were selected in real time from a TIMS-MS survey scan using a non-linear PASEF scheduling algorithm. The polygon filter (200 to 1700 m/z) was designed to cover ions within a specific m/z and ion mobility plane to select multiply charged peptide features rather than singly charged background ions. The quadrupole isolation width was set to 2 Th for m/z < 700 and 3 Th for m/z 800.

*Mass spectrometry data analysis*

Mass spectrometry raw files were processed with MSFragger, v3.1 (www.nesvilab.org). For all searches, a protein sequence database of reviewed Homo sapiens proteins (accessed 07/05/2020 from UniProt) was used. Decoy sequences were generated and appended to the original database for MSFragger. A maximum of two missing cleavages were allowed, the required minimum peptide sequence length was 7 amino acids, and the peptide mass was limited to a maximum of 4600 Da. Carbamidomethylation of cysteine residues was set as a fixed modification, and methionine oxidation and acetylation of protein N termini as variable modifications. The initial maximum mass tolerances were 70 ppm for precursor ions and 35 ppm for fragment ions. A reversed sequence library was generated/used to control the false discovery rate (FDR) at less than 1% for peptide spectrum matches and protein group identifications. Decoy database hits, proteins identified as potential contaminants, and proteins identified exclusively by one site modification were excluded from further analysis. Label-free protein quantification was performed with the IonQuant algorithm (268). All other MsFragger parameters were kept at their default values.

*Analysis software and statistical analysis*

Heat maps were generated using Morpheus (Broad Institute) https://software.*broadinstitute*.org/*morpheus*. mirna functional enrichment analysis was performed using TAM 2.0 (269). Clinical data shown here are in whole based upon data generated by the The Cancer Genome Atlas (TCGA) Research Network: https://www.cancer.gov/tcga. Statistical analyses were performed using GraphPad Prism. Data is presented from three biological replicates per cell line. Abundances of biomolecules of at least 2-fold difference with p values <0.05 to be significantly different. One-way ANOVA and post-hoc Tukey's Test were used to assess statistically significant differences of mean expression values. Results were considered statistically significant for $p$ values < 0.05.

## Results

*Characterization of breast cancer exosomes of varying metastatic potential and breast cancer subtype.*

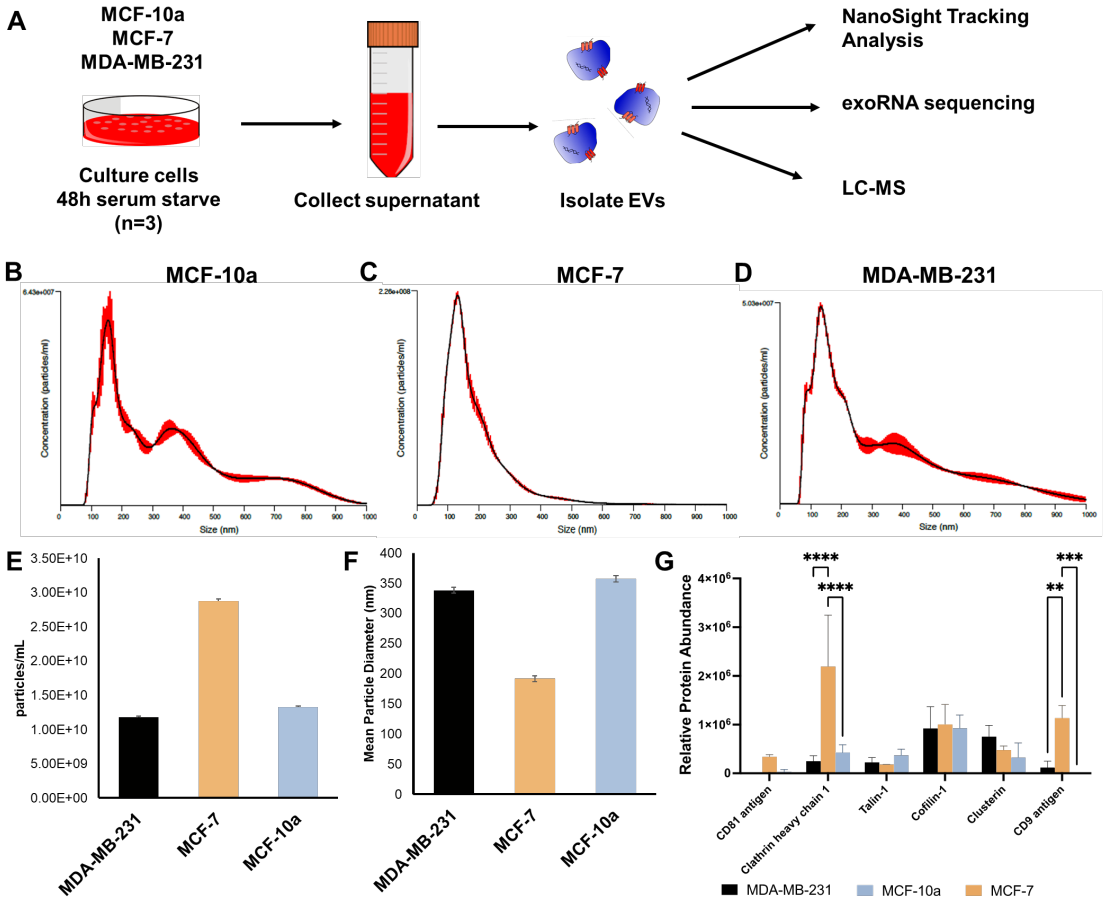


**Figure 1. Characterization of breast cancer exosomes with varying metastatic potential.** A) Experimental design. Breast cancer (BC) cell lines [MCF-10a MCF-7 and MDA-MB-231 (triple-)] were grown to confluency, placed in serum-free media for 48 hours, supernatants were collected, EVs were isolated and processed for downstream analysis. B-D) NanoSight Tracking Analysis was performed, and distribution of isolated vesicles was determined along with E) quantification of vesicle concentration and F) average vesicle size (nm). G) Protein abundance of conventional exosomal markers. Error bars represent standard deviation. n=3/cell line

To compare exosomes representative of breast cancer subtypes and varying behaviors, exosomes were isolated from MCF-10a, MCF-7 and MDA-

MB-231 cells (Fig 1A). Both MCF-10a and MDA-MB-231 vesicles exhibited a range of particle sizes from 100-1000nm in size, but the majority of particles were ~400 nm in size (Fig 1B, D). MCF-7 exosomes displayed a different range of vesicle sizes ranging from 50-400nm (Fig 1C). Additionally, the total exosomal output and particles yielded from $2.0x10^7$ cells per replicate varied across cell lines. MCF-7 cells produced the greatest number of exosomal particles, $2.88x10^{10}$ particles per mL of media (Fig 1E) while MCF-10a and MDA-MB-231 yielded on average $1.33x10^{10}$ and $1.18x10^{10}$ particles/mL, respectively. In general, MCF-10a and MDA-MB-231 cells generated EVs of similar sizes, averaging 357 nm and 338 nm in diameter, respectively; while MCF-7 generated smaller vesicles, averaging 191 nm in diameter (Fig 1F). Common exosomal protein biomarkers (270) were surveyed and confirming the presence of CDE in EV populations (Fig1G) yet significant deviations in abundance across cell lines was observed in 2 of the 6 (Catherin heavy chain 1, CD9 antigen) exosomal markers examined. Additionally, 2 well-utilized exosomal markers characterized for high enrichment in exosomes (CD9, CD81) were not found at significant levels across all cell lines (271)

*RNA exosomal cargo varies between cancer cells of varying breast cancer subtypes.*

Small RNA sequencing, RNA size selection of 20-150bp in length, was utilized to identify small non-coding RNAs differentially abundant in isolated CDEs. Despite size selection and a lack of fragmentation within the sequencing preparation, CDEs primarily packaged protein-coding RNA (Fig 2a-c) at comparable abundance (67-70% of all aligned reads). The composition of non-coding (lincRNA, rRNA, snoRNA, etc) transcripts was also surprisingly highly conserved across cell lines. Of the non-coding transcripts, 33%, 35% and 37% corresponded to pseudogenes (nonfunctional segments that resemble functional genes) in MCF10a, MDA-MB-231 and MCF7 exosomes, respectively

(Fig 2D-F). The most abundant type of non-coding RNA was long intergenic non-coding RNAs (lincRNAs), representing 20% of MCF10a, 20% MDA-MB-231 CDE, 18% of MCF7 total RNA species. Antisense transcripts are single stranded RNAs that prevent transcription of their complementary protein coding gene and function as regulators of mRNA turnover (272). These were the next most abundant subclass of RNA exosomal cargo, representing 17%, 16% and 14% of MCF10a, MDA-MB-231 and MCF7 exosomal RNAs, respectively. Ribosomal RNA (rRNA) and small nucleolar RNA (snoRNA) consistently represented 4% and 2% of exosomal genetic content across all three breast cancer cell types. Small nuclear, snRNAs, represented 3% in both MCF-10a and MDA-MB-231 exosomes and 5% of MCF7 exosomal small RNA content. Lastly, microRNAs (miRNAs), an important class of non-coding RNAs were found in each of the three types of BC exosomes analyzed at various abundances: 3% in MCF10a and MDA-MB-231 and 2% in MCF7.

While the composition of RNA subtypes in CDE were remarkably conserved, the genes expressed were found to be cell line dependent. Unbiased hierarchical clustering of all genes identified from each cell line resulted in a segregation of cancer (MCF7 and MDA-MB-231) from normal epithelia (MCF10a) (Fig 2g). Furthermore, when compared back to MCF10a exosomal RNA profiles, differentially abundant genes were identified (Fig 2h, i) identifying cell type specific exosomal RNA cargo. MCF7 produced exosomes with a more unique RNA profile with 87% of the increased abundant genes unique to this cell line as opposed to 50% of differentially increased genes unique to MDA-MB-231 CDEs. Genes found to be decreased in CDEs were also consistent with this finding as 58% and 24% of decreasing genes compared to MCF10a cells were found to be unique in MCF7 or MDA-MB-231, respectively.

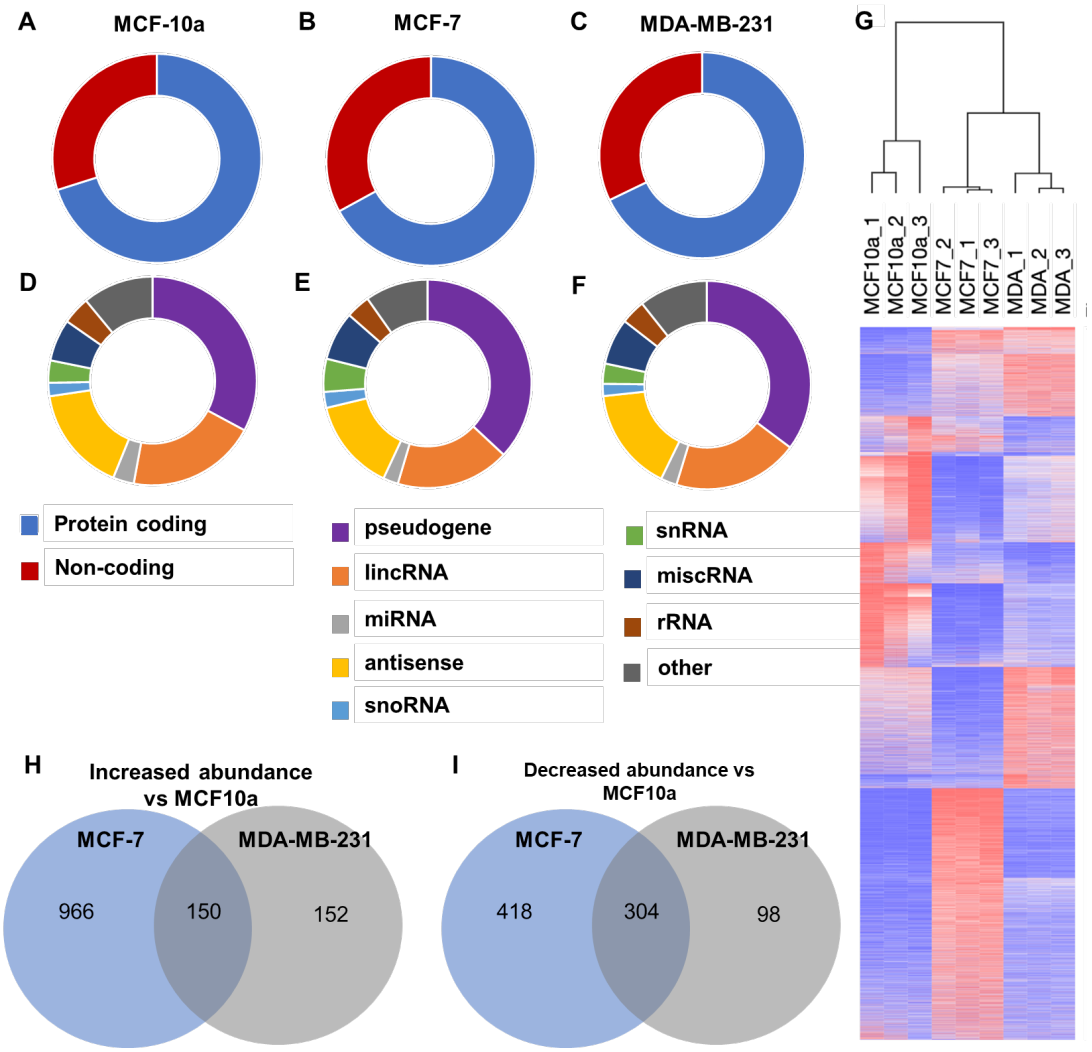


**Figure 2. RNA sequencing (exoRNA sequencing) of breast cancer exosomes.** A-C) Distribution of protein coding to non-coding genes identified in exosomes isolated from each breast cancer cell line: A) MCF-10a, B) MCF-7 and C) MDA-MB-231. D-F) smRNA subtype distribution: long intergenic non-coding RNAs (lincRNA), microRNAs (miRNA), antisense genes, small nucleolar RNAs (snoRNA), small nuclear RNAs (snRNA), miscellaneous RNA (miscRNA), ribosomal RNA (rRNA) and other non-coding regions of low abundance. Quantity of genes G) upregulated and (H) downregulated in exoMCF7 and exoMDA relative to exoMCF10a.

*Cancer derived exosomal miRNAs identify unique functional characteristics associated with cancer behavior.*

MiRNA's represent a well-studied non-coding RNA species with numerous studies identifying functional significance in cancer behavior and

progression (273). Therefore, characterization of miRNAs was further examined in order to identify if exosomal cargo can serve to distinguish cancer types and behaviors. 235 miRNA genes were identified in the exosomal cargo of the cell lines examined with 180 (76.6%) of those differentially abundant in CDE relative to MCF10a. A majority of miRNAs were enriched in MCF10a exosomes relative to cancer cell lines (88% of differentially abundant genes) while minimal upregulation of genes (12%) was observed in CDE relative to those derived from MCF10a cell line (Fig 3a, 3b). Unbiased hierarchical clustering of all miRNAs across cell lines also confirmed an increased similarity between cancer cell lines relative to normal epithelial MCF10a as well as an increased abundance in a majority of miRNA genes relative to the cancer cell lines (Fig 3d). Enrichment of these miRNA populations of interest were analyzed across functional associations of the miRNA based on publication history identifying biological functions potentially altered as a result of the miRNAs identified (Table1-4). Numerous of the biological functions identified play an integral role in tumor biology and cancer progression such as inflammation, angiogenesis, cell death, epithelial to mesenchymal transition (EMT), and differentiation thus implicating possible downstream effects of miRNA in the behavior of cancer. Of note was the lack of enrichment in any biological function in MDA-MB-231 enriched exosomal miRNA. Upon miRNA comparison of both CDE cell lines, 56 miRNAs were found to be enriched in MCF7 exosomal populations while 45 miRNA's were increased in MDA-MB-231 (Fig 3c). Enrichment of biological functions previously identified to be altered by these genes were also found to be cancer related behaviors (Table 5, 6).

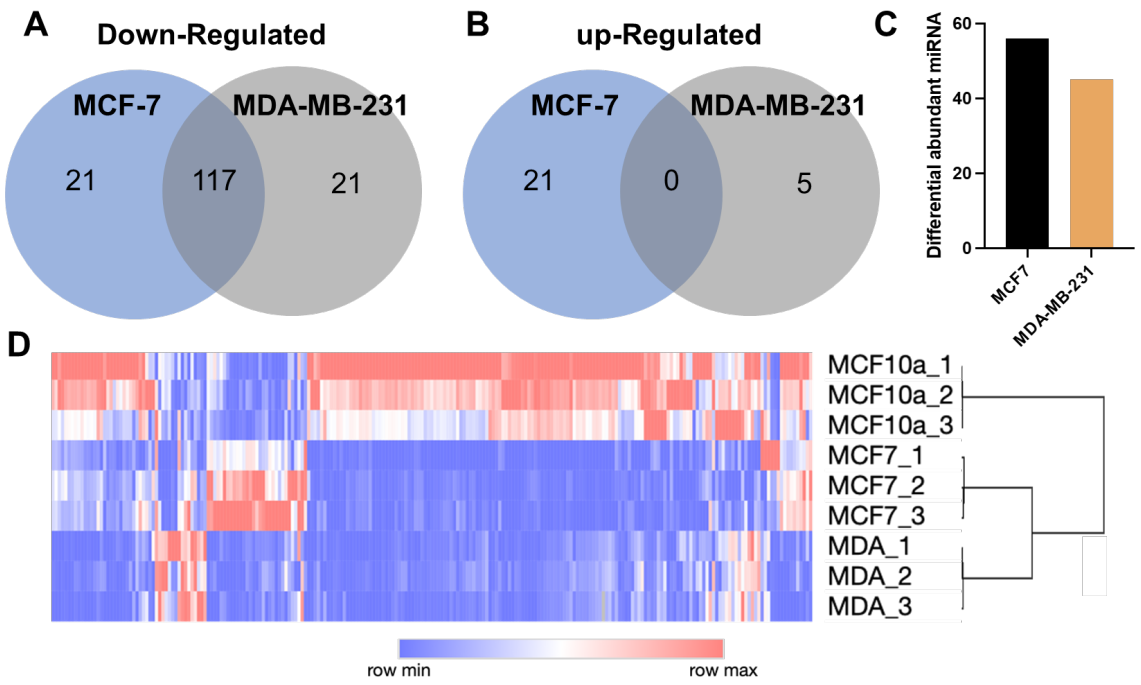


**Figure 3. CDE miRNA cargo analysis.** A, B) Venn diagrams representing convergence of differentially abundant exosomal miRNAs in MCF7 and MDA-MB-231 cells relative to MCF10a. C) Quantitation of differentially abundant miRNA genes identified when comparing MCF7 vs MDA-MB-231. D) Heat map of all miRNA expression across all replicates and hierarchal clustering based on miRNA abundance profiles.

**Table 1. miRNA functional associations decreased in cancer vs MCF10a exosomes.**

| Biological Function | Count | Percent | Fold | P-value | Bonferroni | FDR |
|---|---|---|---|---|---|---|
| Inflammation | 26 | 23% | 4.44 | 9.16E-12 | 6.37E-09 | 1.02E-09 |
| Apoptosis | 25 | 24% | 4.51 | 1.74E-11 | 1.21E-08 | 1.63E-09 |
| Immune Response | 21 | 23% | 4.36 | 1.95E-09 | 1.35E-06 | 1.24E-07 |
| Cell Motility | 10 | 48% | 9.10 | 2.09E-08 | 1.45E-05 | 1.09E-06 |
| DNA Damage Response | 8 | 50% | 9.55 | 3.81E-07 | 2.65E-04 | 1.54E-05 |
| Cell Cycle | 17 | 20% | 3.91 | 4.75E-07 | 3.30E-04 | 1.87E-05 |
| Angiogenesis | 14 | 22% | 4.12 | 2.95E-06 | 2.05E-03 | 8.88E-05 |
| Regulation of Stem Cell | 15 | 19% | 3.63 | 6.76E-06 | 4.70E-03 | 1.77E-04 |
| Chemosensitivity Of Tumor Cells | 5 | 63% | 11.94 | 1.75E-05 | 1.21E-02 | 3.74E-04 |
| Cell Proliferation | 14 | 18% | 3.34 | 3.80E-05 | 2.64E-02 | 7.58E-04 |

**Table 2. miRNA functional associations increased in MCF7 vs MCF10a exosomes.**

| Biological Function | Count | Percent | Fold | P-value | Bonferroni | FDR |
|---|---|---|---|---|---|---|
| Carbohydrate Metabolism | 3 | 33% | 28.21 | 1.14E-04 | 2.98E-02 | 1.35E-02 |
| Epithelial-to-Mesenchymal Transition | 5 | 6% | 5.10 | 2.22E-03 | 5.79E-01 | 1.16E-01 |
| Cell Adhesion | 2 | 25% | 21.15 | 3.57E-03 | 9.32E-01 | 1.67E-01 |

**Table 3. miRNA functional associations decreased in MCF7 vs MCF10a exosomes.**

| Biological Function | Count | Percent | Fold | P-value | Bonferroni | FDR |
|---|---|---|---|---|---|---|
| Inflammation | 8 | 7% | 6.68 | 8.21E-06 | 2.77E-03 | 2.08E-03 |
| Response to Hypoxia | 3 | 25% | 23.38 | 2.15E-04 | 7.24E-02 | 3.47E-02 |
| Apoptosis | 6 | 6% | 5.29 | 5.61E-04 | 1.89E-01 | 6.65E-02 |

**Table 4. miRNA functional associations decreased in MDA-MB-231 vs MCF10a exosomes.**

| Biological Function | Count | Percent | Fold | P-value | Bonferroni | FDR |
|---|---|---|---|---|---|---|
| Inflammation | 7 | 6% | 5.55 | 1.28E-04 | 4.30E-02 | 6.51E-03 |
| Tumor Suppressor MiRNAs | 5 | 8% | 6.83 | 5.68E-04 | 1.90E-01 | 2.40E-02 |
| DNA Damage Repair | 3 | 16% | 14.03 | 1.05E-03 | 3.53E-01 | 3.99E-02 |
| T-helper 17 Cell Differentiation | 3 | 16% | 14.03 | 1.05E-03 | 3.53E-01 | 3.99E-02 |
| Cell Death | 5 | 6% | 5.70 | 1.32E-03 | 4.43E-01 | 4.70E-02 |

**Table 5. miRNA functional associations increased in MDA-MB-231 vs MCF7 exosomes.**

| Biological Function | Count | Percent | Fold | P-value | Bonferroni | FDR |
|---|---|---|---|---|---|---|
| Apoptosis | 13 | 12% | 6.05 | 4.27E-08 | 1.93E-05 | 1.26E-05 |
| Inflammation | 13 | 12% | 5.73 | 8.44E-08 | 3.82E-05 | 2.14E-05 |
| Cell Cycle | 8 | 10% | 4.76 | 1.68E-04 | 7.58E-02 | 1.30E-02 |
| Erythrocyte Differentiation | 3 | 33% | 16.45 | 5.91E-04 | 2.67E-01 | 2.38E-02 |
| Cell Motility | 4 | 19% | 9.40 | 6.65E-04 | 3.01E-01 | 2.46E-02 |

**Table 6. miRNA functional associations increased in MCF7 vs MDA-MB-231 exosomes**

| Biological Function | Count | Percent | Fold | P-value | Bonferroni | FDR |
|---|---|---|---|---|---|---|
| Regulation of Stem Cell | 12 | 15% | 5.29 | 1.01E-06 | 5.32E-04 | 4.97E-05 |
| Inflammation | 14 | 13% | 4.36 | 1.26E-06 | 6.64E-04 | 5.72E-05 |
| Epithelial-to-Mesenchymal Transition | 11 | 13% | 4.62 | 1.23E-05 | 6.50E-03 | 4.45E-04 |
| Immune Response | 11 | 12% | 4.17 | 3.37E-05 | 1.78E-02 | 9.81E-04 |
| Cell Cycle | 10 | 12% | 4.20 | 7.63E-05 | 4.04E-02 | 2.09E-03 |
| Tumor Suppressor MiRNAs | 8 | 12% | 4.29 | 3.78E-04 | 2.00E-01 | 7.82E-03 |
| Cell Adhesion | 3 | 38% | 13.07 | 1.13E-03 | 5.97E-01 | 1.82E-02 |

*Putative small RNA biomarkers of cancer aggressive behavior.*

Other RNA species, representing coding, antisense, intronic, lncRNA, pseudogene, rRNA and snoRNA, may also represent biologically active molecules that denote cancer cellular behavior. Furthermore, MDA-MB-231 cells have been characterized as a highly invasive/metastatic form of BC, MCF7 is a less aggressive cancer type, and MCF10a is non-tumorigenic and considered a model of normal mammary epithelial cells (274). Based on this decreasing aggressive phenotype described amongst cell lines tested, small RNAs of other origins were probed for putative biomarkers of aggressive behavior. 15 genes were identified as genes that have correlative with increases in invasive behavior, from a basal level of expression represented in MCF10a with increasing abundance in MCF7 exosomes and greater abundance in MDA-MB-231 (Fig 4a). The identified genes were all found to be significantly different ($p<0.05$) across cell lines. Conversely, 10 biomarker genes associated decreasing abundance in correlation with aggressive cancer behavior were also identified (Fig 4b).

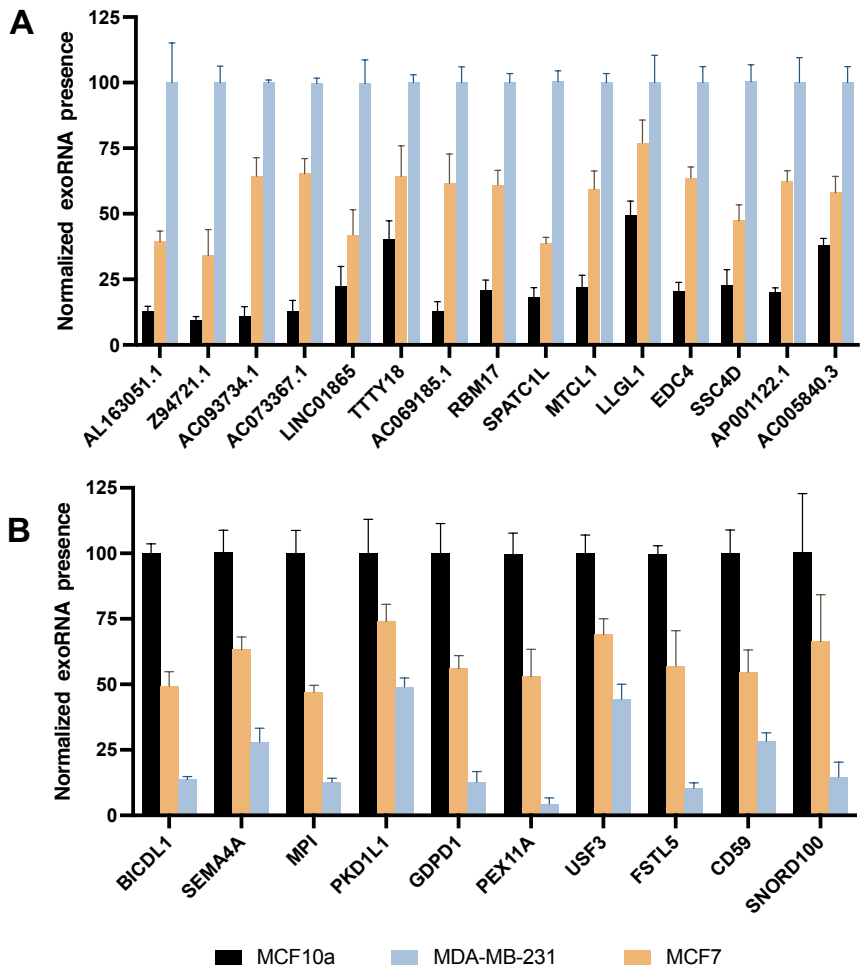


**Figure 4. Exosome-derived candidate biomarkers associated with metastatic disease and normal epithelia.** A) Candidate biomarkers with statistically significant increases in gene expression between exosomes from each cell line, representative of increased invasive/metastatic character. Candidates were only selected based on a statistically significant ($p$-value<0.05) FC<1.5 (fold change) between gene expression of MCF-10a and MCF-7 and also between MCF-7 and MDA-MB-231. Gene expression is normalized as a percentage of maximum expression in MDA-MB-231 exosomes, representative of advanced disease. B) Candidate biomarkers associated with improved disease status. Similarly, biomarkers were selected based on statistically significant decreases (FC>1.5, $p$-value<0.05) between MCF-10a and MCF-7 exosomes; and additionally, between MCF-7 and MDA-MB-231 exosomes to denote candidate biomarkers associated with cancer invasiveness.

*Proteomic analysis of CDEs identifies alternative relationship between cell lines.*

Exosomal proteomic characterization was also performed on CDEs using mass spectrometry. Unbiased hierarchical clustering was performed identifying MCF10a and MDA-MB-231 exosomal populations with increased relatedness relative to MCF7 (Fig5a). Examination of differentially abundant proteins further confirm this finding as 419 proteins were found to be significantly increased in MCF7 exosomes while only 16 were observed different when MDA-MB-231 exosomal proteins were compared to MCF10a. On the other hand, significantly decreased proteins were found to be more abundant in MDA-MB-231 cells (139 proteins) than MCF7 (88 genes) relative to MCF10a (Fig5b). Interestingly, this pattern of abundance indicates an overall decrease in protein abundance in MDA-MB-231 exosomes and an increase in MCF7 relative to MCF10a. Upon comparison of overlapping differentially abundant proteins, CDEs from MDA-MB-231 and MCF7 were found to have opposing effects on 49 proteins in which one cancer cell line increased and the other cancer cell line decreased exosomal protein abundance relative to normal epithelial (MCF10a) exosomes.

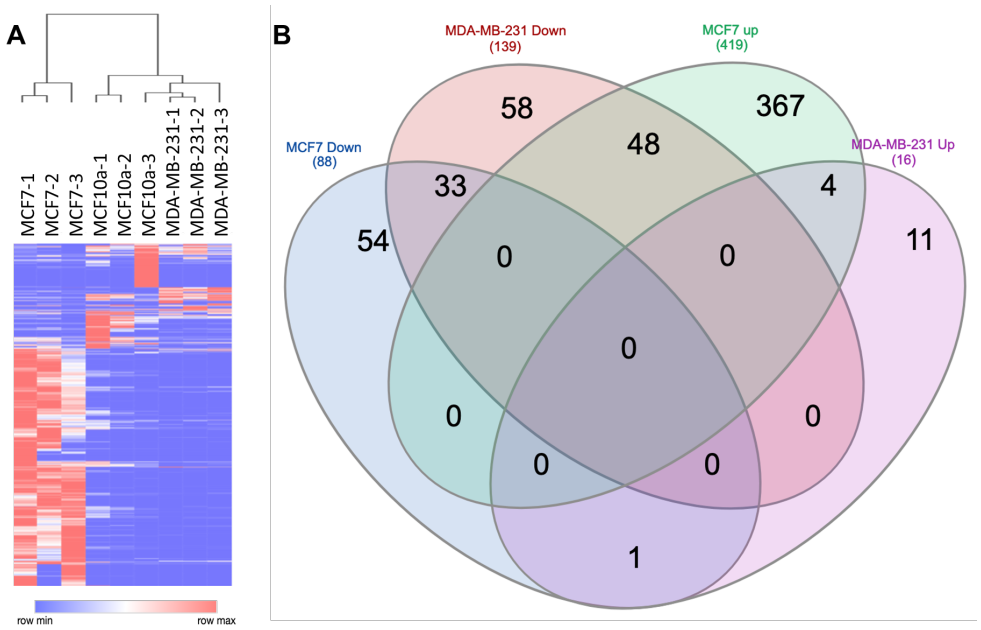


**Figure 5. Exosomal protein cargo in CDEs.** A) Heat map depicting relative protein abundance of all identified proteins in CDEs. B) Shared and unique proteins enriched in breast cancer exosomes (MCF-7 and MDA-MB-231) compared to non-cancerous epithelial cells (MCF10a).

*Clinical relevance of in vitro isolated CDEs*

CDE have been hypothesized to present cell specific biomolecules in a stable and secreted form amenable to non-invasive surveillance in clinical settings (275). The relevance of these pre-clinical, in vitro findings was next examined for utility in relation to clinical data obtained from breast cancer patients using publicly available datasets within The Cancer Genome Atlas (TCGA) (276) Segregation of molecular subtype of BC (MCF10a:Normal; MCF7:Luminal; MDA-MB-231:TNBC) based on transcriptional data generated from in vitro cultured exosomes was confirmed with clinical data from BC patients in 2 miRNAs (hsa-mir-375, has-mir-138-1) (Fig 6a. 6b). Additionally, 2 putative protein biomarkers (FBP1, HLA-A) were also found to match subtype specific abundance patterns identified in BC exosomes with high significance (Fig 6c, 6d).

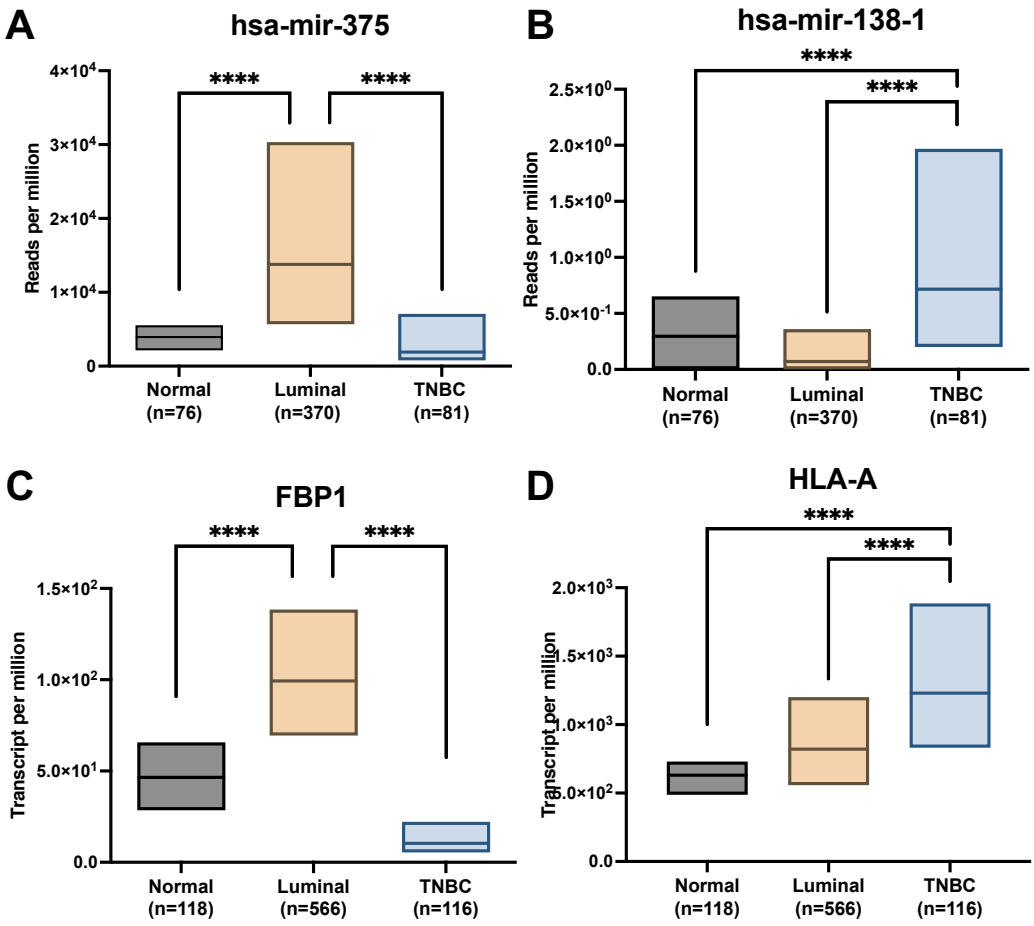


**Figure 6. Breast cancer exosomal contents correlate to clinical data.** Box and Whisker plots of predicted A&B) miRNA and C&D) protein biomarkers identified in this study of in vitro cultured BC cell lines mimics clinical data in correlation to BC subtypes based on data obtained from The Cancer Genome Atlas (TCGA). Line represents median expression and box depicts upper and lower quartile values. **** $p \leq 0.001$

## Discussion

In this study, I identified unique properties of EVs derived from different types of breast cancer cells (normal, luminal, and triple negative origin). Of note, I observed differences in EV particle heterogeneity and generation rate across cell lines. MCF7a cells were found to generate increased abundance of smaller extracellular vesicles while MDA-MB-231 and MCF10a shared common characteristics of size and quantity of extracellular vesicles.

The relatedness of the triple negative MDA-MB-231 cell lines with the normal epithelial MCF10a cell line was also observed upon examination of the protein content within the CDEs. Surprisingly, 6 conventional exosomal protein makers showed variability in abundance across cell lines examined. As a result of this data careful consideration of exosomal marker selection should be examined prior to use of these markers as normalization, quantitation, or enrichment technologies.

Yet upon examination of the transcriptional cargo contained in the CDEs, grater similarity was observed between the two cancer cell lines as opposed to the MCF10a cells. Sequencing of small RNA exosomal cargo identified an abundance of RNA aligning to coding regions of the genome. Due to the size selection process prior to sequencing (25-150 base pairs) these RNA species aligning to coding regions could represent fragments of mRNA that were loaded as a whole or piece of mRNA into exosome or debris in preparation. Further analysis will be required to decipher the origin and significance of these RNA fragments. Interestingly, comparable distribution of smRNA species across cell types was observed in all cell lines tested however the contents were found to be distinct across breast cancer subtype.

Previously unexplored transcript types such as pseudogenes, snoRNAs etc. are surfacing in recent findings as potential new biomarker candidates. For example, survey of lung cancer snoRNAs has suggested that these non-coding RNAs contain both tumor suppressor and tumor promoting properties (277). While our research focused primarily on miRNAs and protein biomarkers, investigation of pseudogenes noted here correlating with breast cancer subtype and metastatic potential are further avenues for validation of clinical significance. This study of breast cancer exosomes found pseudogene transcripts to comprise the majority of non-protein coding genes (33, 35 and 37%) via RNA-sequencing. While previously thought to be redundant and non-

functional, growing evidence reveals that these regions can also not only provide valuable diagnostics of disease but serve as prognostic markers of human cancers as well (278). The full extent to which these gene signatures as well as correlation with disease progression has yet to validated. Future analysis of these differentially abundant genes will focus on validation to clinical tumor and circulating levels from publicly available databases however this analyte is not conventionally collected from clinical samples so pre-clinical studies may be necessary to further this research.

The miRNA cargo within CDEs identified unique profiles specific to the BC cell lines. This species of non-coding RNAs offers an enticing biomarker as the effects of miRNAs in cancer behavior has been well-studied and functional enrichment data is available further allowing predicted function (269,279–281). Functional enrichment performed on miRNAs from CDE in this work highlighted several potential activated/inhibited pathways which warrant future therapeutic or diagnostic investigation. Numerous predictive tools for miRNA targeting to homologous genes are also publicly available and represent an additional established methodology utilized in miRNA research (282,283).

The data generated using basic in vitro culturing techniques was validated with clinical data identifying 4 potential biomarkers (2 miRNA and 2 protein) of BC subtype. It was noted that not all putative biomarkers matched clinical profiles and may represent an exosomal specific differential abundance, non-physiological response, or sampling issues. Despite preliminary promise as a useful analyte in a preclinical setting, increased rigor throughout the exosomal analysis pipeline will add robustness to the impact and understanding of this approach. Specific areas of improvement for futures studies should focus on increasing the breadth of cell lines tested to accommodate for intertumor heterogeneity; increased clinical data associated

with tested samples for further resolution of cancer behaviors from CDEs; longitudinal studies to examine the shifts in exosomal characteristics over the course of disease progression; and increased complexity in preclinical culturing methods to increase clinical impact and to ensure recapitulation of native exosomal packaging/secretion.

The survey of CDE and the biological material cargo encapsulated within displays the utility in analysis of these secreted vesicles as well as its translatability from pre-clinical discovery to clinical significance. In conjunction with data described in previous chapters, future studies will work on discrimination of CDE cargo in ex vivo cultures that can serve diagnostic or prognostic roles. A non-disruptive analyte can serve as a proxy for cancer behavior that can be easily measured from culture media and thus may serve as a valuable metric for preclinical tumor models in longitudinal studies in which retention of native tumor behavior is critical for clinical relevance.

# Chapter 6. Conclusion

Despite breast cancer research driving new advances in therapeutic targets and treatments, triple negative breast cancer remains a difficult to treat disease complicated by lack of targetable receptors, its propensity for aggressiveness, and increased relapse rates. Additionally, the heterogeneity in oncogenic drivers of TNBC induces further difficulty in effective anti-tumor therapies. The utility of pre-clinical models of TNBC has historically been limited by the incomplete recapitulation of the *in vivo* TME. The work presented in this thesis provides insight into behavioral biases imparted by conventional pre-clinical cancer culturing as well as highlighting the dynamic interplay between cancer cells and stromal cell types occupying the primary TME (Fig 1).

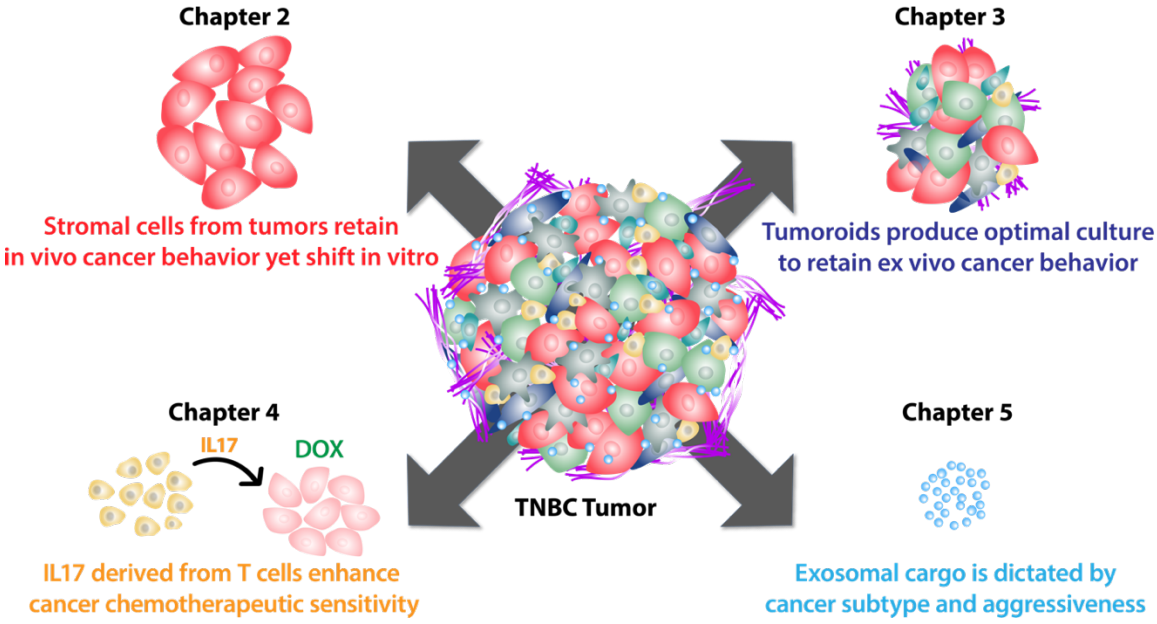


**Figure 1. Summary of project findings.**

A thorough characterization of TNBC 4T1 cells upon differing culture conditions was performed utilizing RNA sequencing technologies and featured in Chapter 2. 4T1 represents an ideal model for TNBC as it is a murine derived TNBC cell line capable of engraftment into fully immune competent animals providing the opportunity to investigate stromal contributions in line with

clinical samples. Additionally, 4T1 cells mimic human metastatic disease (284). My initial hypothesis was that increasing complexity would induce cancer cell behavior more like that of the syngeneic *in vivo* environment. This was proven to be broadly correct however each culturing approach promoted unique gene expression profiles and cellular behaviors suggesting that the cancer cells are rapidly influenced by cues they receive from their surroundings. Monolayer culture was found to prioritize biological processes critical to proliferation; the expression profiles of these cancer cells highlight that these cells are primarily using cellular resources to rapidly expand without engaging in many other types of cellular behaviors. 3-dimensional culture of cancer cell alone introduced more cellular surfaces for cell-cell attachment and established nutrient gradients throughout the spheroids. This culture configuration allowed the cells to synthesize more ECM, and this was quantifiable as a significant increase in many ECM transcripts. It also promoted the expression of genes associated with several differentiation pathways, such as response to hypoxia, cell adhesion, and regulation of cell proliferation; these transcripts were not detected at significant levels in the 2-dimensional cultures.

In general, when similarity matrix analysis was conducted, all the *in vitro* conditions were found to be more similar to each other than to all the *in vivo* conditions examined. Utilizing immunocompromised mice for *in vivo* tumor growth provided insight into the behavior of cancer cells in the absence of immune infiltration or cellular stresses induced by immune cell types such as T-cells that normally function to infiltrate tumors and kill cancer cells, however these mice had other stromal support cells such as fibroblasts and endothelial cells. These tumors were therefore highly informative for assessing the contribution of non-immune stromal components to tumor growth, drug response and other types of cellular morphogenic chances such as EMT. Tumors cultured in these mice did show a significant change in transcripts

associated with rapid proliferation, suggesting that these cancer cells grow slower than *in vitro*. Their transcriptional profiles also suggested that they had a more dynamic interaction with the TME to actively contribute to ECM synthesis. While fibroblasts were originally described by others as the main cell type in the TME to secrete ECM molecules (285), we have found that other cell types in the TME, including cancer cells also expressed robust levels of fibronectin and select collogens in tumors.

The inclusion of a complete immune system provided by growing 4T1 cells orthotopically in BALB/c mice resulted in a transcriptional profile enriched in cell signaling relative to all other *in vivo* and *in vitro* conditions. These cancer cells exhibited a further increase in the ECM and cell signaling programs in cancer cells. These differential processes were found to be facets of an EMT critical to cancer progression. One particular phenotype I aimed to characterize in greater detail in my studies, is how different culture conditions and different cellular components influence the EMT state of cancer cells. Others have previously shown that in skin squamous cell carcinoma tumors, there are 6 transitional EMT states and most of cancer cells tend to reside in early hybrid states in tumor bearing mice with full immune complement, which would be the state most similar to that of human patients (151).

However, that is not the case for cancer cells cultured *in vitro*, these cells are more likely to retain epithelial nature and not undergo EMT. As I increased the complexity *in vitro*, and introduced into the 4T1 cultures additional cell types, I observed that the 4T1 started to rapidly transition away from epithelial cell states that dominate 2D culturing conditions. However, cancer cells undergoing EMT *in vitro* were more likely to rapidly shift to a fully mesenchymal state (as defined by high expression of CD51, CD61, and CD106 markers). This was in sharp contrast with the states present in *in vivo* tumors where only a minority of tumor cells were in the mesenchymal state and most of the cancer cells favored the early intermediate hybrid states. The inclusion

of a full immune component in the TME favored late and hybrid states while NSG tumors lacking immune cells favored an early hybrid state. What became clear was that preserving cancer cells in these intermediate hybrid states *in vitro* would be most challenging and we have yet to determine what are the most critical cellular and molecular components derived from the stroma that are required to recapitulate the *in vivo* phenotype. The union of *in vitro* and *in vivo* methodologies via *ex vivo* culturing was also analyzed and remarkably showed artifacts of both culturing approaches with maintenance of high levels of EMT cells similar to *in vivo* yet these cells also promoted increased shift to a fully mesenchymal state similar to *in vitro* culturing, reemphasizing the challenge we still need to overcome.

To continue the quest of finding the most critical cellular and molecular TME components that would permit human tumors dissected from patients to be cultured *ex vivo* in conditions that preserve their original phenotype, in Chapter 3 I set out to study *ex vivo* cultures longitudinally with the goal of dissecting the *in vivo* complexity to identify the most essential activities that are necessary and sufficient to preserve primary tumors in culture in the most '*in vivo*' state. In this study, I analyzed the effects of time and spatial organization on cancer cells. Tumors were harvested and processed. The dissociated single cell suspensions were next cultures in monolayer and spheroids, in media or in hydrogel. The smaller tumor aggregates or tumoroids were also cultured in media or in hydrogel. Longitudinal studies of these 6 different culturing approaches [(1) monolayer in media; (2) monolayer in gel; (3) spheroid in media, (4) spheroid in gel; (5) tumoroid in media or (6) tumoroid in gel were carried out for 12 days, and cancer cells were assayed at 3-day, 7-day and 12-day time points. I hypothesized that the ECM suspended tumoroid cultures would retain and preserve most of the original tumor cellular heterogeneity, tumor ECM components, and tumor architecture and this condition would best retain the native cancer cell behavior, over time.

Surprisingly tumoroids cultured in media and not those in hydrogel preserved characteristics most closely to the primary tumors and represented the most optimal culturing condition over the course of a 12-day *ex vivo* culture. In sharp contrast with 2D conditions where cancer cells expand at a very rapid rate *in vitro*, the tumor growth was blunted under this condition and the stability of EMT heterogeneity was best maintained under this condition. The insights featured in this work further the understanding of *ex vivo* tumor culture impact through evaluation of cancer cell behavior and heterogeneity. In turn, future studies will focus on further environmental alterations (media composition, tumoroid size, extended culturing time, etc.) to improve the cancer cell and stromal cell retention in *ex vivo* culture for pre-clinical research and/or personalized screenings *in vitro*.

Previously discussed chapters focused solely on the cancer cell behavior, yet a wide range of cell types exist in tumors including immune and non-immune components critical to tumor biology and chemotherapeutic response. Chapter 4 focused on determining the contribution stromal cells can, in a fully immune competent host, have on treatment of TNBC to inform future therapeutic approaches. Following the observation that 4T1 derived TNBC tumors have a polarized response to treatment with anthracycline based chemotherapeutics such as doxorubicin (DOX), in Chapter 4 we applied single cell RNA-sequencing to determine what cell types vary in responders relative to non-responders. Special emphasis was given to identifying alterations in T cell populations, since subtypes of these cells are known to be highly involved in killing tumor cells (286). A minor yet significant T cell subtype CD8 γδ IL17+ was found to play a critical role in secretion of IL17a. IL17a was proven to be a potent cytokine in the TME that can increase the efficacy of the current standard of care treatment with anthracycline chemotherapeutics. The mechanism of action was further characterized through the TNBC cells where coadministration of IL17 and DOX was found to increase toxicity *in vitro* while

also discouraging chronic antigen exposure and exhaustion marker expression leading to a higher population of exhausted, functionally inactive T cell populations in tumors resistant to DOX treatment.

An additional facet of tumor dynamics examined focused on the cell-cell communication of a tumor in Chapter 5 where extracellular vesicle, specifically exosomes, characterization and cargo identification were shown to correlate to BC cancer subtypes and aggressiveness. By surveying of the transcriptomic and proteomic analysis of the cargo, I was able to identify putative biomarkers of BC subtype and metastatic potential. The exosomal cargo identified in this work may serve as a biomarker secreted into biofluids enabling a non-invasive liquid biopsy technology development or serve as a real-time readout in pre-clinical models to assess cancer status and prognosis. Furthermore, the variability identified in protein and small non-coding RNA cargo serves as valuable proof of concept for future work discriminating BC subtypes and behaviors from CDE secreted into culture media.

The molecular and cellular heterogeneity in TNBC tumors identified in this work illustrate the underlying difficulty in attaining effective outcomes from use of standardized cancer treatments. The growing field of personalized medicine offers an alternative approach fueled by targeted therapies catered to each patient's specific tumors. Identifying the optimal combination of therapies that are going to be most effective in eradicating an individualized cancers while having the least adverse effects remains a goal for future cancer care. Current strategies depend heavily on characterization of primary tumors from biopsy samples. Numerous studies have identified therapeutic efficacy strengths and deficiencies based on personal patient factors (age, sex, race, lifestyle, etc), oncogenic driving mutations in addition to other "omics" datasets (proteomic, metabolomic, transcriptomic, pharmacogenomic) (287–289). This data has been utilized to generate treatment selection algorithms promising predictions of increased antitumor efficacy (290,291). Nonetheless the

bottleneck to this methodology remains confirmation of the prognostic value of these methods in a clinically relevant and high-throughput preclinical tumor model. As shown in this research, conventional culturing methodologies do impart tumor phenotypes critical to identification of effective therapies. *In vitro* TME conditions will require careful considerations to retain native tumor behavior and composition while also promoting non-disruptive assay metrics.

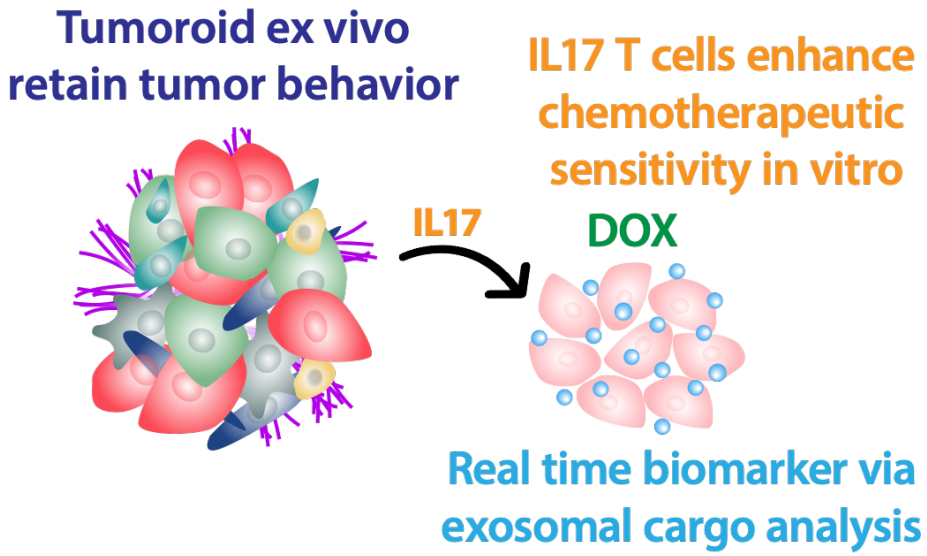


**Future pre-clinical TNBC model.** Utilization of findings from this work can be nto a preclinical model capable of recapitulating stromal induced response of with an exosomal cargo serving as biomarker analyte.

The integration of these findings into improved preclinical models inclusive of the native stromal complexity will continue to remain a goal for future research until cancer will be eradicated, or significant drops in mortality will be achieved. In summation, work presented here lays the foundation for improvements in pre-clinical models of TNBC. Through identification of cancer cell behavior under conventional culturing approaches I was able to focus subsequent efforts on *ex vivo* culturing methodologies in turn identifying a leading method for *ex vivo* retention of the native cancer cell behavior observed in syngeneic tumors comparable to clinical specimens. The importance of retention of *in vivo* complexity in a pre-clinical setting was identified in syngeneic 4T1 tumors where T cell populations inducing a pro-inflammatory

cytokine was proven an influential molecule contributing to chemotherapeutic response and may serve as a prime example for demonstration of a complex *in vitro* tumor model capable of recapitulating this diverse tumor response. Finally, improved metrics integrated into future preclinical may provide additional insights into tumor behavior previously unattainable with current technologies. Here I present exosomal cargo as a novel metric for incorporation into future assays for pre-clinical TNBC models. Despite the complexities and challenges discovered in this work, the promise of decreased health burden and novel therapeutic discovery from TNBC through improving research and pre-clinical screening utilizing research presented here will be the driving force for future studies.

## References

1. Mathers CD. History of global burden of disease assessment at the World Health Organization. Archives Public Heal. 2020;78:77.

2. Siegel RL, Miller KD, Jemal A. Cancer statistics, 2020. Ca Cancer J Clin. 2020;70:7–30.

3. Sung H, Ferlay J, Siegel RL, Laversanne M, Soerjomataram I, Jemal A, et al. Global cancer statistics 2020: GLOBOCAN estimates of incidence and mortality worldwide for 36 cancers in 185 countries. Ca Cancer J Clin. 2021;

4. Ginsburg O, Bray F, Coleman MP, Vanderpuye V, Eniu A, Kotha SR, et al. The global burden of women's cancers: a grand challenge in global health. Lancet. 2017;389:847–60.

5. Mariotto AB, Yabroff KR, Shao Y, Feuer EJ, Brown ML. Projections of the cost of cancer care in the United States: 2010-2020. Jnci J National Cancer Inst. 2011;103:117–28.

6. Harbeck N, Penault-Llorca F, Cortes J, Gnant M, Houssami N, Poortmans P, et al. Breast cancer. Nat Rev Dis Primers. 2019;5:66.

7. Feng Y, Spezia M, Huang S, Yuan C, Zeng Z, Zhang L, et al. Breast cancer development and progression: risk factors, cancer stem cells, signaling pathways, genomics, and molecular pathogenesis. Genes Dis. 2018;5:77–106.

8. Russo J, Russo IH. Innovative Endocrinology of Cancer. Adv Exp Med Biol. 2008;630:52–6.

9. Bombonati A, Sgroi DC. The molecular pathology of breast cancer progression. J Pathology. 2011;223:308–18.

10. Ingegnoli A, D'Aloia C, Frattaruolo A, Pallavera L, Martella E, Crisi G, et al. Flat Epithelial Atypia and Atypical Ductal Hyperplasia: Carcinoma Underestimation Rate. Breast J. 2010;16:55–9.

11. Wellings SR, Jensen HM. On the Origin and Progression of Ductal Carcinoma in the Human Breast2. Jnci J National Cancer Inst. 1973;50:1111–8.

12. Pike MC, Spicer DV, Dahmoush L, Press MF. Estrogens, Progestogens, Normal Breast Cell Proliferation, and Breast Cancer Risk. Epidemiol Rev. 1993;15:17–30.

13. Williams C, Lin C-Y. Oestrogen receptors in breast cancer: basic mechanisms and clinical implications. Ecancermedicalscience. n.d.;7:370.

14. Sircoulomb F, Bekhouche I, Finetti P, Adélaïde J, Hamida AB, Bonansea J, et al. Genome profiling of ERBB2-amplified breast cancers. Bmc Cancer. 2010;10:539.

15. Kirouac DC, Du J, Lahdenranta J, Onsum MD, Nielsen UB, Schoeberl B, et al. HER2+ Cancer Cell Dependence on PI3K vs. MAPK Signaling Axes Is Determined by Expression of EGFR, ERBB3 and CDKN1B. Plos Comput Biol. 2016;12:e1004827.

16. Kartik A, Akshata D, Crystal W, Jingyao X, Yunlong Q, Vaishali R, et al. Triple Negative Breast Cancer – An Overview. Hered Genetics Curr Res. 2013;

17. Beumer IJ, Persoon M, Witteveen A, Dreezen C, Chin S-F, Sammut S-J, et al. Prognostic Value of MammaPrint® in Invasive Lobular Breast Cancer. Biomark Insights. 2016;11:BMI.S38435.

18. McVeigh TP, Kerin MJ. Clinical use of the Oncotype DX genomic test to guide treatment decisions for patients with invasive breast cancer. Breast Cancer Targets Ther. 2017;9:393–400.

19. Nik-Zainal S, Davies H, Staaf J, Ramakrishna M, Glodzik D, Zou X, et al. Landscape of somatic mutations in 560 breast cancer whole-genome sequences. Nature. 2016;534:47–54.

20. Boyle P. Triple-negative breast cancer: epidemiological considerations and recommendations. Ann Oncol. 2012;23:vi7–12.

21. Lund MJ, Trivers KF, Porter PL, Coates RJ, Leyland-Jones B, Brawley OW, et al. Race and triple negative threats to breast cancer survival: a population-based study in Atlanta, GA. Breast Cancer Res Tr. 2009;113:357–70.

22. Bauer KR, Brown M, Cress RD, Parise CA, Caggiano V. Descriptive analysis of estrogen receptor (ER)-negative, progesterone receptor (PR)-

negative, and HER2-negative invasive breast cancer, the so-called triple-negative phenotype. Cancer. 2007;109:1721–8.

23. Davis AA, Kaklamani VG. Metabolic Syndrome and Triple-Negative Breast Cancer: A New Paradigm. Int J Breast Cancer. 2012;2012:809291.

24. Morris GJ, Naidu S, Topham AK, Guiles F, Xu Y, McCue P, et al. Differences in breast carcinoma characteristics in newly diagnosed African–American and Caucasian patients. Cancer. 2007;110:876–84.

25. Dent R, Trudeau M, Pritchard KI, Hanna WM, Kahn HK, Sawka CA, et al. Triple-Negative Breast Cancer: Clinical Features and Patterns of Recurrence. Clin Cancer Res. 2007;13:4429–34.

26. Silva JL da, Nunes NCC, Izetti P, Mesquita GG de, Melo AC de. Triple Negative Breast Cancer: a thorough review of biomarkers. Crit Rev Oncol Hemat. 2019;145:102855.

27. Nagarajan D, McArdle SEB. Immune Landscape of Breast Cancers. Biomed. 2018;6:20.

28. Giordano C, Camera GL, Gelsomino L, Barone I, Bonofiglio D, Andò S, et al. The Biology of Exosomes in Breast Cancer Progression: Dissemination, Immune Evasion and Metastatic Colonization. Cancers. 2020;12:2179.

29. Edechi CA, Ikeogu N, Uzonna JE, Myal Y. Regulation of Immunity in Breast Cancer. Cancers. 2019;11:1080.

30. Gobert M, Treilleux I, Bendriss-Vermare N, Bachelot T, Goddard-Leon S, Arfi V, et al. Regulatory T Cells Recruited through CCL22/CCR4 Are Selectively Activated in Lymphoid Infiltrates Surrounding Primary Breast Tumors and Lead to an Adverse Clinical Outcome. Cancer Res. 2009;69:2000–9.

31. Ruffell B, DeNardo DG, Affara NI, Coussens LM. Lymphocytes in cancer development: Polarization towards pro-tumor immunity. Cytokine Growth F R. 2010;21:3–10.

32. Emens LA. Breast cancer immunobiology driving immunotherapy: vaccines and immune checkpoint blockade. Expert Rev Anticanc. 2014;12:1597–611.

33. Zamarron BF, Chen W. Dual Roles of Immune Cells and Their Factors in Cancer Development and Progression. Int J Biol Sci. 2011;7:651–8.

34. Dunn GP, Bruce AT, Ikeda H, Old LJ, Schreiber RD. Cancer immunoediting: from immunosurveillance to tumor escape. Nat Immunol. 2002;3:991–8.

35. Smyth MJ, Dunn GP, Schreiber RD. Cancer Immunosurveillance and Immunoediting: The Roles of Immunity in Suppressing Tumor Development and Shaping Tumor Immunogenicity. Adv Immunol. 2006;90:1–50.

36. Tu MM, Rahim MMA, Sayed C, Mahmoud AB, Makrigiannis AP. Immunosurveillance and Immunoediting of Breast Cancer via Class I MHC Receptors. Cancer Immunol Res. 2017;5:1016–28.

37. Bu X, Yao Y, Li X. Translational Research in Breast Cancer, Biomarker Diagnosis, Targeted Therapies and Approaches to Precision Medicine. Adv Exp Med Biol. 2017;1026:383–402.

38. Dushyanthen S, Beavis PA, Savas P, Teo ZL, Zhou C, Mansour M, et al. Relevance of tumor-infiltrating lymphocytes in breast cancer. Bmc Med. 2015;13:202.

39. Law AMK, Lim E, Ormandy CJ, Gallego-Ortega D. The innate and adaptive infiltrating immune systems as targets for breast cancer immunotherapy. Endocr-relat Cancer. 2017;24:R123–44.

40. Bussard KM, Mutkus L, Stumpf K, Gomez-Manzano C, Marini FC. Tumor-associated stromal cells as key contributors to the tumor microenvironment. Breast Cancer Res. 2016;18:84.

41. Choi J, Cha YJ, Koo JS. Adipocyte biology in breast cancer: From silent bystander to active facilitator. Prog Lipid Res. 2018;69:11–20.

42. Kim J. Pericyte Biology in Disease. Adv Exp Med Biol. 2019;1147:93–107.

43. Hass R, Ohe J von der, Ungefroren H. Potential Role of MSC/Cancer Cell Fusion and EMT for Breast Cancer Stem Cell Formation. Cancers. 2019;11:1432.

44. Chen S-H, Lin C-Y, Lee L-T, Chang G-D, Lee P-P, Hung C-C, et al. Up-regulation of fibronectin and tissue transglutaminase promotes cell invasion

involving increased association with integrin and MMP expression in A431 cells. Anticancer Res. 2010;30:4177–86.

45. Cirri P, Chiarugi P. Cancer-associated-fibroblasts and tumour cells: a diabolic liaison driving cancer progression. Cancer Metast Rev. 2012;31:195–208.

46. Evrard SM, Lecce L, Michelis KC, Nomura-Kitabayashi A, Pandey G, Purushothaman K-R, et al. Endothelial to mesenchymal transition is common in atherosclerotic lesions and is associated with plaque instability. Nat Commun. 2016;7:11853.

47. Yadav A, Kumar B, Yu J-G, Old M, Teknos TN, Kumar P. Tumor-Associated Endothelial Cells Promote Tumor Metastasis by Chaperoning Circulating Tumor Cells and Protecting Them from Anoikis. Plos One. 2015;10:e0141602.

48. Cardoso F, Senkus E, Costa A, Papadopoulos E, Aapro M, André F, et al. 4th ESO–ESMO International Consensus Guidelines for Advanced Breast Cancer (ABC 4) † † These guidelines were developed by the European School of Oncology (ESO) and the European Society for Medical Oncology (ESMO). Ann Oncol. 2018;29:1634–57.

49. Earl HM, Hiller L, Vallier A-L, Loi S, McAdam K, Hughes-Davies L, et al. 6 versus 12 months of adjuvant trastuzumab for HER2-positive early breast cancer (PERSEPHONE): 4-year disease-free survival results of a randomised phase 3 non-inferiority trial. Lancet. 2019;393:2599–612.

50. Pivot X, Romieu G, Debled M, Pierga J-Y, Kerbrat P, Bachelot T, et al. 6 months versus 12 months of adjuvant trastuzumab for patients with HER2-positive early breast cancer (PHARE): a randomised phase 3 trial. Lancet Oncol. 2013;14:741–8.

51. Ferreira-Gonzalez A. Plasma PIK3CA Mutation Testing in Advanced Breast Cancer Patients for Personalized Medicine: A Value Proposition. J Appl Laboratory Medicine. 2020;5:1076–89.

52. Rusquec P du, Blonz C, Frenel JS, Campone M. Targeting the PI3K/Akt/mTOR pathway in estrogen-receptor positive HER2 negative advanced breast cancer. Ther Adv Med Oncol. 2020;12:1758835920940939.

53. Gonçalves H, Guerra MR, Cintra JRD, Fayer VA, Brum IV, Teixeira MTB. Survival Study of Triple-Negative and Non–Triple-Negative Breast

Cancer in a Brazilian Cohort. Clin Medicine Insights Oncol. 2018;12:1179554918790563.

54. Skinner KE, Haiderali A, Huang M, Schwartzberg LS. Real-world effectiveness outcomes in patients diagnosed with metastatic triple-negative breast cancer. Future Oncol. 2021;17:931–41.

55. (EBCTCG) EBCTCG, Asselain B, Barlow W, Bartlett J, Bergh J, Bergsten-Nordström E, et al. Long-term outcomes for neoadjuvant versus adjuvant chemotherapy in early breast cancer: meta-analysis of individual patient data from ten randomised trials. Lancet Oncol. 2018;19:27–39.

56. Mackey JR, Pieńkowski T, Crown J, Sadeghi S, Martin M, Chan A, et al. Long-term outcomes after adjuvant treatment of sequential versus combination docetaxel with doxorubicin and cyclophosphamide in node-positive breast cancer: BCIRG-005 randomized trial. Ann Oncol. 2016;27:1041–7.

57. Ruan W, Lim HH, Surana U. Mapping Mitotic Death: Functional Integration of Mitochondria, Spindle Assembly Checkpoint and Apoptosis. Frontiers Cell Dev Biology. 2019;6:177.

58. Geisler S, Lønning PE, Aas T, Johnsen H, Fluge O, Haugen DF, et al. Influence of TP53 gene alterations and c-erbB-2 expression on the response to treatment with doxorubicin in locally advanced breast cancer. Cancer Res. 2001;61:2505–12.

59. Nedeljković M, Damjanović A. Mechanisms of Chemotherapy Resistance in Triple-Negative Breast Cancer—How We Can Rise to the Challenge. Cells. 2019;8:957.

60. Mylavarapu S, Das A, Roy M. Role of BRCA Mutations in the Modulation of Response to Platinum Therapy. Frontiers Oncol. 2018;8:16.

61. Diana A, Carlino F, Franzese E, Oikonomidou O, Criscitiello C, Vita FD, et al. Early Triple Negative Breast Cancer: Conventional Treatment and Emerging Therapeutic Landscapes. Cancers. 2020;12:819.

62. Fasching PA, Link T, Hauke J, Seither F, Jackisch C, Klare P, et al. Neoadjuvant paclitaxel/olaparib in comparison to paclitaxel/carboplatinum in patients with HER2-negative breast cancer and homologous recombination deficiency (GeparOLA study). Ann Oncol. 2021;32:49–57.

63. Reinisch M, Ataseven B, Kümmel S. Neoadjuvant Dose-Dense and Dose-Intensified Chemotherapy in Breast Cancer - Review of the Literature. Breast Care. 2016;11:13–20.

64. Emens LA, Kok M, Ojalvo LS. Targeting the programmed cell death-1 pathway in breast and ovarian cancer. Curr Opin Obstetrics Gynecol. 2016;28:142–7.

65. Winer EP, Dang T, Karantza V, Su S-C. KEYNOTE-119: A randomized phase III study of single-agent pembrolizumab (MK-3475) vs single-agent chemotherapy per physician's choice for metastatic triple-negative breast cancer (mTNBC). J Clin Oncol. 2016;34:TPS1102–TPS1102.

66. Kristensen T, Knutsson M, Wehland M, Laursen B, Grimm D, Warnke E, et al. Anti-Vascular Endothelial Growth Factor Therapy in Breast Cancer. Int J Mol Sci. 2014;15:23024–41.

67. Salimifard S, Masjedi A, Hojjat-Farsangi M, Ghalamfarsa G, Irandoust M, Azizi G, et al. Cancer associated fibroblasts as novel promising therapeutic targets in breast cancer. Pathology - Res Pract. 2020;216:152915.

68. Navarrete-Bernal MGC, Cervantes-Badillo MG, Martínez-Herrera JF, Lara-Torres CO, Gerson-Cwilich R, Zentella-Dehesa A, et al. Biological Landscape of Triple Negative Breast Cancers Expressing CTLA-4. Frontiers Oncol. 2020;10:1206.

69. Lee YB, Kim EM, Byun H, Chang H, Jeong K, Aman ZM, et al. Engineering spheroids potentiating cell-cell and cell-ECM interactions by self-assembly of stem cell microlayer. Biomaterials. 2018;165:105–20.

70. Walker C, Mojares E, Hernández ADR. Role of Extracellular Matrix in Development and Cancer Progression. Int J Mol Sci. 2018;19:3028.

71. Depping R, Fallois M von, Landesman Y, Kosyna FK. The Nuclear Export Inhibitor Selinexor Inhibits Hypoxia Signaling Pathways And 3D Spheroid Growth Of Cancer Cells. Oncotargets Ther. 2019;12:8387–99.

72. Achilli T-M, McCalla S, Meyer J, Tripathi A, Morgan JR. Multilayer Spheroids To Quantify Drug Uptake and Diffusion in 3D. Mol Pharmaceut. 2014;11:2071–81.

73. Nath S, Devi GR. Three-dimensional culture systems in cancer research: Focus on tumor spheroid model. Pharmacol Therapeut. 2016;163:94–108.

74. Kim JB, Stein R, O'Hare MJ. Three-dimensional in vitro tissue culture models of breast cancer — a review. Breast Cancer Res Tr. 2004;85:281–91.

75. Arrigoni C, Bersini S, Gilardi M, Moretti M. In Vitro Co-Culture Models of Breast Cancer Metastatic Progression towards Bone. Int J Mol Sci. 2016;17:1405.

76. Nguyen M, Ninno AD, Mencattini A, Mermet-Meillon F, Fornabaio G, Evans SS, et al. Dissecting Effects of Anti-cancer Drugs and Cancer-Associated Fibroblasts by On-Chip Reconstitution of Immunocompetent Tumor Microenvironments. Cell Reports. 2018;25:3884-3893.e3.

77. Chiew GGY, Wei N, Sultania S, Lim S, Luo KQ. Bioengineered three-dimensional co-culture of cancer cells and endothelial cells: A model system for dual analysis of tumor growth and angiogenesis. Biotechnol Bioeng. 2017;114:1865–77.

78. Swaminathan S, Cranston AN, Clyne AM. A Three-Dimensional In Vitro Coculture Model to Quantify Breast Epithelial Cell Adhesion to Endothelial Cells. Tissue Eng Part C Methods. 2019;25:609–18.

79. Grinshpun A, Gavert N, Granit RZ, Masuri H, Ben-Porath I, Breuer S, et al. Ev vivo organ culture as potential prioritization tool for breast cancer targeted therapy. Cancer Biol Ther. 2018;19:1–13.

80. Powley IR, Patel M, Miles G, Pringle H, Howells L, Thomas A, et al. Patient-derived explants (PDEs) as a powerful preclinical platform for anti-cancer drug and biomarker discovery. Brit J Cancer. 2020;122:735–44.

81. Ben-David U, Ha G, Tseng Y-Y, Greenwald NF, Oh C, Shih J, et al. Patient-derived xenografts undergo mouse-specific tumor evolution. Nature genetics. 2017;49:1567–75.

82. Okada S, Vaeteewoottacharn K, Kariya R. Establishment of a Patient-Derived Tumor Xenograft Model and Application for Precision Cancer Medicine. Chem Pharm Bulletin. 2018;66:225–30.

83. Cao X, Shores EW, Hu-Li J, Anver MR, Kelsail BL, Russell SM, et al. Defective lymphoid development in mice lacking expression of the common cytokine receptor γ chain. Immunity. 1995;2:223–38.

84. Shultz LD, Goodwin N, Ishikawa F, Hosur V, Lyons BL, Greiner DL. Human Cancer Growth and Therapy in Immunodeficient Mouse Models. Cold Spring Harb Protoc. 2014;2014:pdb.top073585-pdb.top073585.

85. Day C-P, Merlino G, Dyke TV. Preclinical Mouse Cancer Models: A Maze of Opportunities and Challenges. Cell. 2015;163:39–53.

86. Yang Y, Yang HH, Hu Y, Watson PH, Liu H, Geiger TR, et al. Immunocompetent mouse allograft models for development of therapies to target breast cancer metastasis. Oncotarget. 2017;8:30621–43.

87. Alizadeh AA, Ross DT, Perou CM, Rijn M van de. Towards a novel classification of human malignancies based on gene expression patterns. J Pathology. 2001;195:41–52.

88. Ross DT, Scherf U, Eisen MB, Perou CM, Rees C, Spellman P, et al. Systematic variation in gene expression patterns in human cancer cell lines. Nat Genet. 2000;24:227–35.

89. Mollard S, Mousseau Y, Baaj Y, Richard L, Cook-Moreau J, Monteil J, et al. How can grafted breast cancer models be optimized? Cancer Biol Ther. 2011;12:855–64.

90. Christenson JL, Butterfield KT, Spoelstra NS, Norris JD, Josan JS, Pollock JA, et al. MMTV-PyMT and Derived Met-1 Mouse Mammary Tumor Cells as Models for Studying the Role of the Androgen Receptor in Triple-Negative Breast Cancer Progression. Hormones Cancer. 2017;8:69–77.

91. Blaas L, Pucci F, Messal HA, Andersson AB, Ruiz EJ, Gerling M, et al. Lgr6 labels a rare population of mammary gland progenitor cells that are able to originate luminal mammary tumours. Nat Cell Biol. 2016;18:1346–56.

92. Arun G, Diermeier S, Akerman M, Chang K-C, Wilkinson JE, Hearn S, et al. Differentiation of mammary tumors and reduction in metastasis upon Malat1 lncRNA loss. Gene Dev. 2016;30:34–51.

93. Usary J, Darr DB, Pfefferle AD, Perou CM. Overview of Genetically Engineered Mouse Models of Distinct Breast Cancer Subtypes. Curr Protoc Pharmacol. 2016;72:14.38.1-14.38.11.

94. Herschkowitz JI, Zhao W, Zhang M, Usary J, Murrow G, Edwards D, et al. Comparative oncogenomics identifies breast tumors enriched in functional tumor-initiating cells. Proc National Acad Sci. 2012;109:2778–83.

95. Pfefferle AD, Herschkowitz JI, Usary J, Harrell JC, Spike BT, Adams JR, et al. Transcriptomic classification of genetically engineered mouse models of breast cancer identifies human subtype counterparts. Genome Biol. 2013;14:R125.

96. Pan B-T, Johnstone RM. Fate of the transferrin receptor during maturation of sheep reticulocytes in vitro: Selective externalization of the receptor. Cell. 1983;33:967–78.

97. Zhang Y, Liu Y, Liu H, Tang WH. Exosomes: biogenesis, biologic function and clinical potential. Cell Biosci. 2019;9:19.

98. Llorente A, Skotland T, Sylvänne T, Kauhanen D, Róg T, Orłowski A, et al. Molecular lipidomics of exosomes released by PC-3 prostate cancer cells. Biochimica Et Biophysica Acta Bba - Mol Cell Biology Lipids. 2013;1831:1302–9.

99. Galindo-Hernandez O, Serna-Marquez N, Castillo-Sanchez R, Salazar EP. Extracellular vesicles from MDA-MB-231 breast cancer cells stimulated with linoleic acid promote an EMT-like process in MCF10A cells. Prostaglandins Leukot Essent Fat Acids. 2014;91:299–310.

100. Campos A, Salomon C, Bustos R, Daz J, Martnez S, Silva V, et al. Caveolin-1-containing extracellular vesicles transport adhesion proteins and promote malignancy in breast cancer cell lines. Nanomedicine-uk. 2018;13:2597–609.

101. kia V, Mortazavi Y, Paryan M, Biglari A, Mohammadi-Yeganeh S. Exosomal miRNAs from highly metastatic cells can induce metastasis in non-metastatic cells. Life Sci. 2019;220:162–8.

102. Al-Mayah A, Bright S, Chapman K, Irons S, Luo P, Carter D, et al. The non-targeted effects of radiation are perpetuated by exosomes. Mutat Res Fundam Mol Mech Mutagen. 2015;772:38–45.

103. Ni J, Bucci J, Malouf D, Knox M, Graham P, Li Y. Exosomes in Cancer Radioresistance. Frontiers Oncol. 2019;9:869.

104. Sharma A. Chemoresistance in cancer cells: exosomes as potential regulators of therapeutic tumor heterogeneity. Nanomedicine-uk. 2017;12:2137–48.

105. Kosaka N, Iguchi H, Hagiwara K, Yoshioka Y, Takeshita F, Ochiya T. Neutral Sphingomyelinase 2 (nSMase2)-dependent Exosomal Transfer of Angiogenic MicroRNAs Regulate Cancer Cell Metastasis*. J Biol Chem. 2013;288:10849–59.

106. Chaudhary P, Gibbs LD, Maji S, Lewis CM, Suzuki S, Vishwanatha JK. Serum exosomal-annexin A2 is associated with African-American triple-negative breast cancer and promotes angiogenesis. Breast Cancer Res. 2020;22:11.

107. Maji S, Chaudhary P, Akopova I, Nguyen PM, Hare RJ, Gryczynski I, et al. Exosomal Annexin II Promotes Angiogenesis and Breast Cancer Metastasis. Mol Cancer Res. 2017;15:93–105.

108. Zhou W, Fong MY, Min Y, Somlo G, Liu L, Palomares MR, et al. Cancer-Secreted miR-105 Destroys Vascular Endothelial Barriers to Promote Metastasis. Cancer Cell. 2014;25:501–15.

109. Baroni S, Romero-Cordoba S, Plantamura I, Dugo M, D'Ippolito E, Cataldo A, et al. Exosome-mediated delivery of miR-9 induces cancer-associated fibroblast-like properties in human breast fibroblasts. Cell Death Dis. 2016;7:e2312–e2312.

110. Wen SW, Sceneay J, Lima LG, Wong CSF, Becker M, Krumeich S, et al. The Biodistribution and Immune Suppressive Effects of Breast Cancer–Derived Exosomes. Cancer Res. 2016;76:6816–27.

111. Xing F, Liu Y, Wu S-Y, Wu K, Sharma S, Mo Y-Y, et al. Loss of XIST in Breast Cancer Activates MSN-c-Met and Reprograms Microglia via Exosomal miRNA to Promote Brain Metastasis. Cancer Res. 2018;78:4316–30.

112. Chow A, Zhou W, Liu L, Fong MY, Champer J, Haute DV, et al. Macrophage immunomodulation by breast cancer-derived exosomes requires Toll-like receptor 2-mediated activation of NF-κB. Sci Rep-uk. 2014;4:5750.

113. Wortzel I, Dror S, Kenific CM, Lyden D. Exosome-Mediated Metastasis: Communication from a Distance. Dev Cell. 2019;49:347–60.

114. Kaplan RN, Riba RD, Zacharoulis S, Bramley AH, Vincent L, Costa C, et al. VEGFR1-positive haematopoietic bone marrow progenitors initiate the pre-metastatic niche. Nature. 2005;438:820–7.

115. Karlsson T, Lundholm M, Widmark A, Persson E. Tumor Cell-Derived Exosomes from the Prostate Cancer Cell Line TRAMP-C1 Impair Osteoclast Formation and Differentiation. Plos One. 2016;11:e0166284.

116. Taverna S, Pucci M, Giallombardo M, Bella MAD, Santarpia M, Reclusa P, et al. Amphiregulin contained in NSCLC-exosomes induces osteoclast differentiation through the activation of EGFR pathway. Sci Rep-uk. 2017;7:3170.

117. Raimondi L, Luca AD, Amodio N, Manno M, Raccosta S, Taverna S, et al. Involvement of multiple myeloma cell-derived exosomes in osteoclast differentiation. Oncotarget. 2015;6:13772–89.

118. Pastushenko I, Blanpain C. EMT Transition States during Tumor Progression and Metastasis. Trends Cell Biol. 2019;29:212–26.

119. Meads MB, Gatenby RA, Dalton WS. Environment-mediated drug resistance: a major contributor to minimal residual disease. Nat Rev Cancer. 2009;9:665–74.

120. Lee SS-Y, Bindokas VP, Kron SJ. Multiplex three-dimensional optical mapping of tumor immune microenvironment. Sci Rep-uk. 2017;7:17031.

121. Germano S, O'Driscoll L. Breast cancer: understanding sensitivity and resistance to chemotherapy and targeted therapies to aid in personalised medicine. Curr Cancer Drug Tar. 2009;9:398–418.

122. Dittmer J, Leyh B. The impact of tumor stroma on drug response in breast cancer. Semin Cancer Biol. 2015;31:3–15.

123. Siegel RL, Miller KD, Jemal A. Cancer statistics, 2018. CA: a cancer journal for clinicians. 2018;68:7–30.

124. Siegel RL, Miller KD, Jemal A. Cancer statistics, 2016. Ca Cancer J Clin. 2016;66:7–30.

125. Pampaloni F, Reynaud EG, Stelzer EHK. The third dimension bridges the gap between cell culture and live tissue. Nature Reviews Molecular Cell Biology [Internet]. 2007;8:839–45. Available from: https://www.nature.com/articles/nrm2236.pdf

126. Cagan R, Meyer P. Rethinking cancer: current challenges and opportunities in cancer research. Disease models & mechanisms. 2017;10:349–52.

127. Miura S, Gomez K, Murillo O, Huuki LA, Vu T, Buturla T, et al. Predicting clone genotypes from tumor bulk sequencing of multiple samples. Hancock J, editor. Bioinformatics. 2018;34:4017–26.

128. Zanoni M, Piccinini F, Arienti C, Zamagni A, Santi S, Polico R, et al. 3D tumor spheroid models for in vitro therapeutic screening: a systematic approach to enhance the biological relevance of data obtained. Nature Publishing Group. 2016;6:19103.

129. Dobrolecki LE, Airhart SD, Alferez DG, Aparicio S, Behbod F, Bentires-Alj M, et al. Patient-derived xenograft (PDX) models in basic and translational breast cancer research. Cancer metastasis reviews. 2016;35:547–73.

130. Mak IW, Evaniew N, Ghert M. Lost in translation: animal models and clinical trials in cancer treatment. American journal of translational research. 2014;6:114–8.

131. Dumont S, Jan Z, Heremans R, Gorp TV, Vergote I, Timmerman D. Organoids of epithelial ovarian cancer as an emerging preclinical in vitro tool: a review. Journal of ovarian research. 2019;12:105–11.

132. Engel RM, Chan WH, Nickless D, Hlavca S, Richards E, Kerr G, et al. Patient-Derived Colorectal Cancer Organoids Upregulate Revival Stem Cell Marker Genes following Chemotherapeutic Treatment. Journal of clinical medicine. 2020;9:128.

133. Boj SF, Hwang C-I, Baker LA, Chio IIC, Engle DD, Corbo V, et al. Organoid Models of Human and Mouse Ductal Pancreatic Cancer. Cell. 2015;160:324–38.

134. Saito Y. Establishment of an organoid bank of biliary tract and pancreatic cancers and its application for personalized therapy and future treatment. Journal of gastroenterology and hepatology. 2019;34:1906–10.

135. Mousavi N, Truelsen SLB, Hagel G, Jorgensen LN, Harling H, Timmermans V, et al. KRAS mutations in the parental tumour accelerate in vitro growth of tumoroids established from colorectal adenocarcinoma. International journal of experimental pathology. 2019;100:12–8.

136. Dobin A, Gingeras TR. Mapping RNA-seq Reads with STAR. Current protocols in bioinformatics. 2015;51:11.14.1-19.

137. Risso D, Schwartz K, Sherlock G, Dudoit S. GC-content normalization for RNA-Seq data. BMC bioinformatics. 2011;12:480.

138. Risso D, Ngai J, Speed TP, Dudoit S. Normalization of RNA-seq data using factor analysis of control genes or samples. Nature biotechnology. 2014;32:896–902.

139. Robinson MD, McCarthy DJ, Smyth GK. edgeR: a Bioconductor package for differential expression analysis of digital gene expression data. Bioinformatics. 2010;26:139–40.

140. Chen J, Bardes EE, Aronow BJ, Jegga AG. ToppGene Suite for gene list enrichment analysis and candidate gene prioritization. Nucleic acids research. 2009;37:W305-11.

141. Shannon P, Markiel A, Ozier O, Baliga NS, Wang JT, Ramage D, et al. Cytoscape: a software environment for integrated models of biomolecular interaction networks. Genome research. 2003;13:2498–504.

142. Fabregat A, Jupe S, Matthews L, Sidiropoulos K, Gillespie M, Garapati P, et al. The Reactome Pathway Knowledgebase. Nucleic acids research. 2018;46:D649–55.

143. Sobral-Filho RG, DeVorkin L, Macpherson S, Jirasek A, Lum JJ, Brolo AG. Ex Vivo Detection of Circulating Tumor Cells from Whole Blood by Direct Nanoparticle Visualization. ACS nano. 2018;12:1902–9.

144. Stuart T, Butler A, Hoffman P, Hafemeister C, Papalexi E, III WMM, et al. Comprehensive Integration of Single-Cell Data. Cell. 2019;177:1888-1902.e21.

145. Feitelson MA, Arzumanyan A, Kulathinal RJ, Blain SW, Holcombe RF, Mahajna J, et al. Sustained proliferation in cancer: Mechanisms and novel therapeutic targets. Seminars in cancer biology. 2015;35 Suppl:S25–54.

146. Sever R, Brugge JS. Signal transduction in cancer. Cold Spring Harbor perspectives in medicine. 2015;5:a006098–a006098.

147. Parker BS, Rautela J, Hertzog PJ. Antitumour actions of interferons: implications for cancer therapy. Nature Reviews Cancer. 2016;16:131–44.

148. Brabletz T, Kalluri R, Nieto MA, Weinberg RA. EMT in cancer. Nature Reviews Cancer. 2018;18:128–34.

149. Atkinson SP, Collin J, Irina N, Anyfantis G, Kyung BK, Lako M, et al. A putative role for the immunoproteasome in the maintenance of pluripotency in human embryonic stem cells. Stem cells (Dayton, Ohio). 2012;30:1373–84.

150. Au-Yeung N, Mandhana R, Horvath CM. Transcriptional regulation by STAT1 and STAT2 in the interferon JAK-STAT pathway. JAK-STAT. 2013;2:e23931.

151. Pastushenko I, Brisebarre A, Sifrim A, Fioramonti M, Revenco T, Boumahdi S, et al. Identification of the tumour transition states occurring during EMT. Nature. 2018;556:463–8.

152. Tsubakihara Y, Moustakas A. Epithelial-Mesenchymal Transition and Metastasis under the Control of Transforming Growth Factor ß. International journal of molecular sciences. 2018;19:3672.

153. Wang W-L, Huang H-C, Kao S-H, Hsu Y-C, Wang Y-T, Li K-C, et al. Slug is temporally regulated by cyclin E in cell cycle and controls genome stability. Oncogene. 2015;34:1116–25.

154. Jolly MK, Tripathi SC, Jia D, Mooney SM, Celiktas M, Hanash SM, et al. Stability of the hybrid epithelial/mesenchymal phenotype. Oncotarget. 2016;7:27067–84.

155. Hong T, Watanabe K, Ta CH, Villarreal-Ponce A, Nie Q, Dai X. An Ovol2-Zeb1 Mutual Inhibitory Circuit Governs Bidirectional and Multi-step Transition between Epithelial and Mesenchymal States. Stumpf MPH, editor. PLoS computational biology. 2015;11:e1004569.

156. Jordan NV, Johnson GL, Abell AN. Tracking the intermediate stages of epithelial-mesenchymal transition in epithelial stem cells and cancer. Cell Cycle. 2011;10:2865–73.

157. Nieto MA, Huang RY-J, Jackson RA, Thiery JP. EMT: 2016. Cell. 2016;166:21–45.

158. McKeown SR. Defining normoxia, physoxia and hypoxia in tumours—implications for treatment response. The British Journal of Radiology. 2014;87:20130676.

159. Reuter S, Gupta SC, Chaturvedi MM, Aggarwal BB. Oxidative stress, inflammation, and cancer: How are they linked? Free Radical Biology and Medicine. 2010;49:1603–16.

160. Pompili L, Porru M, Caruso C, Biroccio A, Leonetti C. Patient-derived xenografts: a relevant preclinical model for drug development. Journal of experimental & clinical cancer research : CR. 2016;35:189.

161. Rous P. THE INFLUENCE OF DIET ON TRANSPLANTED AND SPONTANEOUS MOUSE TUMORS. J Exp Medicine. 1914;20:433–51.

162. Bleijs M, Wetering M, Clevers H, Drost J. Xenograft and organoid model systems in cancer research. Embo J. 2019;38:e101654.

163. Gupta N, Liu JR, Patel B, Solomon DE, Vaidya B, Gupta V. Microfluidics-based 3D cell culture models: Utility in novel drug discovery and delivery research. Bioeng Transl Medicine. 2016;1:63–81.

164. Mittal R, Woo FW, Castro CS, Cohen MA, Karanxha J, Mittal J, et al. Organ-on-chip models: Implications in drug discovery and clinical applications. J Cell Physiol. 2019;234:8352–80.

165. Wong CH, Siah KW, Lo AW. Estimation of clinical trial success rates and related parameters. Biostatistics. 2019;20:273–86.

166. Niu N, Wang L. In vitro human cell line models to predict clinical response to anticancer drugs. Pharmacogenomics. 2015;16:273–85.

167. Krepler C, Xiao M, Sproesser K, Brafford PA, Shannan B, Beqiri M, et al. Personalized Preclinical Trials in BRAF Inhibitor–Resistant Patient-Derived Xenograft Models Identify Second-Line Combination Therapies. Clin Cancer Res. 2016;22:1592–602.

168. Navone NM, Weerden WM van, Vessella RL, Williams ED, Wang Y, Isaacs JT, et al. Movember GAP1 PDX project: An international collection of serially transplantable prostate cancer patient-derived xenograft (PDX) models. Prostate. 2018;78:1262–82.

169. Ravi M, Paramesh V, Kaviya SR, Anuradha E, Solomon FDP. 3D Cell Culture Systems: Advantages and Applications. J Cell Physiol. 2015;230:16–26.

170. Kämpfer AAM, Urbán P, Gioria S, Kanase N, Stone V, Kinsner-Ovaskainen A. Development of an in vitro co-culture model to mimic the human intestine in healthy and diseased state. Toxicol In Vitro. 2017;45:31–43.

171. Drost J, Jaarsveld RH van, Ponsioen B, Zimberlin C, Boxtel R van, Buijs A, et al. Sequential cancer mutations in cultured human intestinal stem cells. Nature. 2015;521:43–7.

172. Gjorevski N, Sachs N, Manfrin A, Giger S, Bragina ME, Ordóñez-Morán P, et al. Designer matrices for intestinal stem cell and organoid culture. Nature. 2016;539:560–4.

173. Drost J, Clevers H. Organoids in cancer research. Nat Rev Cancer. 2018;18:407–18.

174. Bühler P, Wolf P, Katzenwadel A, Schultze-Seemann W, Wetterauer U, Freudenberg N, et al. Primary prostate cancer cultures are models for androgen-independent transit amplifying cells. Oncol Rep. 2010;23:465–70.

175. Zhang YS, Duchamp M, Oklu R, Ellisen LW, Langer R, Khademhosseini A. Bioprinting the Cancer Microenvironment. Acs Biomater Sci Eng. 2016;2:1710–21.

176. Nair RR, Padhee S, Das T, Green R, Howell M, Mohapatra SS, et al. Three- and Four-Dimensional Spheroid and FiSS Tumoroid Cultures: Platforms for Drug Discovery and Development and Translational Research. Crit Rev Ther Drug. 2017;34:185–208.

177. Ma L, Hernandez MO, Zhao Y, Mehta M, Tran B, Kelly M, et al. Tumor Cell Biodiversity Drives Microenvironmental Reprogramming in Liver Cancer. Cancer Cell. 2019;36:418-430.e6.

178. Januškevičienė I, Petrikaitė V. Heterogeneity of breast cancer: the importance of interaction between different tumor cell populations. Life Sci. 2019;239:117009.

179. Kent DM, Steyerberg E, Klaveren D van. Personalized evidence based medicine: predictive approaches to heterogeneous treatment effects. Bmj. 2018;363:k4245.

180. Kleinman HK, Martin GR. Matrigel: Basement membrane matrix with biological activity. Semin Cancer Biol. 2005;15:378–86.

181. Badea MA, Balas M, Hermenean A, Ciceu A, Herman H, Ionita D, et al. Influence of Matrigel on Single- and Multiple-Spheroid Cultures in Breast Cancer Research. Slas Discov. 2019;24:563–78.

182. Hum NR, Sebastian A, Gilmore SF, He W, Martin KA, Hinckley A, et al. Comparative Molecular Analysis of Cancer Behavior Cultured In Vitro, In Vivo, and Ex Vivo. Cancers. 2020;12:690.

183. Yu T, Di G, Center D of BS Fudan University Shanghai Cancer, China D of O Shanghai Medical College, Fudan University, Shanghai 200032,. Role of tumor microenvironment in triple-negative breast cancer and its prognostic significance. Chinese J Cancer Res. 2017;29:237–52.

184. Hinshaw DC, Shevde LA. The Tumor Microenvironment Innately Modulates Cancer Progression. Cancer Res. 2019;79:4557–66.

185. Kalluri R. The biology and function of fibroblasts in cancer. Nat Rev Cancer. 2016;16:582–98.

186. Katti KS, Molla MS, Karandish F, Haldar MK, Mallik S, Katti DR. Sequential culture on biomimetic nanoclay scaffolds forms three-dimensional tumoroids. J Biomed Mater Res A. 2016;104:1591–602.

187. Zhu H, Sarkar S, Scott L, Danelisen I, Trush M, Jia Z, et al. Doxorubicin Redox Biology: Redox Cycling, Topoisomerase Inhibition, and Oxidative Stress. React Oxyg Species. 2016;1:189–98.

188. Wang L, Chen Q, Qi H, Wang C, Wang C, Zhang J, et al. Doxorubicin-Induced Systemic Inflammation Is Driven by Upregulation of Toll-Like Receptor TLR4 and Endotoxin Leakage. Cancer Res. 2016;76:6631–42.

189. Khan MA, D'Ovidio A, Tran H, Palaniyar N. Anthracyclines Suppress Both NADPH Oxidase- Dependent and -Independent NETosis in Human Neutrophils. Cancers. 2019;11:1328.

190. Rong Y, Yuan C-H, Qu Z, Zhou H, Guan Q, Yang N, et al. Doxorubicin resistant cancer cells activate myeloid-derived suppressor cells by releasing PGE2. Sci Rep-uk. 2016;6:23824.

191. Soma CE, Dubernet C, Barratt G, Benita S, Couvreur P. Investigation of the role of macrophages on the cytotoxicity of doxorubicin and doxorubicin-loaded nanoparticles on M5076 cells in vitro. J Control Release. 2000;68:283–9.

192. Alizadeh D, Trad M, Hanke NT, Larmonier CB, Janikashvili N, Bonnotte B, et al. Doxorubicin Eliminates Myeloid-Derived Suppressor Cells and Enhances the Efficacy of Adoptive T-Cell Transfer in Breast Cancer. Cancer Res. 2014;74:104–18.

193. Park JY, Jang MJ, Chung YH, Kim KY, Kim SS, Lee WB, et al. Doxorubicin enhances CD4+ T-cell immune responses by inducing expression of CD40 ligand and 4-1BB. Int Immunopharmacol. 2009;9:1530–9.

194. McAleer JP, Kolls JK. Directing traffic: IL-17 and IL-22 coordinate pulmonary immune defense. Immunol Rev. 2014;260:129–44.

195. Welte T, Zhang XH-F. Interleukin-17 Could Promote Breast Cancer Progression at Several Stages of the Disease. Mediat Inflamm. 2015;2015:1–6.

196. Ma Y, Aymeric L, Locher C, Mattarollo SR, Delahaye NF, Pereira P, et al. Contribution of IL-17–producing γδ T cells to the efficacy of anticancer chemotherapy. J Exp Med. 2011;208:491–503.

197. Mattarollo SR, Loi S, Duret H, Ma Y, Zitvogel L, Smyth MJ. Pivotal Role of Innate and Adaptive Immunity in Anthracycline Chemotherapy of Established Tumors. Cancer Res. 2011;71:4809–20.

198. Wang JT, Li H, Zhang H, Chen YF, Cao YF, Li RC, et al. Intratumoral IL17-producing cells infiltration correlate with antitumor immune contexture and improved response to adjuvant chemotherapy in gastric cancer. Ann Oncol. 2019;30:266–73.

199. Faustino-Rocha A, Oliveira PA, Pinho-Oliveira J, Teixeira-Guedes C, Soares-Maia R, Costa RG da, et al. Estimation of rat mammary tumor volume using caliper and ultrasonography measurements. Lab Animal. 2013;42:217–24.

200. Reich M, Liefeld T, Gould J, Lerner J, Tamayo P, Mesirov JP. GenePattern 2.0. Nat Genet. 2006;38:500–1.

201. Ishikawa F, Yasukawa M, Lyons B, Yoshida S, Miyamoto T, Yoshimoto G, et al. Development of functional human blood and immune systems in NOD/SCID/IL2 receptor γ chainnull mice. Blood. 2005;106:1565–73.

202. Shultz LD, Lyons BL, Burzenski LM, Gott B, Chen X, Chaleff S, et al. Human Lymphoid and Myeloid Cell Development in NOD/LtSz-scid

IL2Rγnull Mice Engrafted with Mobilized Human Hemopoietic Stem Cells. J Immunol. 2005;174:6477–89.

203. Szabo PA, Levitin HM, Miron M, Snyder ME, Senda T, Yuan J, et al. Single-cell transcriptomics of human T cells reveals tissue and activation signatures in health and disease. Nat Commun. 2019;10:4706.

204. Best JA, Blair DA, Knell J, Yang E, Mayya V, Doedens A, et al. Transcriptional insights into the CD8+ T cell response to infection and memory T cell formation. Nat Immunol. 2013;14:404–12.

205. Hashimoto M, Kamphorst AO, Im SJ, Kissick HT, Pillai RN, Ramalingam SS, et al. CD8 T Cell Exhaustion in Chronic Infection and Cancer: Opportunities for Interventions. Annu Rev Med. 2018;69:301–18.

206. Zhang Z, Liu S, Zhang B, Qiao L, Zhang Y, Zhang Y. T Cell Dysfunction and Exhaustion in Cancer. Frontiers Cell Dev Biology. 2020;8:17.

207. Kim K, Park S, Park SY, Kim G, Park SM, Cho J-W, et al. Single-cell transcriptome analysis reveals TOX as a promoting factor for T cell exhaustion and a predictor for anti-PD-1 responses in human cancer. Genome Med. 2020;12:22.

208. Thommen DS, Schumacher TN. T Cell Dysfunction in Cancer. Cancer Cell. 2018;33:547–62.

209. Crinier A, Milpied P, Escalière B, Piperoglou C, Galluso J, Balsamo A, et al. High-Dimensional Single-Cell Analysis Identifies Organ-Specific Signatures and Conserved NK Cell Subsets in Humans and Mice. Immunity. 2018;49:971-986.e5.

210. Atsaves V, Leventaki V, Rassidakis GZ, Claret FX. AP-1 Transcription Factors as Regulators of Immune Responses in Cancer. Cancers. 2019;11:1037.

211. Tsai Y-F, Huang C-C, Lin Y-S, Hsu C-Y, Huang C-P, Liu C-Y, et al. Interleukin 17A promotes cell migration, enhances anoikis resistance, and creates a microenvironment suitable for triple negative breast cancer tumor metastasis. Cancer Immunol Immunother. 2021;1–13.

212. Roussel L, Houle F, Chan C, Yao Y, Bérubé J, Olivenstein R, et al. IL-17 Promotes p38 MAPK-Dependent Endothelial Activation Enhancing

Neutrophil Recruitment to Sites of Inflammation. J Immunol. 2010;184:4531–7.

213. Fabre JAS, Giustinniani J, Garbar C, Merrouche Y, Antonicelli F, Bensussan A. The Interleukin-17 Family of Cytokines in Breast Cancer. Int J Mol Sci. 2018;19:3880.

214. Dawod B, Liu J, Gebremeskel S, Yan C, Sappong A, Johnston B, et al. Myeloid-derived suppressor cell depletion therapy targets IL-17A-expressing mammary carcinomas. Sci Rep-uk. 2020;10:13343.

215. Dökümcü K, Farahani RM. Evolution of Resistance in Cancer: A Cell Cycle Perspective. Frontiers Oncol. 2019;9:376.

216. Haibe-Kains B, Desmedt C, Leo AD, Azambuja E, Larsimont D, Selleslags J, et al. Genome-wide gene expression profiling to predict resistance to anthracyclines in breast cancer patients. Genom Data. 2013;1:7–10.

217. Hatzis C, Pusztai L, Valero V, Booser DJ, Esserman L, Lluch A, et al. A Genomic Predictor of Response and Survival Following Taxane-Anthracycline Chemotherapy for Invasive Breast Cancer. Jama. 2011;305:1873–81.

218. Gilad Y, Eliaz Y, Yu Y, Han SJ, O'Malley BW, Lonard DM. Drug-induced PD-L1 expression and cell stress response in breast cancer cells can be balanced by drug combination. Sci Rep-uk. 2019;9:15099.

219. Chen L, He J, Zhou J, Xiao Z, Ding N, Duan Y, et al. EIF2A promotes cell survival during paclitaxel treatment in vitro and in vivo. J Cell Mol Med. 2019;23:6060–71.

220. Esparza-López J, Medina-Franco H, Escobar-Arriaga E, León-Rodríguez E, Zentella-Dehesa A, Ibarra-Sánchez MJ. Doxorubicin induces atypical NF-κB activation through c-Abl kinase activity in breast cancer cells. J Cancer Res Clin. 2013;139:1625–35.

221. Reinhardt HC, Aslanian AS, Lees JA, Yaffe MB. p53-Deficient Cells Rely on ATM- and ATR-Mediated Checkpoint Signaling through the p38MAPK/MK2 Pathway for Survival after DNA Damage. Cancer Cell. 2007;11:175–89.

222. Zhou L, Kuai F, Shi Q, Yang H. Doxorubicin restrains osteogenesis and promotes osteoclastogenesis in vitro. Am J Transl Res. 2020;12:5640–54.

223. Gallo S, Spilinga M, Albano R, Ferrauto G, Gregorio ED, Casanova E, et al. Activation of the MET receptor attenuates doxorubicin-induced cardiotoxicity in vivo and in vitro. Brit J Pharmacol. 2020;177:3107–22.

224. Korga A, Ostrowska M, Iwan M, Herbet M, Dudka J. Inhibition of glycolysis disrupts cellular antioxidant defense and sensitizes HepG2 cells to doxorubicin treatment. Febs Open Bio. 2019;9:959–72.

225. House IG, Savas P, Lai J, Chen AXY, Oliver AJ, Teo ZL, et al. Macrophage-Derived CXCL9 and CXCL10 Are Required for Antitumor Immune Responses Following Immune Checkpoint Blockade. Clin Cancer Res. 2020;26:487–504.

226. Korbecki J, Grochans S, Gutowska I, Barczak K, Baranowska-Bosiacka I. CC Chemokines in a Tumor: A Review of Pro-Cancer and Anti-Cancer Properties of Receptors CCR5, CCR6, CCR7, CCR8, CCR9, and CCR10 Ligands. Int J Mol Sci. 2020;21:7619.

227. Z F, G K, V P, N KE. Interleukins Associated with Breast Cancer. Cureus. 2018;10:e3549.

228. Nagai S, Toi M. Interleukin-4 and breast cancer. Breast Cancer-tokyo. 2000;7:181–6.

229. Kawakami K, Kawakami M, Husain SR, Puri RK. Potent antitumor activity of IL-13 cytotoxin in human pancreatic tumors engineered to express IL-13 receptor α2 chain in vivo. Gene Ther. 2003;10:1116–28.

230. Lyon DE, McCain NL, Walter J, Schubert C. Cytokine comparisons between women with breast cancer and women with a negative breast biopsy. Nursing research. 2008;57:51–8.

231. Joimel U, Gest C, Soria J, Pritchard L-L, Alexandre J, Laurent M, et al. Stimulation of angiogenesis resulting from cooperation between macrophages and MDA-MB-231 breast cancer cells: proposed molecular mechanism and effect of tetrathiomolybdate. Bmc Cancer. 2010;10:375.

232. Ahmad N, Ammar A, Storr SJ, Green AR, Rakha E, Ellis IO, et al. IL-6 and IL-10 are associated with good prognosis in early stage invasive breast cancer patients. Cancer Immunol Immunother. 2018;67:537–49.

233. Bilska M, Pawłowska A, Zakrzewska E, Chudzik A, Suszczyk D, Gogacz M, et al. Th17 Cells and IL-17 As Novel Immune Targets in Ovarian Cancer Therapy. J Oncol. 2020;2020:1–15.

234. Lee M-H, Chang JT-C, Liao C-T, Chen Y-S, Kuo M-L, Shen C-R. Interleukin 17 and peripheral IL-17-expressing T cells are negatively correlated with the overall survival of head and neck cancer patients. Oncotarget. 2018;9:9825–37.

235. Zhang Q, Liu S, Ge D, Zhang Q, Xue Y, Xiong Z, et al. Interleukin-17 Promotes Formation and Growth of Prostate Adenocarcinoma in Mouse Models. Cancer Res. 2012;72:2589–99.

236. Cochaud S, Giustiniani J, Thomas C, Laprevotte E, Garbar C, Savoye A-M, et al. IL-17A is produced by breast cancer TILs and promotes chemoresistance and proliferation through ERK1/2. Nature Publishing Group. 2013;3:3456–10.

237. Kryczek I, Wei S, Szeliga W, Vatan L, Zou W. Endogenous IL-17 contributes to reduced tumor growth and metastasis. Blood. 2009;114:357–9.

238. Zhang X, Weng W, Xu W, Wang Y, Yu W, Tang X, et al. Prognostic significance of interleukin 17 in cancer: a meta-analysis. Int J Clin Exp Med. 2014;7:3258–69.

239. Martin-Orozco N, Muranski P, Chung Y, Yang XO, Yamazaki T, Lu S, et al. T Helper 17 Cells Promote Cytotoxic T Cell Activation in Tumor Immunity. Immunity. 2009;31:787–98.

240. Muranski P, Boni A, Antony PA, Cassard L, Irvine KR, Kaiser A, et al. Tumor-specific Th17-polarized cells eradicate large established melanoma. Blood. 2008;112:362–73.

241. You R, DeMayo FJ, Liu J, Cho S-N, Burt BM, Creighton CJ, et al. IL17A Regulates Tumor Latency and Metastasis in Lung Adeno and Squamous SQ.2b and AD.1 Cancer. Cancer Immunol Res. 2018;6:canimm.0554.2017.

242. Chen X, Wan J, Liu J, Xie W, Diao X, Xu J, et al. Increased IL-17-producing cells correlate with poor survival and lymphangiogenesis in NSCLC patients. Lung Cancer. 2010;69:348–54.

243. Sui G, Qiu Y, Yu H, Kong Q, Zhen B. Interleukin-17 promotes the development of cisplatin resistance in colorectal cancer. Oncol Lett. 2019;17:944–50.

244. Gonzalez-Angulo AM, Morales-Vasquez F, Hortobagyi GN. Breast Cancer Chemosensitivity. Adv Exp Med Biol. 2007;608:1–22.

245. Nyström L, Andersson I, Bjurstam N, Frisell J, Nordenskjöld B, Rutqvist LE. Long-term effects of mammography screening: updated overview of the Swedish randomised trials. Lancet. 2002;359:909–19.

246. Moss SM, Cuckle H, Evans A, Johns L, Waller M, Bobrow L, et al. Effect of mammographic screening from age 40 years on breast cancer mortality at 10 years' follow-up: a randomised controlled trial. Lancet. 2006;368:2053–60.

247. Pashayan N, Antoniou AC, Ivanus U, Esserman LJ, Easton DF, French D, et al. Publisher Correction: Personalized early detection and prevention of breast cancer: ENVISION consensus statement. Nat Rev Clin Oncol. 2020;17:716–716.

248. Trentham-Dietz A, Kerlikowske K, Stout NK, Miglioretti DL, Schechter CB, Ergun MA, et al. Tailoring Breast Cancer Screening Intervals by Breast Density and Risk for Women Aged 50 Years or Older: Collaborative Modeling of Screening Outcomes. Ann Intern Med. 2016;165:700.

249. Stahl PD, Raposo G. Extracellular Vesicles: Exosomes and Microvesicles, Integrators of Homeostasis. Physiology. 2019;34:169–77.

250. Skotland T, Sandvig K, Llorente A. Lipids in exosomes: Current knowledge and the way forward. Prog Lipid Res. 2017;66:30–41.

251. Muller L, Hong C-S, Stolz DB, Watkins SC, Whiteside TL. Isolation of biologically-active exosomes from human plasma. J Immunol Methods. 2014;411:55–65.

252. Robbins PD, Morelli AE. Regulation of immune responses by extracellular vesicles. Nat Rev Immunol. 2014;14:195–208.

253. Ham S, Lima LG, Chai EPZ, Muller A, Lobb RJ, Krumeich S, et al. Breast Cancer-Derived Exosomes Alter Macrophage Polarization via gp130/STAT3 Signaling. Front Immunol. 2018;9:871.

254. Jabalee J, Towle R, Garnis C. The Role of Extracellular Vesicles in Cancer: Cargo, Function, and Therapeutic Implications. Cells. 2018;7:93.

255. Azmi AS, Bao B, Sarkar FH. Exosomes in cancer development, metastasis, and drug resistance: a comprehensive review. Cancer Metast Rev. 2013;32:623–42.

256. Nedaeinia R, Manian M, Jazayeri MH, Ranjbar M, Salehi R, Sharifi M, et al. Circulating exosomes and exosomal microRNAs as biomarkers in gastrointestinal cancer. Cancer Gene Ther. 2017;24:48–56.

257. Hoshino A, Costa-Silva B, Shen T-L, Rodrigues G, Hashimoto A, Mark MT, et al. Tumour exosome integrins determine organotropic metastasis. Nature. 2015;527:329–35.

258. Jia Y, Chen Y, Wang Q, Jayasinghe U, Luo X, Wei Q, et al. Exosome: emerging biomarker in breast cancer. Oncotarget. 2015;5:41717–33.

259. Li M, Zeringer E, Barta T, Schageman J, Cheng A, Vlassov AV. Analysis of the RNA content of the exosomes derived from blood serum and urine and its potential as biomarkers. Philosophical Transactions Royal Soc B Biological Sci. 2014;369:20130502.

260. Hannafon BN, Trigoso YD, Calloway CL, Zhao YD, Lum DH, Welm AL, et al. Plasma exosome microRNAs are indicative of breast cancer. Breast Cancer Res. 2016;18:90.

261. Zhou M, Chen J, Zhou L, Chen W, Ding G, Cao L. Pancreatic cancer derived exosomes regulate the expression of TLR4 in dendritic cells via miR-203. Cell Immunol. 2014;292:65–9.

262. Madeo M, Colbert PL, Vermeer DW, Lucido CT, Cain JT, Vichaya EG, et al. Cancer exosomes induce tumor innervation. Nat Commun. 2018;9:4284.

263. Brown J, Pirrung M, McCue LA. FQC Dashboard: integrates FastQC results into a web-based, interactive, and extensible FASTQ quality control tool. Bioinformatics. 2017;33:3137–9.

264. Dobin A, Gingeras TR. Optimizing RNA-Seq Mapping with STAR. Methods in molecular biology (Clifton, NJ). 2016;1415:245–62.

265. Ritchie ME, Phipson B, Wu D, Hu Y, Law CW, Shi W, et al. limma powers differential expression analyses for RNA-sequencing and microarray studies. Nucleic Acids Res. 2015;43:e47–e47.

266. Silveira WA da, Hazard ES, Chung D, Hardiman G. Tumor Profiling, Methods and Protocols. Methods Mol Biology. 2019;1908:185–204.

267. Meier F, Brunner A-D, Koch S, Koch H, Lubeck M, Krause M, et al. Online Parallel Accumulation–Serial Fragmentation (PASEF) with a Novel Trapped Ion Mobility Mass Spectrometer*. Mol Cell Proteomics. 2018;17:i–2545.

268. Yu F, Haynes SE, Teo GC, Avtonomov DM, Polasky DA, Nesvizhskii AI. Fast Quantitative Analysis of timsTOF PASEF Data with MSFragger and IonQuant. Mol Cell Proteomics. 2020;19:1575–85.

269. Li J, Han X, Wan Y, Zhang S, Zhao Y, Fan R, et al. TAM 2.0: tool for MicroRNA set analysis. Nucleic Acids Res. 2018;46:gky509-.

270. Wang W, Zhu N, Yan T, Shi Y-N, Chen J, Zhang C-J, et al. The crosstalk: exosomes and lipid metabolism. Cell Commun Signal. 2020;18:119.

271. Willms E, Cabañas C, Mäger I, Wood MJA, Vader P. Extracellular Vesicle Heterogeneity: Subpopulations, Isolation Techniques, and Diverse Functions in Cancer Progression. Front Immunol. 2018;9:738.

272. Xu J, Zhang J, Zhang W. Antisense RNA: the new favorite in genetic research. J Zhejiang Univ-sc B. 2018;19:739–49.

273. Dilsiz N. Role of exosomes and exosomal microRNAs in cancer. Futur Sci Oa. 2020;6:FSO465.

274. Sun N, Xu HN, Luo Q, Li LZ. Oxygen Transport to Tissue XXXVIII. Adv Exp Med Biol. 2016;923:121–7.

275. Halvaei S, Daryani S, Eslami-S Z, Samadi T, Jafarbeik-Iravani N, Bakhshayesh TO, et al. Exosomes in Cancer Liquid Biopsy: A Focus on Breast Cancer. Mol Ther - Nucleic Acids. 2018;10:131–41.

276. Chang K, Creighton CJ, Davis C, Donehower L, Drummond J, Wheeler D, et al. The Cancer Genome Atlas Pan-Cancer analysis project. Nat Genet. 2013;45:1113–20.

277. Mourksi N-E-H, Morin C, Fenouil T, Diaz J-J, Marcel V. snoRNAs Offer Novel Insight and Promising Perspectives for Lung Cancer Understanding and Management. Cells. 2020;9:541.

278. Poliseno L, Marranci A, Pandolfi PP. Pseudogenes in Human Cancer. Frontiers Medicine. 2015;2:68.

279. Borgmästars E, Weerd HA de, Lubovac-Pilav Z, Sund M. miRFA: an automated pipeline for microRNA functional analysis with correlation support from TCGA and TCPA expression data in pancreatic cancer. Bmc Bioinformatics. 2019;20:393.

280. Kern F, Fehlmann T, Solomon J, Schwed L, Grammes N, Backes C, et al. miEAA 2.0: integrating multi-species microRNA enrichment analysis and workflow management systems. Nucleic Acids Res. 2020;48:gkaa309-.

281. Zagganas K, Vergoulis T, Paraskevopoulou MD, Vlachos IS, Skiadopoulos S, Dalamagas T. BUFET: boosting the unbiased miRNA functional enrichment analysis using bitsets. Bmc Bioinformatics. 2017;18:399.

282. Zhang J, Tian X-J, Zhang H, Teng Y, Li R, Bai F, et al. TGF-ß–induced epithelial-to-mesenchymal transition proceeds through stepwise activation of multiple feedback loops. Science Signaling. 2014;7:ra91–ra91.

283. Riffo-Campos ÁL, Riquelme I, Brebi-Mieville P. Tools for Sequence-Based miRNA Target Prediction: What to Choose? Int J Mol Sci. 2016;17:1987.

284. Pulaski BA, Ostrand-Rosenberg S. Mouse 4T1 breast tumor model. Current protocols in immunology. 2001;Chapter 20:Unit 20.2-20.2.16.

285. Liu T, Zhou L, Li D, Andl T, Zhang Y. Cancer-Associated Fibroblasts Build and Secure the Tumor Microenvironment. Frontiers Cell Dev Biology. 2019;7:60.

286. Waldman AD, Fritz JM, Lenardo MJ. A guide to cancer immunotherapy: from T cell basic science to clinical practice. Nat Rev Immunol. 2020;20:651–68.

287. Jeibouei S, Akbari ME, Kalbasi A, Aref AR, Ajoudanian M, Rezvani A, et al. Personalized medicine in breast cancer: pharmacogenomics approaches. Pharmacogenomics Personalized Medicine. 2019;12:59–73.

288. Basu B, Basu S. Correlating and Combining Genomic and Proteomic Assessment with In Vivo Molecular Functional Imaging: Will This Be the Future Roadmap for Personalized Cancer Management? Cancer Biother Radio. 2016;31:75–84.

289. Uzilov AV, Ding W, Fink MY, Antipin Y, Brohl AS, Davis C, et al. Development and clinical application of an integrative genomic approach to personalized cancer therapy. Genome Med. 2016;8:62.

290. Dumbrava EI, Meric-Bernstam F. Personalized cancer therapy—leveraging a knowledge base for clinical decision-making. Mol Case Stud. 2018;4:a001578.

291. Krzyszczyk P, Acevedo A, Davidoff EJ, Timmins LM, Marrero-Berrios I, Patel M, et al. The growing role of precision and personalized medicine for cancer treatment. Technology. 2019;06:79–100.